Micronization of Proteins

by

Jet Milling

Dissertation

zur Erlangung des Doktorgrades der Naturwissenschaften
(Dr. rer. nat.)
der Fakultät Chemie und Pharmazie
der Universität Regensburg

vorgelegt von

Axel Ehmer

aus Hünfeld

2009

Diese Doktorarbeit entstand in der Zeit von August 2004 bis September 2009 am Lehrstuhl für Pharmazeutische Technologie an der Universität Regensburg.

Die Arbeit wurde von Herrn Prof. Dr. Achim Göpferich angeleitet.

Promotionsgesuch eingereicht am: 23. Oktober 2009

Datum der mündlichen Prüfung: 01. Dezember 2009

Prüfungsausschuss:	Vorsitzender:	Prof. Dr. Franz
	Erstgutachter:	Prof. Dr. Göpferich
	Zweitgutachter:	Prof. Dr. Schlossmann
	Drittprüfer:	Prof. Dr. Heilmann

Meiner Familie

in Liebe und Dankbarkeit gewidmet

"The most exciting phrase to hear in science, the one that heralds new discoveries, is not 'Eureka!' (I found it!) but 'That's funny ...' "

Isaac Asimov

Table of Contents

Chapter 1

Introduction

and

Goals of the Thesis

Introduction

Powders are not only intermediate products, but they have a significant impact on drug performance or are used directly as dosage forms. Particle size and size distribution are very important characteristics of powders having significant effects on flowability [1], dissolution properties [2], release kinetics [3] etc. Therefore, particle engineering is a very important step in the processing of pharmaceutical solids. For many applications particles with special requirements, like sizes in the lower micrometer range, are needed. The positive effects of micronization on the solubility of poorly soluble drugs [4], the homogeneous distribution within long term release matrices [5] or effective pulmonary application [6] are just some examples. Several methods for the processing of pharmaceutical powders are available and very well validated. However, only few detailed studies exist for micronization of proteins.

Proteins belong to a group of drugs so-called biopharmaceuticals (recombinant proteins, monoclonal antibodies and nucleic acid-based drugs) [7], which were established on the market during the last decades. Starting with the approval of the first recombinant insulin in the early 1980s, biopharmaceuticals have more and more been used as highly potent drugs. Facilitated by advances in molecular biology and immunology and description of diseases at the molecular level rational drug design was enabled [8]. And due to the improvement of biotechnical methods to modify DNA there are now virtually unlimited options to create recombinant proteins for every demand. Especially in the fields of cancer, diabetes, growth disturbances, hemophilia and hepatitis [7], new therapeutic options were made possible by the development of biopharmaceutical drugs. The immense variability in structure and the possibility to evoke very specific effects in the body are the most salient characteristics of biopharmaceuticals.

But as always, there are two sides of the coin: stability problems of the amino acids backbone especially in presence of water are well known. Proteins are prone to many different types of chemical degradation e.g. deamidation, hydrolysis, β-elimination, oxidation or disulfide exchange [9]. Additionally, physical changes in the secondary or tertiary structure e.g. by unfolding are fatal for the bioactivity of proteins [10]. Another drawback is the fact that the Holy Grail, the oral administration of these drugs, has still not been found. The challenges are e.g. digestive enzymes, intestinal flora, acetic gastric environment and the hindered absorption [11], which block this preferred way of application. Therefore, as long as no satisfying solutions are available, innovative new ways of application have to be found for these challenging molecules. Creating alternatives to the parenteral delivery with its unpleasant

injections and short administration intervals was the focus in drug delivery research during the last years. Several new ways of application were developed, like nasal [12], pulmonary [13], buccal [14], ocular [15], rectal [16], implantable long term release systems [3], needle free powder injections [17] and transdermal delivery [18]. For most of these applications proteins are not only processed in solid state but also delivered as a solid. This concept is based on the dramatically increased stability of proteins in solid state compared to solutions [19]. From the beginning of protein galenics most protein drugs were stored as freeze dried solids being disssolved before parenteral application. So longer shelf lives were obtained. However, for the new administration strategies not only the stability of the solid drugs but also the properties of the solid itself played an important role. Now being delivered in solid form protein drugs had to fulfill the same requirements as any other pharmaceutical powder e.g. flowability, particle size and size distribution of the protein particles. Especially pulmonary delivery or incorporation into long term release systems has special demands on these powder characteristics. A particle is no longer seen as a passive carrier, but rather as an essential part of the drug delivery system [20]. Hence processes have to be found, which allow the production of micron sized protein particles. Ideally existing micronization methods can be used from the powder processing of small molecular drugs, but maintaining their bioactivity during these sometimes harsh processes is a challenging task.

Obtaining micron sized protein particles– an overview

There are generally two different methods to obtain protein particles in the lower micrometer range starting with a protein solution. For one the solidification and particle forming of the proteins take place in one step. Spray drying, spray freeze drying and precipitation (incl. supercritical fluid methods) are typical examples. The second option almost always starts with freeze drying of the protein solution. Afterwards the dry cake is micronized by different size reduction processes like jet milling, pearl milling or high pressure homogenization. These different methods of obtaining small protein particles will now be discussed in more detail.

One step processes

Spray drying

Spray drying is the most often used and best investigated process of forming protein particles in the lower micrometer range. A liquid feed is atomized into a hot gas. The resulting fine droplets generate a large amount of air-water interfacial area, so that the water evaporates very rapidly. The whole drying process takes tens of seconds to a few seconds [21]. Due to the evaporation of the solvent a critical increase in temperature is prevented and the temperature of the formed particles remains significantly lower than the temperature of the drying gas [22]. However, for spray drying of proteins a lower inlet air temperature is used in practice to reduce the potential thermal stress [23]. Afterwards the particles are removed from the gas stream by cyclone separators. This separation step was improved during the last years so that the yield could be increased from $20 - 50\%$ [24] to more than 70% by the development of high-performance cyclones. The quality of the product is significantly influenced by the chosen process parameters. And apart from the classical trial and error attempts experimental statistical design techniques were applied to optimize the process [25]. Especially lack of control over particle size and size distribution are challenges [26,27].

The resulting particle morphology after spray drying is not necessarily spherical. After drying the particles may have convoluted surfaces, asperities, holes and voids [21]. For most of the mentioned spray drying experiments particle sizes below 10 μm were obtained. The median diameters were in a size range from 2 to 6 μm. Therefore, spray drying is often used for the production of particles for pulmonary delivery [28].

Thermal stressing is more or less avoided due to the evaporative cooling, but high shear rates originating from the atomization process may denature proteins. For example, human growth hormone (hGH) was denatured at the air-liquid interface whereas for tissue-type

plasminogen activator (t-PA) no negative effects were detectable [29]. Pure lysozyme lost about 10 % and catalase lost nearly 50 % of their initial bioactivity [30]. To overcome these problems different excipients for stabilization of proteins during and after the spray drying process were tested. By adding sucrose, trehalose, polyvinyl alcohol and mixtures thereof lysozyme and catalase retained almost full activity. Lactose showed good stabilization of a recombinant humanized anti-IgE monoclonal antibody [31] and combinations of lactose with dipamitoylphosphatidylcholine prevented the dimerization of hGH by spray drying [32]. Surfactants were recognized as useful tools to prevent the accumulation of proteins at the air-liquid interface of the atomized droplets. Due to their amphiphilic character proteins normally tend to concentrate on the surface of these droplets and are then prone to aggregation and unfolding. Added surfactants displace the proteins and promote their stability [33].

While spray drying is the best established method for preparation of micron sized protein particles, a disadvantage may be the high amounts of excipients that are necessary to stabilize the proteins during the process.

Spray freeze drying (SFD)

The principle of SFD was first introduced in 1990 [34]. Similar to spray drying a solution is atomized, but instead of rapid drying by hot air the droplets are sprayed into a vessel containing a cryogenic liquid, such as liquid nitrogen. While traveling through the cryogenic gas the droplets begin to freeze [35] and are completely frozen after entering the liquid cryogen. After freeze drying micron size particles were obtained [36].

Due to the absence of hot air drying no solvent evaporation takes place and the resulting porous particles keep their spherical shape [17]. An advantage is the high product yield. At identical spraying conditions SFD resulted in larger (8 − 10 μm) but more porous particles with a larger specific surface area than at spray drying (3 μm) [37]. Nevertheless, particle size and morphology can be strongly influenced by varying the process parameters [38].

Similar to spray drying problems with protein aggregation and denaturation can occur. Ziegler et al. [17] determined a constant loss of 30 % bioactivity of catalase due to the SFD process. By systematically studying the effect of the separate steps of the process (spraying, freezing, drying) the large gas-liquid interface in the spraying step was identified as the primary cause of protein aggregation of recombinant human interferon-γ [39] and lysozyme [40]. During the freezing step concentrations of protein and other solutes like electrolytes increase markedly in the remaining unfrozen solution, which further contributes to protein aggregation and

denaturation [41]. Therefore, modifications were developed to minimize the time of exposure to the air liquid interface during the atomization step and increasing the freezing velocity.

It was not the new concept to spray the protein solution on top of the cryogenic liquid but directly in the cryogenic liquid by using an insulated nozzle. It was first developed for enhancing the dissolution of poorly soluble drugs [42]. The ultra rapid freezing of the formed droplets prevents phase separation and also prevents crystal growth in frozen water. By spray freezing into liquid (SFL) an amorphous glass is formed before any relaxation events take place in the concentrated solution [41].

The particle morphology was quite similar to SFD particles. Very porous particles with large specific surface areas were optained. Yu et al. produced particles of insulin and BSA with a median diameter of 5 μm. By sonication in methylene chloride BSA particles were further micronized to about 0.4 μm [40,43].

Comparing results from SFD and SFL showed a significant increase in protein activity and stability for protein particles produced by SFL. The monomer loss of BSA was reduced from about 5 % for SFD to 0.5 % for SFL [44], for the enzyme lysozyme 97 % activity for SFL made particles and 86 % for SFD made ones were obtained [40]. For insulin which tends to deamidation and aggregation no differences in stability compared to the bulk substance were determined [43]. Even for fragile lactate dehydrogenase (LDH) 98 % bioactivity were measured after SFL, which was similar to the freeze dried control and significantly higher than after SFD where about 80 % activity were determined [45]. This effect was attributed to the very short exposure time to the gas-liquid interface which was 2 orders of magnitude faster than for SFD.

SFD and SFL are a further development of spray drying and the higher expense seems to be justified by the good results.

Precipitation of protein crystals

Precipitation was one of the first methods to purify proteins or to obtain protein crystals for structural analysis. Generally, proteins are precipitated by the reduction of solubility due to the addition of specific compounds or the change in process conditions. Salting-out, precipitation by polyelectrolytes and nonionic polymers, isoelectric precipitation and addition of organic solvents are common methods. Detailed information about crystallization conditions and crystal data for several thousand proteins can be found in the Biological Macromolecular Crystallization Database (BMCD) [46]. However, these data originated mainly from approaches to generate X-ray quality crystals for structural analysis, but for the

use in pharmaceutical formulations the aims are quite different. Narrow size distribution, high yield and quick processing are challenges for the use of precipitation in pharmaceutical processes [47].

There are different hints that proteins in crystallized form are more stable than in their amorphous form [48,49]. The crystalline form is thermodynamically more stable, which is the reason for the lower stability and higher reactivity of amorphous substances [50]. Additionally, it is possible to influence the release behavior by modifying crystal properties due to different excipients or by utilizing possible crystal polymorphisms [51]. In spite of these advantages with exception of insulin nearly no protein is used in crystallized form in pharmaceutics. Reasons for this are 1. the hard to be controlled crystallization process which often results in broad size distributions and 2. that not all proteins cannot easily be crystallized.

Lee et al. produced uniform spherical microcrystals of α-lactalbumin of 1-2 μm by using a pH-shift method in presence of PEG as a stabilizer [52]. Three monoclonal antibodies (rutiximab, trastuzumab and infliximab) were successfully crystallized by Yang et al. [53]. As precipitation agents different amounts and types of PEG and salts were utilized. Depending on the conditions needles, rice-shaped crystals or star clusters formed in a quite homogenous way. The obtained size range was between 10 to 60 μm. All antibodies retained their full stability and activity. Reichert et al. patented a method to produce crystalline interferon alpha for pulmonary delivery [54]. The protein was dissolved in zinc acetate/sodium acetate containing medium at 4°C. Crystallization was achieved by using a temperature induction method. It was increased over 6 hours up to 22°C and maintained there for 5 days. The resulting crystal sizes ranged from 100 to less than 1 μm. After further processing it was possible to isolate a fraction with an average diameter of 1.8 μm. The bioactivity of interferon was not distinguishable from the unprocessed control.

These are some promising results but as mentioned before the practical use in drug formulation has not yet been established.

Supercritical fluid technology

Supercritical fluids (SCFs) are gases or liquids at temperatures and pressures above their critical points (critical temperature T_c, critical pressure P_c). The 3-phase diagram indicates that the higher the temperature of a gas is the higher the pressure has to be to liquefy it (fig 1.1). At high pressures the density of the gaseous phase increased so much that it is impossible to

distinguish between gas and liquid. T_c is now the highest temperature at which gaseous and liquid phase are separated and P_c is the highest pressure where this is possible [23].
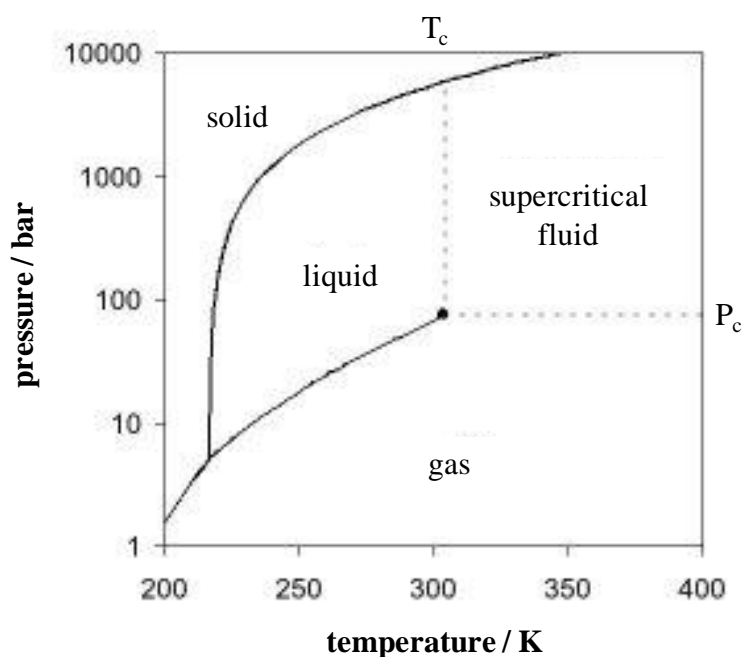

Fig. 1.1 Carbon dioxide pressure-temperature phase diagram

In practice the term supercritical fluids is assigned to substances in a pressure and temperature range of $T_r = 1.01$ to 1.10 and $P_r = 1.01$ to 1.5 ($T_r = T/T_c$ and $P_r = P/P_c$) [55]. SCFs are characterized by special thermophysical properties. Liquid-like densities combined with very large compressibility and higher thermal diffusivities and viscosities than liquids make them an interesting tool. They are utilized for extraction of plant ingredients [56,57], supercritical fluid chromatography [58], particle production for pulmonary delivery [59], as solvents for enzymatic reactions [60] and several other applications. Carbon dioxide (CO_2) is the most widely used substance, because of its low costs and nontoxic properties and its easily accessible critical point (304.1 K and 72.8 bar) [61].

Several methods were developed to use these super critical fluids for preparation of protein microparticles. SCFs may be used as solvents or antisolvents for the proteins to be precipitated. For the first variant the increased dissolving power of the SCFs is utilized to dissolve the proteins. Afterwards the solution is fed via an orifice into a vessel where by rapid expansion the protein is precipitated because of the decreasing dissolving power. This method is limited by the fact that only some proteins are soluble in SFCs. The second and most often used option is similar to the use of anti-solvent in solvent-based crystallization processes [62]. Proteins are dissolved in good solvents like dimethylsulfoxide (DMSO) or ethanol water

mixtures. The high solubility of supercritical CO_2 in these solvents leads to volume expansion when the fluids get into contact. Due to this the solvent density is reduced and the solvation capacity drops which leads to nucleation and particle precipitation [22].

Different proteins were tested at different process conditions. Cyclosporine particles of 150 nm were obtained by rapid expansion, but the particles were highly aggregated [63]. Insulin and catalase were micronized down to 3 μm respectively smaller 1 μm by using CO_2 as an antisolvent [64].

Muhrer and Mazotti investigated the effect of different parameters on the size of lysozyme particles precipitated from a DMSO solution. The resulting amorphous particles had a size of about 250 nm, but were aggregated to particles of 20-30 μm with no big influence of any process parameter. After the process 75 % biological activity relative to the standard material was retained [65]. Thiering et al. described the relation between process temperature and lysozyme bioactivity, which was decreased to 60 % by increasing the temperature from 25 to 45°C [66]. Insulin precipitated from DMSO formed particles with 90 % smaller than 4 μm. The FT-IR spectra showed an increase of β-sheet content with concomitant decrease in α-helix contents. However, after dissolving the particles in 0.01 M HCl the spectra were nearly identical to the commercial powder [67]. Bioactivity tests in rats showed no difference to the unprocessed insulin [68].

Bustami et al. sprayed an aqueous solution of lysozyme and rhDNase into pressurized CO_2 with a mole fraction of 0.2 ethanol added. Lysozyme retained all bioactivity, but rhDNase was totally denatured. No monomers of rhDNase could be detected after processing at 45°C. Even after lowering the temperature to 20°C two-thirds were denatured, which was related to the acetic environment in this process [69].

This relatively new technique seems to be quite promising, but the process is complex and applicable to a few proteins only.

Two step processes

Lyophilization

Lyophilization or freeze-drying is the most common and best investigated method to obtain solid proteins. However, the resulting solids have to be further processed to get homogeneously distributed particles in the micrometer range and freeze drying is just the first of the two preparation steps. The process of freeze-drying is very well investigated and often reviewed in literature [19,70–75]. Therefore, this process will not be discussed in detail here, as it would exceed the scope of this thesis. The critical steps during the three process stages

(freezing, primary drying and secondary drying), e.g. by freezing and drying stresses like solute concentration, formation of ice crystals, pH changes and effect of different excipients, are well known and often reviewed but still not totally understood [19,76]. Wang stated, that in order to get the optimal result for each protein it takes an enormous amount of time and labor, because there is no single, short and mature pathway to follow in formulating such a product [19]. This might be true for all protein processing methods.

Anyhow, even by taking the potential risks into account, lyophilization is a very useful and well analyzed method to obtain stable solid proteins and most commercially available proteins are freeze-dried powders.

Co-lyopilization of proteins with poly(ethylene glycol) (PEG)

Morita et al. developed a method to conceive spherical protein microparticles after lyophilization in presence of PEG 6000 [77]. PEG was chosen because of its solubility in different media, which allows the co-lyophilization with proteins in an aqueous media and the complete removal with an organic solvent afterwards. Secondly, PEG served as a phase separation inducer. Protein and PEG have to be mixed in a protein specific ratio and then solved in water to form a clear solution. During the freezing process protein and PEG are separated in a continuous PEG-phase and a disperse protein-phase. Afterwards the PEG phase is removed by methylene chloride and the protein microparticles remain.

The resulting spherical particles had a narrow size distribution with an average particle size of 3-4 µm and high purity for BSA, superoxide dismutase and horseradish peroxidase. The activity of superoxide dismutase and horseradish peroxidase was completely maintained after the process. Castellanos et al. investigated the activity of γ-chymotrypsin after encapsulation of the protein particles in PLGA microsperes and 92 % of the initial activity was measured [78]. Koennings et al. described the incorporation of interleukin-18 particles produced by co-lyphilization into lipidic matrices without any loss in bioactivity [79]. The method was also adapted for the preparation of dextran microspheres. Depending on molecular weight of PEG and dextran particles in the range of 200 nm to 10 µm were obtained [80].

This method seems to be very useful for the processing of very small amounts of proteins.

Milling

Size reduction of solids by milling is the oldest method to obtain small particles and is a basic operation in the processing of many powdered pharmaceutical excipients or drugs.

Nevertheless, for the production of protein microparticles these techniques are applied quite rarely until now.

Jet milling

Micronization by jet milling is the most common method to produce particles in the lower micrometer range. In brief, the raw material with a maximum size of about 1 to 2 mm is introduced into the milling chamber via a gas stream. Within the milling chamber a circular gas stream accelerates the particles which are micronized by collision with each other or with the wall of the chamber. The ground particles are removed from the milling chamber by the gas stream, while the larger ones stay inside due to centrifugal forces.

Platz et al. described the jet milling of different proteins after freeze drying [81]. After micronization of human growth hormone 40 % of the powder was insoluble in water. It was possible to reduce this fraction to 2.5 to 7.5 % by exchanging some silver soldered joints and copper gas lines with more inert materials like stainless steel. Interferone-β was freeze dried with different mixtures of human serum albumin, NaCl and sorbitol. 50 % of the micronized particles were smaller than 3 μm and the mixture containing the sorbitol withstood the milling without significant loss of activity while the activity of the other mixtures was reduced by about 35 %. For granulocyte-colony stimulating factor soluble aggregates were detected after jet milling. Adding sorbitol to the protein solution before freeze drying reduced these aggregates to less than 4 %. By using HPLC no degradation of the protein was visible.

Phillips et al. investigated the effect of the milling pressure on 5 amorphous proteins and peptides [82]. The improvement in size reduction by increasing the pressure was visible for all proteins but the dimension of the effect was different. For all tested materials mean particle sizes between 1.5 and 3.5 μm were measured. No impact on initial or long term storage stability or on the bioactivity was determined.

Horseradish peroxidase was jet milled after co-precipitation with carbomer [83]. The activity of the protein was significantly reduced by the milling process, but the author stated that the way of co-precipitation had a much greater effect on protein stability than the milling process itself. It is worth while mentioning that after grinding the powder for 10 min in a mortar nearly no remaining activity of the peroxidase was measurable.

Insulin was micronized in combination with sodium caprate as an absorption enhancer for pulmonary application [84]. The mixture was milled down to an average size of 2 μm and significant plasma insulin levels of insulin and a drop in glucose concentration were measured after pulmonary application to five dogs. Similar results were found for the pulmonary

activity of salmon calcitonin which was micronized after freeze drying with lactose and absorption enhancers. Particle sizes of 4 µm were achieved and significant blood levels of calcitonin were determined within rats [85].

Jet milling is besides spray drying the gold standard for the production of inhalable particles of small molecular drugs. For the processing of proteins and peptides the results are quite different and the reasons for the loss of activity of some proteins is not clear yet and has to be further investigated before it will be regularly used for these substances, too.

Tribomechanical milling

Tribomechanics is a field in physics which deals with phenomena occurring during fine milling under dynamic conditions. The milling equipment consists of two rotor discs placed against each other. On each disc several concentric rings of metal teeth are placed. During the milling process the discs rotate in opposite directions (10.000 – 22.000 rpm) while the product enters the center of the discs via an air stream. By collision and friction size reduction takes place.

The system was tested in food industry on different whey protein powders with 60 % (WPC-60) respectively 80 % (WPC-80) protein content at a feed rate of 5 kg/min and rotor speeds between 16.000 and 22.000 rpm [86]. The resulting particle size decreased with increasing rotor speeds. For WPC-60 the average size was reduced from 59.7 µm to 13.3 – 17.8 µm and for the WPC-80 from 76.7 µm down to 45.1 – 46.6 µm. While solubility of the WPC-60 powder in water increased even a little bit from 88 % to about 90 % the solubility of the WPC-80 powder with the higher protein content decreased from 85 % to about 76 %. Additionally changes in the rheological properties of the milled powder were determined [87]. For pharmaceutical applications the size reduction potential is not high enough and the changes in protein integrity have to be further investigated. Furthermore, the needed amounts of powder are very large and not practicable for the small amount of expensive protein drugs.

Media pearl milling

In this process a liquid is used as a medium during milling. A rotating milling chamber is filled with small pearls with a diameter of 0.6 to 1.1 mm. The protein is suspended in the liquid and circulates from a reservoir to the milling chamber. In most cases the whole setup was combined with a cryostat for cooling.

Lizio et al. micronized cetrorelix acetate suspended in heptafluoropropane (HFA 227) [88]. The milling chamber and pearls were provided with abrasion resistant materials, such as

iridium-stabilized ZrO_2. During the process the system was cooled down to -44°C or -60°C. Resulting cetrorelix particles had an average diameter of 2.1 µm and were absolutely stable under the used conditions. Due to the modified materials no contaminants from the process were detected.

Irngartinger et al. performed also experiments with cetrorelix acetat with nearly the same setup [26]. The milling setup was cooled down to -70°C by using ethanol 96 % as coolant. Particles with a diameter of 1.58 µm were obtained and again no degradation products could be determined.

This process seems to be useful to directly produce suitable suspensions for pressurized metered dose inhalers. For other applications the use of a dispersion medium may be a disadvantage.

High pressure homogenization

High pressure homogenization is a well known method for the preparation of stable nanoemulsions [89] and nanosuspensions [90] or for the preparation of solid lipid nanoparticles [91]. A disperse system (emulsion or suspension) is forced through a small slit by applying high pressure up to 1500 bar. During the passage of the small slit the dynamic pressure increases while the static pressure decreases, which was described by Bernoulli. If the static pressure falls below the vapor pressure of the liquid it begins to boil. Behind the slit the static pressure suddenly increases and the small gas bubbles implode. This cavitation effect originates high forces which disrupt the emulsion droplets or solid particles.

Maschke et al. tested this process for the micronization of insulin suspended in miglyol®812 [92]. The insulin crystals were micronized at different pressures and the homogenization process was repeated up to 6 homogenization cycles. The average particle size was reduced from 15.8 µm to 3.7 µm after homogenizing 6 times at 1500 bar. By HPLS-MS no degradation products were visible and full bioactivity was determined in a chondrocyte proliferation assay.

The results for insulin are promising, but results for other more sensitive proteins have to be determined before the process can be finally evaluated.

Summary

For the production of small protein particles numerous methods and techniques were developed or modified. Achieving the desired particle sizes and size distributions does not seem to be the major problem, maintaining protein stability and bioactivity are the challenges. Adding excipients for the stabilization of sensitive proteins is the commonly used and good working solution at the moment. Each process has its own advantages and disadvantages and no method can really outrun the others. The use of organic solvents is always critical and has to be carefully evaluated to prevent contamination of the final product. Cost and time consumption are important factors which have an impact on the development, too. It also depends on the form in which your purchased protein is available. If it is a solution the on-step methods may be favored and if it is already available as a powder it would be a good idea to avoid the critical dissolving step and process the powder directly.

At the moment for each protein and each application it is more or less a trial and error process to find the optimal method.

Jet milling – theoretical background

Jet milling is a well established micronization method and the process has been investigated since the 1950s and is besides hammer mills and ball mills the most often used technique for ultrafine grinding (<10 µm) [93]. So the principles of size reduction are well known for this method and it is applied to many different substances ranging from technical powders, like laser printer toner [94], to pharmaceutical drugs for pulmonary applications [95]. The often mentioned advantages are achievable particle sizes below 10 µm, very low risk of product contamination e.g. by attrition or lubricants and grinding of heat sensitive materials due to the cooling effect of the expanding gas stream. Nevertheless, only few results exist for the micronization of proteins.

To understand the size reduction processes and identify important parameters, which may have an impact on the micronized product concerning particle size and stability, knowledge about the theoretical background is indispensable [96].

Assembly of a jet mill

A jet mill consists of a cylindrical milling chamber with 4 to 8 nozzles implemented into its wall (fig. 1.2). The nozzles are symmetrically aligned with an angle between 52°-60° [97] so that a circular gas stream with high rotational speed results within the chamber, when pressure is applied. Additionally a feed injection nozzle is installed. Due to the existing negative relative pressure above the venturi nozzle the added powder is continuously introduced into the milling chamber with the gas stream. Inter-particle collisions and impact on the wall of the milling chamber are the size reduction mechanisms. The ground particles are carried out of the milling chamber with the gas stream and are collected in a cyclone separator. It is a main difference to other grinding methods that jet mills contain no moving parts, which reduces the risk of product contamination by attrition or by lubricants.
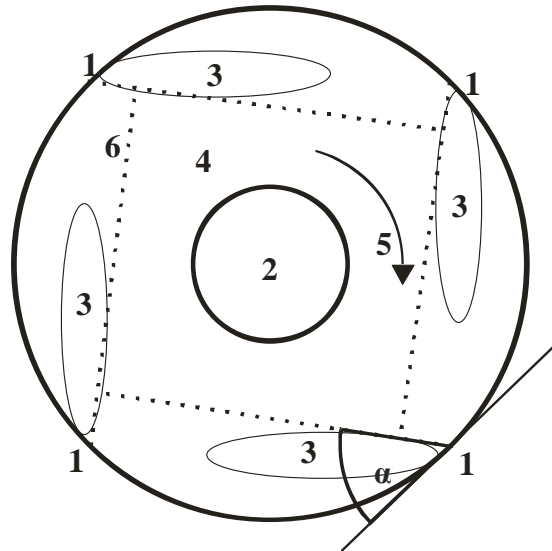
Fig.1.2: Milling chamber of a jet mill: (1) Nozzle, (2) gas outlet, (3) grinding zone, (4) separation zone, (5) circular gas stream, (6) jet of gas out of nozzles (dotted line)

Particles in a gas stream

The principle of micronization by jet milling is the collision of particles within a fast gas jet. The processes responsible for size reduction and separation within the milling chamber were investigated intensively in the 1960s by Rumpf and Kuerten [98,99]. By using triboluminescent substances like sucrose it was possible to have a closer look on the size reduction mechanisms. Triboluminescent substances emit light during size reduction due to the formation of an electrical field between the breakage surfaces. The light emission pattern during the milling process was analyzed by using a transparent milling chamber. Figure 1.2 illustrates the different detected areas in a milling chamber during the milling process.

Size reduction mainly takes place at the backside of the gas streams coming out of the nozzles. Due to the circular motion of gas within the milling chamber, these jets are deformed (fig. 1.3) and within the resulting vortices at the backside, the probability of collisions of particles with different relative velocities dramatically increases.
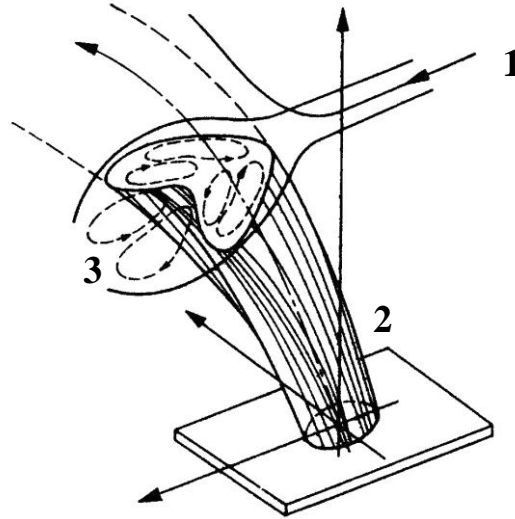
Fig. 1.3: jet of gas in a cross flow (adapted from Abramovich [100]) (1) cross flow, (2) gas jet out of nozzle, (3) vortical gas streams

For size reduction special prerequisites for collisions have to be fulfilled and the relative velocities of the colliding particles have to be large enough. Collisions are possible if the average free path length (averaged distance between two single particles) between the particles is smaller than their flight path length (distance the particle will fly starting with a specific velocity taking air resistance into account). If you start from the assumption that the velocity of the particles is spatial equally distributed within the chamber, the average free path length can be calculated by equation 1.1:

$$\bar{\lambda} \approx \frac{x}{10*(1-q)} \tag{1.1}$$

$[\bar{\lambda}] = m$ average free path length
$[x] = m$ particle diameter
q particle free volume portion on chamber volume

Flight path length of particles is described by equation 1.2 [101]:

$$s_0 = \frac{x^2*\rho_s*v_0}{18*\eta} \tag{1.2}$$

$[s_0] = m$ flight path length
$[x] = m$ particle diameter
$[\rho_s] = kg * m^{-3}$ density of solid

$[v_0] = m * s^{-1}$ particle velocity at time zero

$[\eta] = Pa * s$ dynamic viscosity of milling gas

Fig. 1.4 shows average free path lengths and flight path length depending on particle size at different typical velocities and loading of the milling chamber for jet milling.
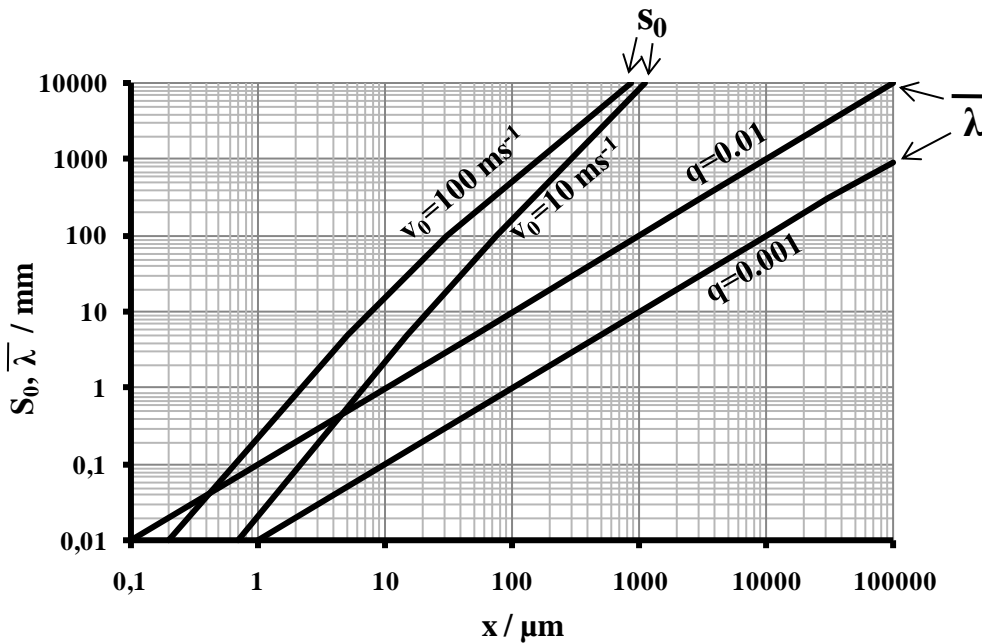

Fig. 1.4: maximal flight path length (S_0) and average free path length $\overline{\lambda}$) depending on the size x of spherical particles (ρ=1 g/cm^3) in air (20°C) [102]

It becomes obvious that there is a natural grinding limit by using jet milling. If the flight path length gets shorter than the average free path length, no collisions will take place or the velocities are much too low to initiate particle breakage. For typical conditions in a jet mill the grinding limit is at about 0.1 to 1 µm, depending on the applied pressure, type of milling gas and used substance. The grinding process is influenced by the frequency of collisions and the intensity of these collisions. Therefore, the results depend on the concentration of solid in the milling chamber and on the impact velocity. Hence, the feed rate is an important parameter to facilitate a successful milling process. It has to be high enough to allow inter-particle collisions, but if it is too high, on the one side the acceleration before impact is too short and on the other side the gas stream is slowed down and the milling process is not efficient.

In the center of the circular milling chamber you find the separation area (fig. 1.2 (4)). Particles are affected by the gas flow, which leaves the chamber, and by occurring centrifugal forces. The gas stream leads the particles to the center of the milling chamber to the outlet

opening, while the centrifugal forces resulting from the circular motion push the particles to the periphery. Theoretically a particle size limit can be calculated where 50 % of particles leave the milling chamber, while the other 50 % stay within the milling chamber for further micronization. Assuming laminar flow around the particles the drag force can be expressed by the equation of Stokes [103]. This leads to the following equation (3) for this size limit [104]:

$$x_{lim} = \sqrt{\frac{18*\eta*v_r*r_i}{(\rho_s-\rho_g)*u_i^2}} \qquad\qquad (1.3)$$

$[x_{lim}] = m$ particle size limit
$[\eta] = Pa*s$ dynamic viscosity of milling gas
$[v_r] = m*s^{-1}$ radial velocity
$[r_i] = m$ radius
$[\rho_s] = kg*m^{-3}$ density of solid
$[\rho_g] = kg*m^{-3}$ density of milling gas
$[u_i] = m*s^{-1}$ circumferential speed at a circle of radius r_i

Based on this process small particles below the limit are removed out of the milling chamber, while large ones are hold back for further grinding. Therefore, jet milling results in narrow particle size distributions as milling and size fractioning are combined in one process. This separation mechanism however, is influenced by the angle of the nozzles in the milling chamber; the particle size limit is lowered with higher circumferential speed and with lower radial velocity at the outlet. A compromise has to be found between large angles, which allow good acceleration of the particles, and low angles, which are necessary for a good separation step [96]. Angles between 52° and 60° were found to be optimal for jet mill grinding [97].

Particle breakage

As mentioned before, the prerequisites for particle collisions must be fulfilled to facilitate size reduction, but not every collision results in breakage of the two particles. Conditions for and processes during particle breakage will be described in the following part.

The powder particles are accelerated by the gas stream. When collisions with other particles take place, elastic deformations are the consequence. Thus tension areas are induced, which concentrate on small cracks or flaws within the particle. If the tension exceeds a critical value crack extension occurs. It was demonstrated that treating particles with blasts before

micronization enhances the milling result by inducing microcracks [105], proving the importance of these flaws for particle breakage.

Two prerequisites have to be fulfilled that particle breakage takes place: the differential and the integral breakage condition [106]. To start the fracture the crack extension force must exceed the surface energy of the created surfaces (differential breakage condition). The crack is only able to propagate through the whole particle if the complete needed energy is stored within the tension field (integral breakage condition), because the crack propagation is so fast that no further energy can be supplied from the surrounding.

In practice however, the needed fracture energy is orders of magnitude larger than the surface energy of the just created surface areas. Most of the applied energy is consumed by structural changes, kinetic energy of the formed fragments, emission of light (triboluminescence) and heat consumption. Especially during crack propagation high temperatures may occur at the new created surfaces. For ground glass up to 3200 K were measured at the breakage area [107]. After the propagation of the crack however, the surfaces cool down very rapidly within less than 10^{-6} seconds [108]

Grinding limit

As described before, one limiting factor for particle size reduction by jet milling is dependent on average free path length and flight path length, which determines the likelihood of collisions. Another limiting factor is the particle size itself. The smaller the particles the smaller is the probability of cracks and flaws, which are essential prerequisites for particle breakage. Therefore, it can be observed, that the particle strength increases while the particle size decreases, which can be explained by more and more perfect crystal structures. The particle strength is defined as the ratio of the force acting on the particle at the breakage point divided by a nominal particle cross-section [109]. For example, the particle strength of a 10 µm quartz particle is 350 MPa. This value raises up to 800 MPa for a 5 µm particle. Another reason for this size depending effect is that the particles have to be big enough to store the elastic energy needed for the particle breakage. The critical size is described by equation (1.4) [108]:

$$l \geq \frac{\beta}{W_{bV}} = \frac{2 * e * \beta}{\sigma_b^2} \qquad\qquad (1.4)$$

$[\beta] = J * m^{-2}$ surface energy
$[l] = m$ particle size

$[W_{bV}] = J\,m^{-3}$ breakage energy related to the volume
$[e] = J\,m^{-3}$ Young´s modulus
$[\sigma_b] = J\,m^{-3}$ breakage tension

For most particles this limit is below one micrometer, but often instant reagglomeration takes place increasing the measured particle sizes [106].

Predicting particle sizes after the milling process

Three factors determine the milling behavior of a substance: the mechanical properties of the material, the initial particle size distribution of the powder and the chosen milling conditions [110]. However, the mechanical properties of the material and depending on that the specific energy consumption for breakage are hard to determine. They depend on a lot of factors like Young´s modulus, hardness, number of cracks and flaws. Therefore, the energy consumption can hardly be estimated and no exact efficiency factor is available for jet mill grinding. It is estimated that only 0.05 to 2 % of the energy supplied by the milling gas are used for the size reduction process [111]. At the moment there are still no methods, which allow a good prediction of milling behavior of particles based on material properties and milling technique. For that reason a lot of effort has to be put in the optimization of milling processes of new or unknown powders.

Different approaches were undertaken to formulate a "law of comminution". The three most known ones are the hypotheses of Rittinger (1867) (eq. 1.5), Kick (1855) (eq. 1.6) and Bond (1951) (eq. 1.7) [112,113].

$$W_{Rittinger} = c_R * \left[\frac{1}{d_p} - \frac{1}{d_f}\right] \tag{1.5}$$

$$W_{Kick} = c_K * \log\left(\frac{d_f}{d_p}\right) \tag{1.6}$$

$$W_{Bond} = c_B * \left(\sqrt{\frac{1}{d_p}} - \sqrt{\frac{1}{d_f}}\right) \tag{1.7}$$

$[W_x] = J * kg^{-1}$ specific grinding energy
$[c_x]$ constant of the material concerned, work indices
$[d_f] = m$ size of feed
$[d_p] = m$ size of product

These "laws of comminution" are useful tools for the extrapolation of milling results, but their scope is limited and the best-fitting equation has to be chosen for each single experimental setup. The material constants have to be determined experimentally, which means a lot of effort. A large list exists for the Bond work indices, which is the reason why it is the most popular one of these three hypotheses [114]. Nevertheless, no exact estimations of the grinding energy are available until now, which is certainly attributed to the fact that energy loss occurs throughout all milling processes, what is not taken into account for these estimations.

Due to this gap, a field of research formed to solve this problem starting from a theoretical statistical approach. Nearly all of them are based on two different processes. First, the "selection function" that describes the fraction of particles destroyed in an experiment. Second, the "breakage function" describing the size distribution of the fragments after breakage, not considering the undestroyed particles [115]. Again the main problem is to find easy ways of obtaining all necessary particle properties like size of initial flaws, hardness or surface energy.

Several groups are working in this field [110,115–119]. The results are quite promising, but the transfer to practical applications in pharmaceutical industry will take a longer time. Therefore, still experimental optimization has to be performed for every new substance or machine. A possibility to reduce time and costs for these experiments may be the utilization of statistical experimental design, which is used for process optimization in many other fields.

Goals of the thesis

To meet the demand of the pharmaceutical industry to process and deliver proteins in solid state it is necessary to establish methods, which allow a customized particle design. As abovementioned jet milling is one of the most effective micronization methods, but its potential for the micronization of proteins has not yet been tested to the full extend. Therefore, the aim of this thesis was to provide more information about the jet milling of proteins. For this investigation three important points have to be considered:

1. Which particle size distributions can be obtained by jet milling and is there a difference between different proteins?

2. Which are the important process parameters and how can the process be optimized to improve the size reduction and size distribution?

3. Are there any negative effects on stability or activity of the investigated proteins due to the milling process?

To address these questions, first of all the setup of the jet mill had to be optimized. One big problem was to deal with the air humidity in standard lab environment. It is well known that it leads to agglomeration of micronized particles (e.g. powdered sugar) and also may influence the activity and stability of processed proteins [120]. Additionally a cryogenic grinding setup as an additional investigated parameter had to be developed and evaluated, which also reinforces the need for the exclusion of humidity. These customization steps are described in **chapter 3**.

As mentioned before, many pharmaceutical applications demand protein particle sizes below 10 μm. For many of the low molecular weight drugs this is performed by jet milling, but for protein drugs only very few investigations exist. Are there detectable differences between different proteins? Are crystalline or amorphous proteins micronized differently? These questions were investigated by using three model proteins with known properties and different characteristics: bovine insulin, hen egg white lysozyme and bovine serum albumin. Their size distributions were analyzed after milling by laser light diffraction analysis and were verified by scanning electron microscopy of the resulting protein powder. The effect of milling pressure, number of milling cycles and of the milling gas temperature on the resulting particle size was analyzed by using statistical experimental design (**chapter 4**).

Nevertheless, particle size is only one important parameter. For proteins the conservation of chemical and structural stability and of their bioactivity is even more important. Therefore, the proteins were analyzed for changes after the milling process by HPLC, MALDI ToF, CD- and fluorescence spectroscopy. Lysozyme and insulin were chosen as model proteins, because for both well established bioactivity assays are available. The bioactivity of insulin was tested in cell culture experiments, where the dose dependent effect of insulin on the proliferation and quality of the extracellular matrix of chondrocytes was utilized (**chapter 5**). The enzymatic activity of lysozyme was tested by using the well established micrococcus assay (**chapter 6**). For BSA, chosen because of its wide spread use and higher molecular weight, it occurred that changes in its solubility in water were the most prominent altered property due to the jet milling process and the main hurdle for further investigations (**chapter 7**). If it was possible, the effects of the micronization process on the investigated parameters of the proteins would be analyzed by using the statistical experimental design to identify the impact of the single milling parameters.

Inspired by different methods for the preparation of lipid microparticles, like solvent evaporation and spray congealing methods and difficulties to obtain small and homogeneous distributed particles, the suitability of jet milling for this task was tested. Additionally the easy measurable heat effects on lipid powders were utilized to get a closer look on the impact of jet milling on heat sensitive substances. Glycerol tripalmitate (Dynasan 116[®]) was jet milled at different conditions and afterwards characterized by laser light diffraction, scanning electron microscopy and DSC measurements (**chapter 8**).

Chapter 2

Materials

and

Methods

Materials

Bovine insulin crystals were a gift from Sanofi-Aventis (Frankfurt, Germany), chicken egg white lysozyme lyophilized powder, albumin from bovine serum (BSA), albumin from bovine serum essentially fatty acid free, l-glutathione oxidized and l-glutathione reduced were purchased from Sigma Aldrich (Taufkirchen, Germany). We acquired the HPLC-grade acetonitrile from Baxter (Deventer, The Netherlands), trifluoroacetic acid (TFA) from Riedel-De-Haen (Sigma Aldrich, Taufkirchen, Germany) and isobutanol from Merck-Schuchardt (Hohenbrunn, Germany). Water was double-distilled and filtered through a cellulose nitrate filter (pore size 0.2 µm, from Sartorius, Göttingen, Germany) prior to use. Glycerol tripalmitate (Dynasan116®) was purchased from Sasol AG (Witten, Germany). Thrombin was provided by Baxter (Unterschleißheim, Germany) and bovine fibrinogen, lyophilized micrococcus lysodeikticus cells ATCC No. 4698, calcium chloride, potassiumphosphat buffer, 8-anilino-1-naphtalenesolfonic acid ammonium salt (ANS), Ellman´s reagent 5,5´-dithiobis(2-nitrobenzoic acid) (DTNB) and dieethylenetriamine-pentacetic acid (Detapac) were purchased from Sigma-Aldrich (Taufkirchen, Germany). Knee joints from 3-month-old bovine calves were obtained from a local abattoir within 12–18 h of slaughter. Type II collagenase and papainase were purchased from Worthington (CellSystem, St. Katharinen, Germany). Dulbecco's Modified Eagle's Medium (DMEM) with 4.5 g/l glucose, fetal bovine serum (FBS), MEM non-essential amino acid solution, penicillin, streptomycin, HEPES buffer, and phosphate buffer solution (PBS) were obtained from Gibco (Karlsruhe, Germany). 149 µm pore size polypropylene filters were purchased from Spectrum (Rancho Dominguez, CA, USA). Hoechst 33258 dye was obtained from Polysciences (Warrington, PA, USA). All cell culture plastics were purchased from Corning Costar (Bodenheim, Germany).

Methods

Storage of sugar at 75 % rel. humidity

In order to store micronized sugar exactly at 75 % rel. humidity a saturated sodium chloride solution was prepared in a chromatography chamber. The humidity was allowed to equilibrate for one day. The open vial with the micronized sugar was inserted in the chamber and stored for one day. Afterwards the sugar was dried under vacuum and SEM pictures were taken.

Micronization of proteins by jet milling

For micronization a modified MC One® jet mill (Jetpharma, Balerna, Switzerland) was used. The mill was equipped with a custom made cryogenic cooling device and a temperature measurement unit (N9001 thermometer with air temperature sensor, Comark Limited, Stevanage, UK). For cryogenic grinding the milling gas was piped through a coiled tube inserted into a dewar vessel filled with liquid nitrogen. Therefore, it was possible to cool the milling gas down to approximately -60°C. Temperature of milling gas was measured within the gas stream shortly behind the milling chamber. To exclude effects of air humidity [121], the complete experimental setup was integrated in an isolator filled with dry nitrogen atmosphere (RH <2 %; hygrometer testo 608-H2, Testo, Lenzkirch, Germany). Nitrogen with a purity of 99.999 % was used as the milling gas. For each experiment 500 mg of protein was micronized. The milling pressure ranged from 6 to 14 bar (the feeding pressure was kept 1 bar above to prevent blow back of the powder). The feeding rate was kept constant at a rate of 120 mg/min for all experiments to allow milling at all used milling pressures without accommodating the feed rate.

Micronization of glycerol tripalmitate

Before micronization glycerol tripalmitate was carefully ground by using an agate mortar and was sieved through a 1000 μm mesh to obtain particles which were able to pass the feed opening of the jet mill. 600 mg of were fed to the mill (120 mg/min) and ground at different milling pressures.

Experimental design

A full factorial face centered central composite design (CCF) was performed to investigate the effect of three different process parameters on resulting particle size. The effects of milling pressure, number of milling cycles and temperature of the milling gas were analyzed. Milling pressure and number of milling cycles were investigated on three levels. Milling gas temperature was defined as an uncontrolled factor to take fluctuations during different cycles into account. Table I provides a survey of the varied parameters and conditions. Overall, 22 individual experiments were performed for each protein (table 2.1); the first half at room temperature, the second part of experiments at about -60°C. Coefficients based on quadratic polynomial equation (2.1) were estimated by using Partial least Squares (PLS) fitting.

$$y=b_0+b_1x_1+b_2x_2+b_3x_3+b_4x_1^2+b_5x_2^2+b_6x_3^2+b_7x_1x_2+b_8x_1x_3+b_9x_2x_3+\varepsilon \qquad (2.1)$$

Variable	Level -1	Center point	Level +1
x_1: milling pressure	6 bar	10 bar	14 bar
x_2: number of milling cycles	1	2	3
x_3: cooling device	on (approx. -60°C)		off (room temperature)

table 2.1 parameters of the experimental design

Where y represents the investigated response, b_0 the constant part of the term, b_1-b_3 the linear, b_4-b_6 the quadratic and b_7-b_9 the interaction coefficients and ε the error. The PC software MODDE 7.0.0.1 (Umetrics, Umea, Sweden) was used to both generate the experimental design and analyze the resulting data. The influences of the scaled and centered coefficients of equation (1) were investigated by using an F-Test at a confidence interval of 0.95. A coefficient was recognized as having an effect on the response (d90 value) if it was significantly different from zero. The insignificant terms were excluded from the model and the coefficients were recalculated.

Particle size determination

Protein particles

The protein particles were suspended in 18 ml degassed isobutanol (refractive index 1.39) and particle size distribution was measured using a Mastersizer 2000 (Malvern Instruments, Herrenberg, Germany) equipped with a Hydro 2000µP dispersion unit. Mie scattering theory was used to calculate particle sizes (insulin refractive index 1.54, absorption 0.1 [92], BSA and lysozyme refractive index 1.55, absorption 0.01 [122]). For disaggregation of agglomerates an integrated device was used to apply ultrasound (48 kHz, 20 W) for ten seconds before measurement. Each sample was measured for 20 seconds and 5 measurements were averaged. As characteristic values for particle size distribution the d90 and d50 (percentage of particles that are smaller than the given value) were analyzed as response parameters.

Glycerol tripalmitate microparticles

For lipid microparticles (refractive index 1.5, absorption 0) a Hydro S dispersion unit (Malvern Instruments, Herrenberg, Germany) was used. The particles were suspended in ethanol 68.2 % (V/V) (refractive index 1.361). The measurement was performed as described for the protein particles.

Changes in particle size during storage of BSA

To investigate if there is a change in particle size during the storage in the freezer, we measured the particle size of each sample of BSA directly after the micronization process and after four weeks of storage in the freezer at about -20°C under nitrogen atmosphere by using the described protocol for the size measurement by laser light diffraction.

Morphology of micronized particles

Pictures were taken by using a scanning electron microscope (JSM 840; Jeol, Japan) at 3kV. The particles were fixed on aluminum stups using conductive carbon tape (LeitTabs; Plannet GmbH, Germany) and coated with gold by sputtering three times for 20 seconds (SEM Autocoating unit E2500; Polaron equipment LTD, UK).

HPLC analysis of the model proteins

All proteins and peptides were analyzed for changes due to the micronization process by HPLC. A HPLC System with a degasser (Knauer, Berlin, Germany), LC-10AT pump, FCV-10AT$_{vp}$ gradient mixer, SIL-10Ad$_{vp}$ autosampler, CTO-6a oven, SPD-10AV UV-Detector, RF-551 fluorescence detector and SCL-10Avp controller (all from Shimadzu, Duisburg, Germany) and a C_{18}-reversed phase precolumn (LC318, 4.6x20 mm; Supelco, Bellefonte, USA) combined with an analytical C_{18}-reversed phase column (Supelcosil, LC318, 4.6x250 mm; Supelco) was used.

Insulin

Chemical stability of bovine insulin was determined by a previously described method [92]. One milligram of insulin was dissolved in 1 ml 0.01 M HCl. 50 μl of this solution were injected into the HPLC system at 37°C. During measurement, a linear gradient was applied (mobile phase A: 90 % H_2O, 10 % acetonitrile, 0.1 % TFA; mobile phase B: 90 % acetonitrile, 10 % H_2O and 0.1 % TFA; flow rate of 1 ml/min). The fraction of phase B was increased from 20 % to 36 % over 22 min (total run time 30 min). Signals were recorded using UV detection (210 nm and 274 nm).

Lysozyme

One milligram of lysozyme was dissolved in 1 ml bidistilled water. 50 μl were injected into the HPLC system at 40°C. The same mobile phases as for insulin were used, but phase B changed from 25 % to 40 % over 35 min (total run time 40 min). Signals were recorded using UV detection (210 nm and 274 nm).

BSA

Five milligrams of BSA were dissolved in 1 ml bidistilled water. 50 µl were injected into the HPLC system at 40°C. Mobile phase A consists of water and 0.1 % TFA, phase B of 90 % acetonitrile, 10 % water and 0.1 % TFA. The analytical run started with 3 min with 27 % of phase B. Afterwards the fraction of phase B was increased from 27 % to 54 % over 12 min. The concentration was kept at this concentration for additional 10 min. Signals were recorded using UV detection (210 nm and 274 nm).

GSH

2.5 milligrams of GSH were dissolved in 1 ml bidistilled water. 50 µl were injected into the HPLC system at 40°C. Mobile phase A consists of water and 0.1 % TFA, phase B of 90 % acetonitrile, 10 % water and 0.1 % TFA. The analytical run started with 100 % phase A for 3 min. Afterwards the fraction of phase B was increased to 20 % during 17 min and was kept at this concentration for 5 min. At the end phase B was reduced to 0 % in 1 min and the run was finished after total time of 30 min. Signals were recorded by UV absorption at 210 nm.

MALDI analysis of insulin and lysozyme

As matrix α-cyanohydroxy-cinnamic acid dissolved in 50 % acetonitrile and 0.1 % TFA was used. Protein was solved in 0.1 % TFA and diluted in the matrix to a concentration of 5 µM. Samples were analyzed with Maldi ToF/ToF (4700 Proteomics Analyzer; Applied biosystems, USA) in linear mode.

Determination of insulin-bioactivity

Bioactivity of three differently treated samples of micronized insulin were investigated using a three-dimensional chondrocyte cell culture system utilizing fibrin gels as a carrier as described elsewhere [123]. These groups are: insulin micronized three times at 6 bar at room temperature, insulin micronized three times at 14 bar at room temperature and insulin micronized three times with 14 bar with cool milling gas. Two groups one without insulin and one with untreated insulin were used as controls. For all groups three experiments were performed (n=3). The effect of the insulin samples on cell proliferation due to interaction with the IGF receptor was investigated. In brief, primary chondrocytes where isolated from the surface of the femoral patellar groove of a three-month-old bovine calve. The cartilage was enzymatically digested overnight in DMEM containing 4.5 g/l glucose, 10 % FBS, 584 mg/l glutamine, 0.1 mM MEM non-essential amino acids, 10 mM HEPES, 0.4 mM proline, 50 mg/ml ascorbic acid, 50 U/ml penicillin, 50 mg/ml streptomycin, and 470 U/ml of type II

collagenase. The digest was repipetted, filtered through a 149 µm mesh, and washed three times with PBS. The cell number was determined using a hemocytometer. $1x10^{-6}$ freshly isolated chondrocytes were resuspended in a fibrinogen solution (fibrinogen 50 mg/ml, $CaCl_2$ 20 mM at pH of 7.0). Gels were formed by adding the same volume of thrombin solution. Each resulting fibrin disc (diameter 5 mm, thickness 2 mm) was put in a six-well plate and covert with 4 ml culture media containing 0.5 or 2.5 µg/ml of each insulin (control without insulin). The constructs were cultivated for 5 weeks, changing culture media three times a week. Afterwards the cell-fibrin constructs were analyzed. The constructs were weighed (=wet weight) and cut in parts. One section of each construct was lyophilized, then digested with 1ml of a papainase solution (3.2 U/ml in buffer) for 18 h at 60°C and used for the determination of cell number. The cell number per construct was determined by measuring DNA content using Hoechst 33258 dye [124]. Another section of each construct was successively fixed with a mixture of glutaraldehyde and formaldehyde for histological analysis. The samples were embedded in paraffin and cross-sectioned into 5 µm sections. After deparaffinization sections were stained with safranin-O.

Determination of lysozyme-bioactivity

The activity of lysozyme was analyzed using a method described by Shugar [125]. Lysozyme was dissolved in 66 mM potassiumphosphat buffer at pH 6.24. 100 µl of this solution were mixed with 2.5 ml cell suspension of micrococcus lysodeicticus. The decrease in absorption at 450 nm wavelength due to lyses of the cells was measured in 12 second-intervals for 1 min (Uvikon; Kontron Instruments, UK). The kinetic rate, indicating the enzyme activity, was obtained from the slope of the linear part of the curve. Activity was calculated using a calibration curve measured with a solution of unprocessed lysozyme of the same batch. Additionally some samples were tested in the presence of 1 mM Detapac to complex possibly present iron.

Obtaining lysozyme crystals

In order to obtain lysozyme crystals a batch crystallization method described by Elkordy et al. [49] was used. 4 g of lysozyme were dissolved in 100 ml of 0.1M sodium acetat buffer pH 4.6. In another bottle 100 ml of a 10% sodium chloride solution were prepared. Both solutions were filtered using a sterile filter with pores of 0.2 µm. After mixing both solutions the mixture was stored for 24 h in the fridge at 4°C. Then the suspension was filtered by using

a 0.4 µm filter and the remainder was washed with isopropanol. Afterwards it was dried in the glovebox at a rel. humidity <2% for 24 h.

Determination of the water insoluble fraction of BSA

For the solubility determination of BSA approximately 10 mg of the micronized BSA samples were weighed into eppendorf cups of known weight. For the PEG BSA mixtures an amount corresponding to approximately 10 mg of pure BSA was weighed into the cups. Afterwards 2 ml of water were added. Every 20 min the cup was vortexed for 5 seconds. After one hour the mixture was centrifuged at 13 000 rpm for 10 min. The supernatant was removed and 1 ml water was added to the remainder. Every 10 min it was vortexed for 5 seconds. After 30 min it was centrifuged again. This step was repeated three times. Afterwards the remainder was freeze dried and the eppendorf cup was weighed again after this process. As control samples without BSA and with unprocessed BSA were used.

Finding a solvent for the insoluble BSA fraction

To perform further analysis of the insoluble fraction occurring after jet milling BSA a suitable solvent had to be found. 10 mg of the micronized BSA powder were mixed with 2 ml of a solvent or solvent mixture. Every 10 min it was homogenized on a vortex shaker for 10 s. After one hour the vessel was controlled for not dissolved particles.

List of tested solvents:

-water

-isopropanol

-ethanol 68 %

-acetonitril

-ethanol 68 %, acetonitril 1:1

-89 % water, 10 % acetonitril, 1 % TFA

-6 M urea

-6 M guanidine HCl

-0.1 % SDS

-10 mM dithioreythritol + 1 mM EDTA

-6 M urea + 10 mM dithioreythritol + 1 mM EDTA

-6 M guanidine HCl + 10 mM dithioreythritol + 1 mM EDTA

-0.1 % SDS + 10 mM dithioreythritol + 1 mM EDTA

Determiation of free sulfhydryl (SH) groups for BSA

The experiment was performed analog to the description of Aitken and Learmonth [126]. Unprocessed BSA was dissolved in 0.1 N phosphate buffer pH 8 at a concentration of 50 mg/ml. 3 ml of buffer were added into a cuvet. 100 µl of 10mM solution of Ellman´s reagent 5,5´-dithiobis(2-nitrobenzoic acid) (DTNB) were added. Finally 200 µl of the protein solution were added and the absorption of the anion (TNB^{2-}) was measured at 412 nm. The concentration of thiols was calculated from the molar absorbance of the TNB anion ($E_{412}TNB^{2-} = 1.415*10^4 \, cm^{-1}M^{-1}$).

Blocking the free sulfhydryl group of BSA

The free sulfhydryl group of bovine serum albumin was alkylated with iodoacetamide according to a modified literature procedure [127]. The pH of a BSA solution (15 mg/ml) was raised to 8 with 0.1 N NaOH. The reaction vessel was covered with aluminum foil and then approximately 2 mol of iodoacetamide per mol of sulfhydryl were added. The mixture was allowed to react for one hour at room temperature, while stirred with a magnetic stirring bar. Afterwards the mixture was centrifuged in a Vivaspin 20® vessel with a cutoff filter of 30 000 Da at 4°C. The remainder was washed with water three times. A control group without the addition of iodoacetamide was analyzed, too, to evaluate the effect of the process on the protein.

Co-lyophilization of BSA with PEG

1 g of different ratios of PEG 10 000 and BSA were dissolved in 10 ml of bidistilled water. The solutions were frozen at -25°C within a benchtop freeze-dryer (Beta 2-16 with LMC-2 system control, Christ, Osterode, Germany). Afterwards the frozen samples were freeze dried at 6°C and 0.12 mbar for 24 hours. For complete drying the temperature was increased to 20°C for additional 6 hours. The vacuum was removed by filling the chamber with dry nitrogen. The samples were stored at -20°C for further analysis.

Investigating changes in the secondary structure of insulin and lysozyme by CD spectroscopy

To investigate changes in secondary structure of the proteins due to the micronization process circular dichroism spectroscopy (spectropolarimeter J-710, Jasco, Gross-Umstadt, Germany) was used. CD spectra of protein solutions (15 µM in 66mM phosphate buffer pH 6.24) were recorded 190 nm to 260 nm at a scanspeed of 20 nm/min and temperature of 22°C in a quartz

cuvette with 0.1 cm path length. Five measurements were accumulated to reduce noise. Afterwards the secondary structure composition was estimated by using the CDNN algorithm [128] (CD spectra deconvolution software CDNN 2.1).

Measurement of intrinsic fluorescence

Lysozyme and BSA (0.1 mM) were dissolved in 10 mM phosphate buffer at pH 6.2. Measurements were performed using a LS55 fluorescence spectrometer (PerkinElmer, Waltham, USA) at 295 nm (excitation wavelength, slit = 5 nm), $300 - 500$ nm (emission wavelength, slit = 5 nm) and scanspeed of 10 nm/s. For insulin measurements a stock solution in 0.01 M hydrochloric acid was prepared, which was diluted with phosphate buffer to concentration of 0.1 mM. The excitation wavelength for insulin was 280 nm because it does not contain any tryptophan. Fluorescence emission spectra were measured in the range from 290 to 450 nm. Four measurements were accumulated and the background measured with pure buffer was subtracted.

For BSA a stock solution was prepared and the insoluble fraction was removed by centrifugation. Afterwards the concentration of BSA was determined by UV measurements at 280 nm using solutions with known concentration as reference.

Measurement of surface hydrophobicity

A method described by Lechevalier et al. was used to determine the surface hydrophobicity of proteins [129]. ANS is a probe multiplying its fluorescence intensity when it is in a hydrophobic environment and is therefore often utilized to investigate surface properties of macromolecules in solution. Each sample was dissolved in phosphate buffer (10 mM, pH 7) at 6 different concentrations in the range of $0.005 - 0.05\%$. Insulin was dissolved in 0.01 M hydrochloric acid before dilution in phosphate buffer. 15 µl of an 8 mM ANS solution were added to 1 ml protein solution. The maximal fluorescence intensity of ANS was measured for 5 s at 470 nm emission wavelength (excitation at 390 nm). Excitation and emission slits were 10 nm and a cutoff filter of 430 nm was used. The fluorescence intensity was plotted against the protein concentration and the slope was calculated by linear regression analysis as an index of protein surface hydrophobicity (PSH). The relative surface hydrophobicity (RSH) was calculated as follows:

$$RSH = (PSH \text{ of sample})/(PSH \text{ of control})$$

Determination of iron content by inductively coupled plasma – optical emission spectroscopy (ICP-OES)

ICP measurements were performed to investigate, whether there was an increase of iron content within the protein powder due to the micronization process. For these measurements a JY40+ from Jobin Yvon (Unterhaching, Germany) with argon as plasma gas (16 l/min) and as carrier gas (2 l/min) was used. A specific amount of lysozyme was dissolved in 10 ml water. Calibration of the instrument was performed by using iron(III)chloride standards of 1, 10 and 100 ppm.

FT-IR measurements

For FT-IR measurements a Tensor 27 spectrometer (Bruker, Ettlingen, Germany) with a single reflection ATR unit (Harrik MVP, Harrik Scientific, New York, USA) was used. For measurement the not micronized samples were ground in an agate mortar while the micronized ones were used without further processing. The samples were measured from $4000 - 600 \, cm^{-1}$ wave number. For each sample 100 interferograms were collected and averaged using a resolution of $4 \, cm^{-1}$. Second-derivative spectra were created using the OPUS 4 software (Bruker, Ettlingen, Germany). Afterwards the data was transferred to GRAMS 8.0 software (Thermo Fisher Scientific Inc.). With GRAMS, each spectrum was attenuated to the amide I region ($1700 - 1610 \, cm^{-1}$), baseline corrected and normalized to an area of unity [130]. The area under each band was correlated to different protein secondary structures as described by Krimm et al. [131]

Differential scanning calorimetric (DSC) measurements of micronized lipid

Micronized lipid microparticles were analyzed for structural changes by differential scanning calorimetry (DSC 2920, TA Instruments, Alzenau, Germany). 2 to 4 mg of each sample were weighed into AutoDSC aluminium sample pans (TA Instruments, Alzenau, Germany) and sealed with the TA Instuments encapsulating press. An empty sealed pan served as reference. The samples were equilibrated for 10 min at -20°C and the measurement was performed applying a heating rate of 5 K/min up to 100°C.

Statistics

Data were analyzed by applying ANOVA and then Tukey´s test. All measurements were performed in triplicate. The design of experiment data was analyzed by using MODDE 7.0.0.1 Software (Umetrics, Umea, Sweden).

Chapter 3

Customizing

the

Jet Mill

Introduction

As mentioned before, jet milling is a well established and common micronization method, but it is normally utilized for processing big amounts of powder, starting from several grams up to kilograms of substance. However, most therapeutic proteins are very potent drugs and on the other side often are a very expensive class of substances. Both factors are causing the fact that for the processing of solid proteins only small amounts are available for process tests. Therefore, a special milling setup had to be found to allow sensible processing of proteins.

Basic setup of the jet mill

Taking the typically low available amounts of proteins and high costs into account, it was aimed to work with as little protein as possible for the milling experiments. Therefore, a small, laboratory scale jet mill was purchased: MC One®, Jetpharma. The details of the mill are described in table 3.1 and the setup is schematically shown in fig. 3.1.

diameter of milling chamber	3.34 cm
number of nozzles	4
diameter of nozzles	1 mm
nozzle angle	55°
material	AISI stainless steel 316L
metal contamination of product	< 1 ppm
milling pressure	6 – 12 bar
max. volume flow	10.8 Nm^2/h
process gas temperature	0°C – 50°C
batch size	0.2 – 100 g

Tab. 1.1: Specifications of MC One® by Jetpharma
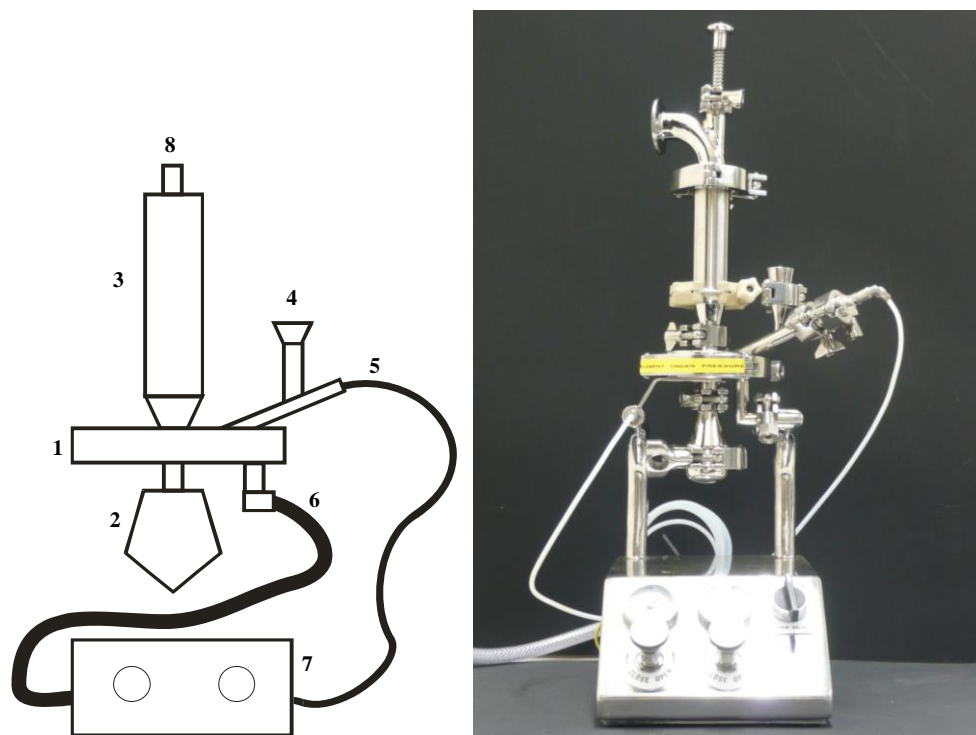
Fig. 3.1: schematic diagram of the used jet mill: (1) milling chamber, (2) product collection container with cyclone separator, (3) exhaust gas filtration unit, (4) product feed by venturi injector, (5) gas feed for venturi injector, (6) gas feed for milling chamber, (7) control device for applied pressure on milling chamber and venturi.

It is a so-called "pancake" mill regarding the flat circular milling chamber. The whole mill is made off stainless steel and completely decomposable for easy cleaning. The connections between the different parts are sealed by Teflon (PTFE) gaskets. Jetpharma specifies that small batch grinding down to 200 milligrams of powder is possible with good yield. Although, this setup seemed to be very good, some modifications had to be installed in order to optimize the setup for protein grinding. In chapter 1 the negative effect of grinding on some proteins is described and therefore, some additional parameters should be tested for their stabilizing effect on the investigated proteins.

In consideration of the sensitive product it can be assumed that the high temperatures created on the particle surfaces by impact breakage [107] may have a negative effect on product stability and activity. Therefore, the effect of cryogenic grinding on proteins should be investigated. Cryogenic grinding is seldom used in pharmaceutical industry because of its high costs [132]. The main applications for cryogenic grinding are the milling of heat sensitive substances like plants for food industry [133], grinding of herbs for medicinal usage [134] or the milling of elastic, rubber-like substances [135] or recycling of rubber tires [136]. At low temperatures the brittleness of many elastic or ductile materials is dramatically increased thus the mechanical size reduction process is improved [137]. The major

disadvantages as mentioned before are the much higher costs due to the special equipment and the consumption of liquid nitrogen [138]. However, for proteins both mentioned advantages may be possible, so that the higher costs may be outweighed by a better grinding performance and more stable products.

Cryogenic setup

In order to facilitate cryogenic grinding by jet milling the temperature within the milling chamber had to be cooled down below -50°C e.g. by liquid nitrogen. The lower temperature limit of the integrated valves of the MC One® is 0°C (tab. 1.1). Therefore, the cooling had to take place by bypassing the valves to assure safe work with the jet mill. For the remaining parts the low temperatures were not expected to be a problem, because they are made of steel and Teflon.

The first idea was adding liquid nitrogen parallel to the product feed into the milling chamber (fig. 3.2). A tank containing liquid nitrogen was installed right next to the opening for the powder feed. Powder and liquid nitrogen were blown into the milling chamber by the venturi nozzle.
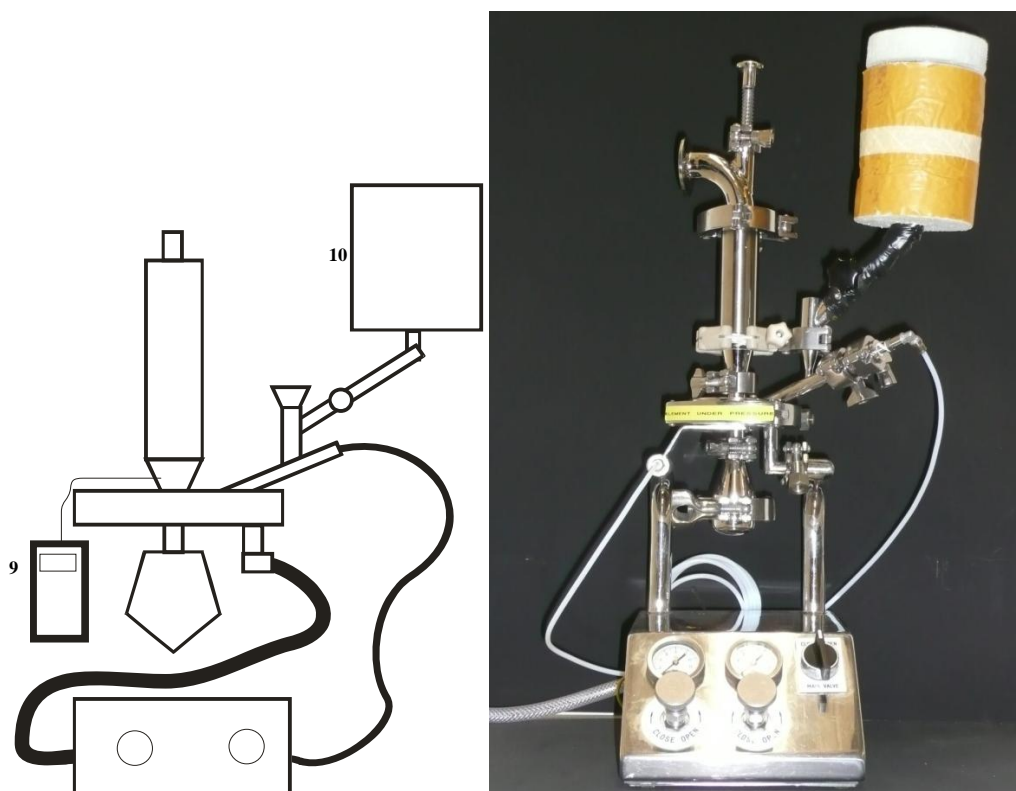
Fig. 3.2: First cryogenic setup; (9) temperature sensor, (10) liquid nitrogen tank

Measuring the milling gas temperature just behind the milling chamber (fig. 3.2(9)) results in a temperature of -20 to -30°C. Lower temperatures could not be obtained. A problem occurred

due to the fact that liquid nitrogen entered the milling chamber and evaporated there by disturbing the normal gas flow. For this reason results from this setup were not comparable with the experiments at room temperature, because possible differences may have been provoked by the temperature difference or by uncontrollable turbulences in the gas flow.

To overcome these problems no liquid nitrogen was added into the mill, but the gas pipes for the milling chamber and the venturi injector were modified. The pipes were elongated and each fitted into liquid nitrogen-containing tanks (fig. 3.3).
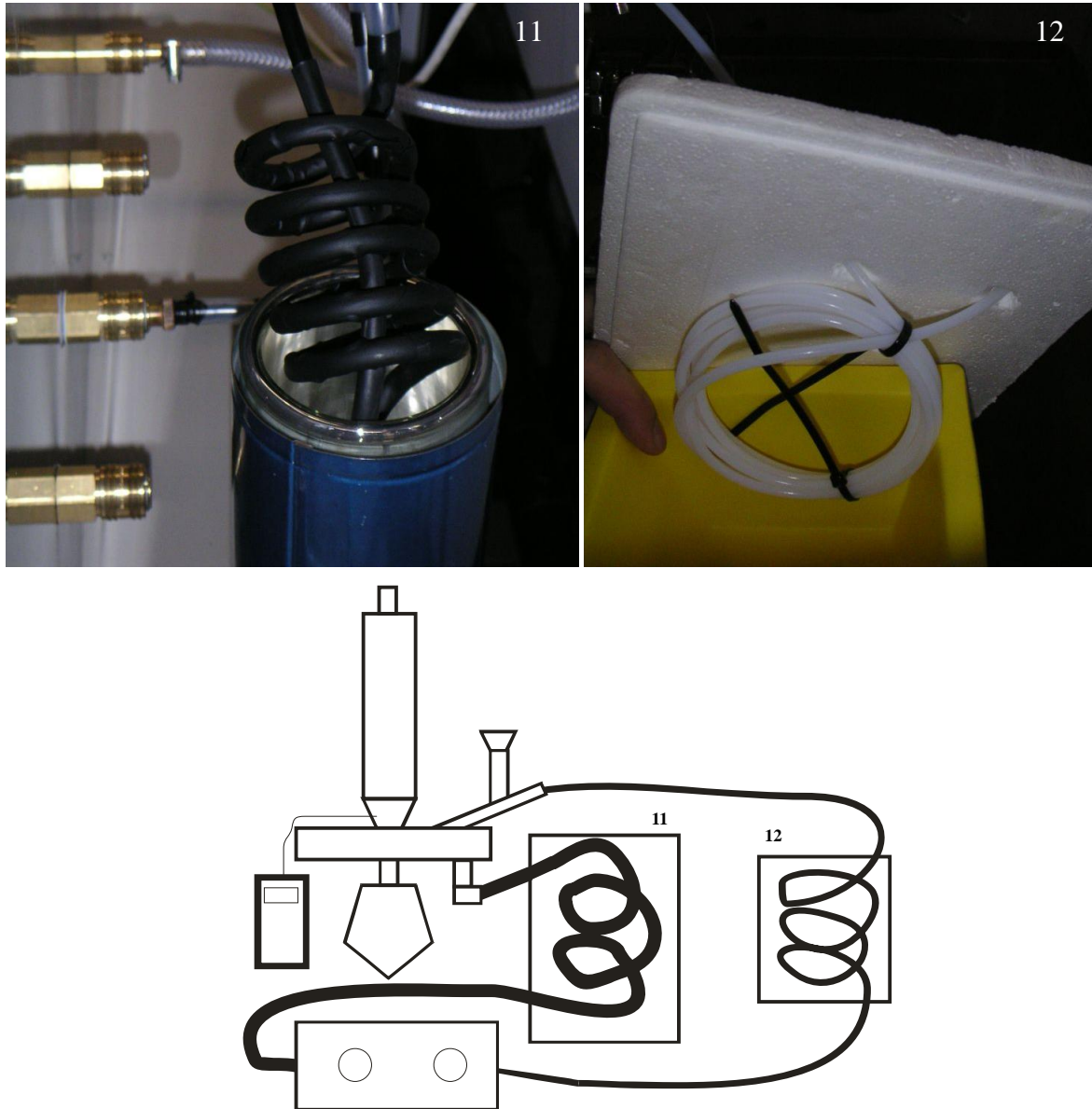
Fig. 3.3: second cryogenic setup. (11) Gas feed for milling chamber within liquid nitrogen tank, (12) gas feed for venturi injector within liquid nitrogen tank

Testing the new setup at different milling pressures resulted in temperatures of about -60°C (fig. 3.4). Small temperature differences at the different pressures are due to the cooling effect of the expanding gas in the milling chamber, which is higher at higher pressures.
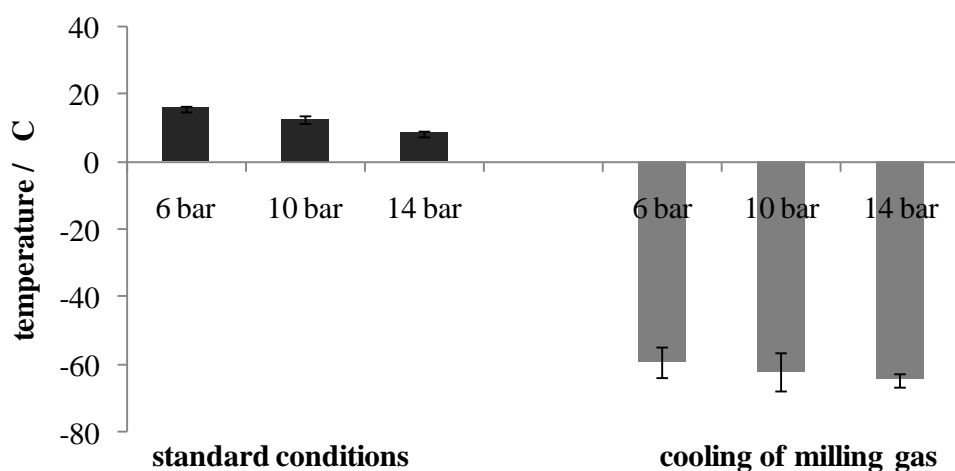
Fig. 3.4: milling gas temperatures at standard conditions compared to temperatures with use of the cryogenic setup at different milling pressures

The next step was to exclude air humidity from the whole process to avoid negative effects on particle size due to agglomeration and on stability and activity of the micronized protein powder [120].

Excluding air humidity

During this test phase the need for humidity exclusion got very prominent. Due to the cold temperatures humidity condensed not only on the cold machine parts but also on the micronized product. To investigate the effect of humidity on the resulting powder 500 mg of sugar as a cheap test substance was micronized. In order to exclude humidity from the product two options were tested. First, 10 ml of isobutanol were filled in the product collection container (fig. 3.1(2)), so that the product is directly collected in the particle size measurement media without any contact with the surrounding air. The second option was to integrate the whole jet mill setup in a glovebox filled with a dry nitrogen atmosphere (fig. 3.5). A hygrometer was installed within the glovebox to check the air humidity permanently. All experiments within the glovebox were performed at rel. humidity lower than 2 %. After micronization the samples were stored in a desiccator for one day.
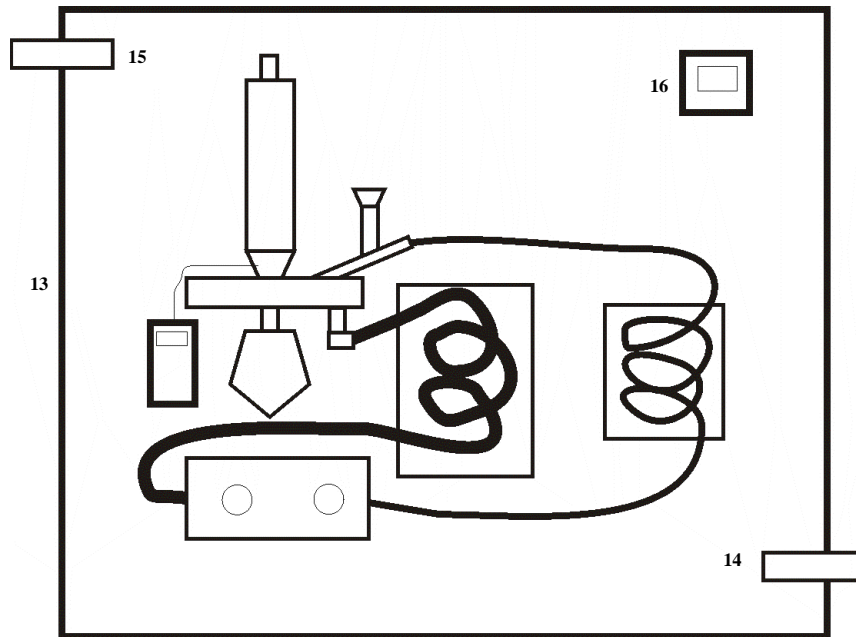
Fig. 3.5: Cryogenic setup integrated into nitrogen filled glovebox. (13) glovebox, (14) nitrogen inlet, (15) nitrogen outlet, (16) hygrometer

The product yield of the micronized sugar was about 80 %. Particle size measurements showed that even under non cryogenic conditions agglomeration due to humidity took place (fig. 3.6). After one day storage the sample collected in isobutanol showed a narrow size distribution with particle up to 27 µm (d90 6.7 µm). A small shift to higher sizes was visible for the samples micronized in the glovebox. Some particles up to 500 µm (d90 12.1 µm) were

detectable. Under normal ambient conditions a clear shift to higher particles sizes was detectable with a d90 value of 123 μm. This demonstrated the effect of humidity on the resulting particle size.
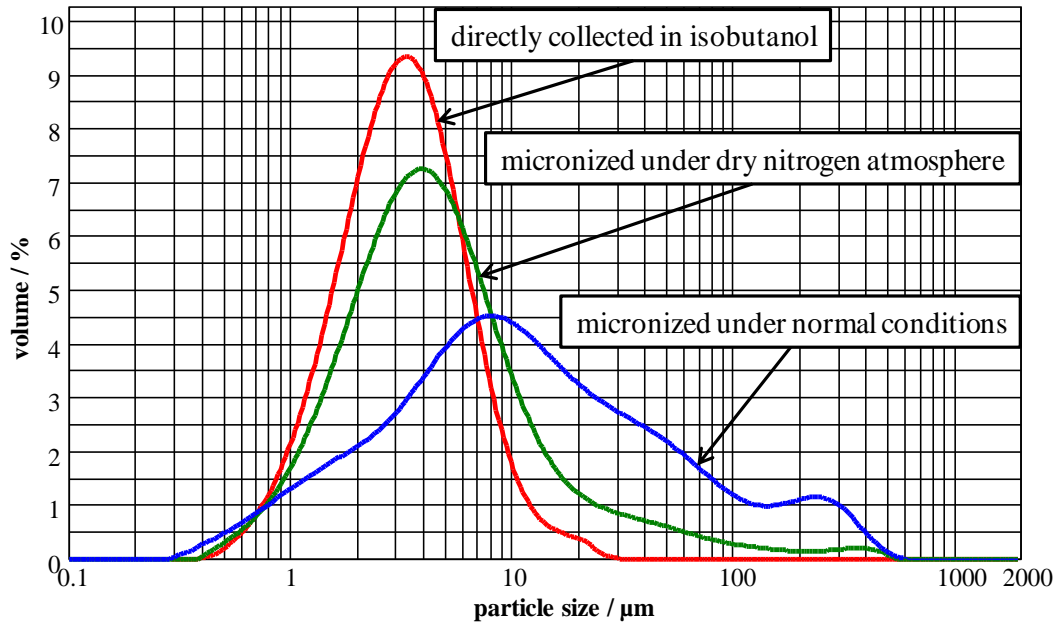
Fig. 3.6: size distribution of sugar micronized under different conditions at 8 bar after 1 day storage in an desiccator

To illustrate the consequences of air humidity on micronized sugar one sample was stored one day at 75 % rel humidity, was vacuum dried afterwards and SEM micrographs were taken (fig. 3.7).
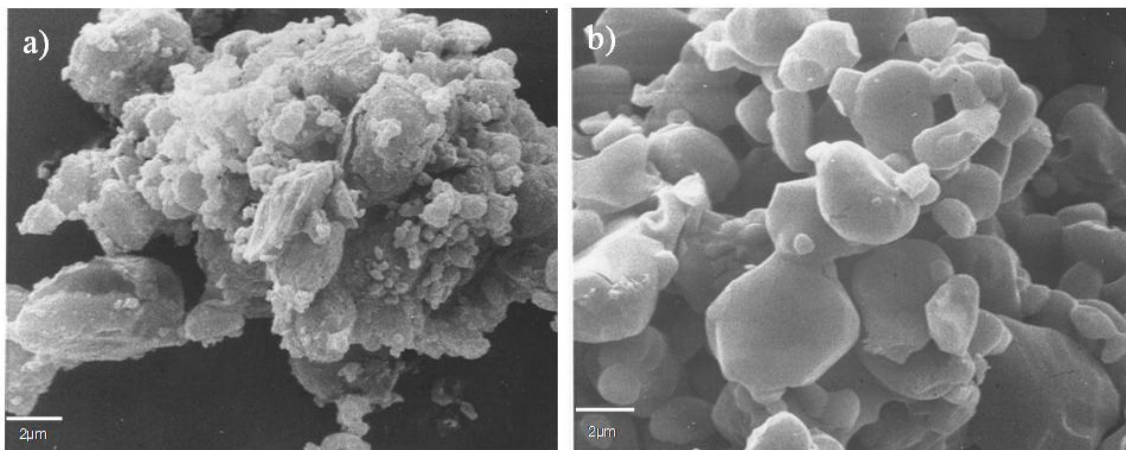
Fig. 3.7: SEM pictures of micronized sugar a) stored at dry conditions and b) stored at 75 % rel. humidity

The differences were obvious, no sharp edges were detectable anymore and the particle surfaces appeared very smooth. Single particles were still identifiable, but solid connections were formed. Due to the humidity the single particles visible in fig. 3.7 a) were irreversibly agglomerated (fig. 3.7 b)), which is a good explanation for the particle growth detected by laser light diffraction. However, for proteins not only agglomeration would be a problem, it is well known that humidity also results in degradation or denaturation of proteins [139,140]. Therefore, all the following experiments were performed with the milling setup integrated within the glovebox.

Summary

Overall a jet milling system was established, which allowed the micronization of very small batches down to 200 mg with yield of about 80 % and cryogenic grinding at temperatures of about -60°C. Air humidity was recognized as a critical factor for micronization processes; therefore, it was totally excluded from the whole milling process, so that no impact on particle sizes or stability and activity data of the proteins should be expected.

Chapter 4

Size Reduction

of

Proteins

by

Jet Milling

Introduction

The most important outcomes for size reduction obviously are resulting particle size and size distribution of the product. Additionally, important factors for the suitability of such a process are controllability and reproducibility to guarantee unchanged quality of the product.

But even if the process is well characterized, for establishing the processing of a new substance or class of substances the process has to be validated from scratch on. Different properties like hardness, density, brittleness, size etc. of a new material make the transfer of parameters of other substances very difficult. Therefore, the establishment of size reduction processes and defining the right parameters for a new substance is very time- and in most cases also substance-consuming. This is especially true by using the traditional COST approach (**c**hanging **o**ne **s**eparate factor at a **t**ime) to optimize a process and find the optimal adjustments of the variable parameters. Especially when interactions between the investigated parameters exist, the probability of indicating an optimum far from the real optimum is high [141].

To overcome this problem statistical factorial design, also called Design of Experiments (DoE), for the planning of the single experiments was developed. With this approach all relevant parameters are varied simultaneously. By optimizing the experimental setup it is possible to reduce the number of necessary experiments without significant loss of information. The obtained data can be analyzed to yield valid and objective conclusions for the investigated parameters and interactions can be revealed. In principle DoE can be applied for the optimization of all processes with process relevant parameters, which can be varied on specific levels. Because of these advantages this method was established in many kinds of different fields like biotechnology [142,143], material sciences [144] and engineering [145]. In spite of these advantages the progress in displacing the COST-approach is not that fast. However, even in new guidelines e.g. of the ICH these methods are incorporated [146].

Therefore, DoE was applied to investigate the jet milling process of proteins for the identification and optimization of important process parameters. The suitability of the process was investigated by processing three different model proteins: bovine insulin, hen egg-white lysozyme and bovine serum albumin (BSA). Differing in molecular weight, structure, particle size and particle morphology these well characterized proteins should give a good impression of the impact of jet milling on this class of drugs. A closer look on the characteristics of the

three substances will be given at the beginning of the following chapters 5 – 7, where the focus is on the impact of the micronization process on chemical stability, structure and bioactivity.

In this chapter the influence of the three process parameters milling gas pressure, number of milling cycles and temperature of the milling gas on particle size, size distribution and particle morphology was investigated.

Results and Discussion

Particle size and size distribution

The yield of the proteins after one milling cycle starting with 500 mg was at about 83 %. After 3 cycles it was possible to regain 40 % of the initially applied amount.

To investigate the efficiency of the micronization process the resulting particle size distribution of each milling experiment was determined. Milling gas pressure, number of milling cycles and temperature of the milling gas were varied on specific levels (tab. 4.1). Figures 4.1 to 4.3 show typical size distributions for the investigated proteins. Detailed information about the obtained sizes is shown in table 4.2 for each experiment. For all three proteins particle sizes drastically decreased and the process resulted in very narrow size distributions. Using one milling cycle at 6 bar the d90 value of insulin was reduced from 30.19 µm to 6.13 µm and for three cycles at 14 bar 3.30 µm were achieved. The much larger and broader distributed lysozyme and BSA particles (d90 of 673.66 µm and 919 µm) were micronized to 8.56 µm by milling once at 6 bar and to 4.07 µm at 3x14 bar for lysozyme and to 21.5 µm and 6.48 µm for BSA respectively. A small rest of coarser particles after milling lysozyme and BSA one time at 6 bar was traceable (fig. 4.2 and 4.3), which is probably due to the larger particles of the bulk material. Nevertheless, most d50 values were in the range of 2 to 5 µm. These sizes are comparable to results in other publications where mean particle sizes of 3 µm for IFN-β containing sorbitol [81], sizes between 1.5 and 3.5 µm for five different proteins and peptides [82] and 2 µm and 4 µm, respectively, for insulin and calcitonin [84] were determined after jet milling. For the model proteins higher pressure and more milling cycles led to smaller particle sizes. With higher pressure more energy was provided to the milling chamber likely contributing to the smaller particle sizes. The most effective milling cycle regarding size reduction was the first one. Additional grinding cycles only had a small impact on the d50 value but the d90 was further decreased indicating a narrower size distribution (see table 4.2). A prerequisite for breakages of particles by all milling processes are existing cracks and flaws within the particles. With decreasing particle size the probability of those imperfections is reduced [147]. Therefore, there is a so-called grinding limit where only plastic deformation and no further breakage can take place [148]. This limit seemed to be at a d90 between 3 and 5 µm for the investigated proteins using this experimental setup, which corresponds to the results in the other studies. Furthermore, the residence time of small particles within the milling chamber is much shorter than that of larger ones, because they are taken out of the milling chamber with the gas stream much faster while the larger ones are

held back by the centrifugal forces. In our study the slight differences between the tested proteins after the first milling cycle are likely due to the different particle sizes of the unprocessed bulk materials. These differences could not be totally removed after three milling cycles, which indicates that the results are also influenced by other parameters, which are specific for each protein.

For lysozyme and BSA an effect of the milling gas temperature on the resulting particle size was measured. With cooling slightly larger particles were measured for lysozyme, but for BSA the cooling resulted in smaller particles. The effect of the low milling gas temperature on BSA is maybe due to an increased brittleness at these temperatures. This is the main reason for cryogenic grinding, a more efficient grinding of elastic, rubber-like materials. The cooling restricts the molecule flexibility and therefore stress cannot be reduced by stretching any more. The energy saved as elastic deformation is concentrated within a smaller area and the tension and also the fracture probability increased [149].

Variable	Level -1	Center point	Level +1
x_1: milling pressure	6 bar	10 bar	14 bar
x_2: number of milling cycles	1	2	3
x_3: cooling device	on (approx. -60°C)		off (room temperature)

Tab. 4.1 parameters of the experimental design

experiment	pressure	cycles	temperature			d90			d50			span		
			insulin	lysozyme	BSA	insulin	lysozyme	BSA	insulin	lysozyme	BSA	insulin	lysozyme	BSA
1	6	1	15	17	17	6.19	8.60	21.50	3.06	3.87	8.77	1.620	1.739	2.60
2	14	1	8	8	8	5.47	5.26	8.87	2.84	2.90	4.65	1.472	1.252	1.388
3	6	3	15	16	16	4.92	5.28	10.64	2.62	2.76	5.63	1.430	1.422	1.395
4	14	3	8	10	10	3.30	4.07	6.48	2.00	2.22	3.77	1.131	1.314	1.137
5	6	2	46	17	17	5.32	6.28	12.64	2.77	3.36	6.46	1.498	1.341	1.486
6	14	2	9	8	8	3.78	4.68	6.92	2.24	2.50	3.89	1.180	1.362	1.215
7	10	1	12	15	15	4.40	7.36	11.38	2.50	3.26	4.99	1.266	1.732	1.782
8	10	3	11	13	13	3.47	4.37	6.53	2.06	2.44	3.65	1.158	1.259	1.209
9	10	2	12	13	13	3.94	4.92	7.38	2.26	2.70	3.91	1.239	1.288	1.355
10	10	2	12	14	14	3.64	4.81	8.44	2.13	2.70	4.52	1.195	1.235	1.347
11	10	2	12	13	13	3.52	5.62	8.12	2.12	2.89	4.36	1.118	1.459	1.334
12	6	1	-53	-58	-58	7.13	11.99	15.13	3.39	5.05	6.47	1.704	1.934	1.917
13	14	1	-61	-65	-65	4.18	7.62	9.71	2.36	3.39	3.63	1.271	1.763	2.174
14	6	3	-65	-57	-57	5.06	7.06	7.95	2.72	3.79	4.39	1.401	1.338	1.267
15	14	3	-67	-64	-64	3.51	4.93	6.85	2.08	2.61	3.60	1.162	1.391	1.365
16	6	2	-64	-58	-58	5.89	7.62	9.84	3.18	4.04	5.25	1.399	1.359	1.376
17	14	2	-65	-66	-66	3.87	5.64	7.30	2.35	2.87	3.60	1.090	1.475	1.472
18	10	1	-63	-53	-53	4.44	9.80	12.80	2.54	4.77	5.54	1.225	1.582	1.865
19	10	3	-73	-61	-61	3.33	5.22	6.70	2.02	2.78	3.73	1.084	1.346	1.224
20	10	2	-67	-57	-59	3.58	6.60	7.24	2.14	3.61	3.65	1.113	1.290	1.458
21	10	2	-64	-60	-59	4.18	6.07	9.43	2.35	3.07	4.69	1.297	1.462	1.511
22	10	2	-65	-59	-57	4.44	6.93	9.51	2.44	3.63	4.72	1.343	1.408	1.518

Tab. 4.2 results of the micronization experiments
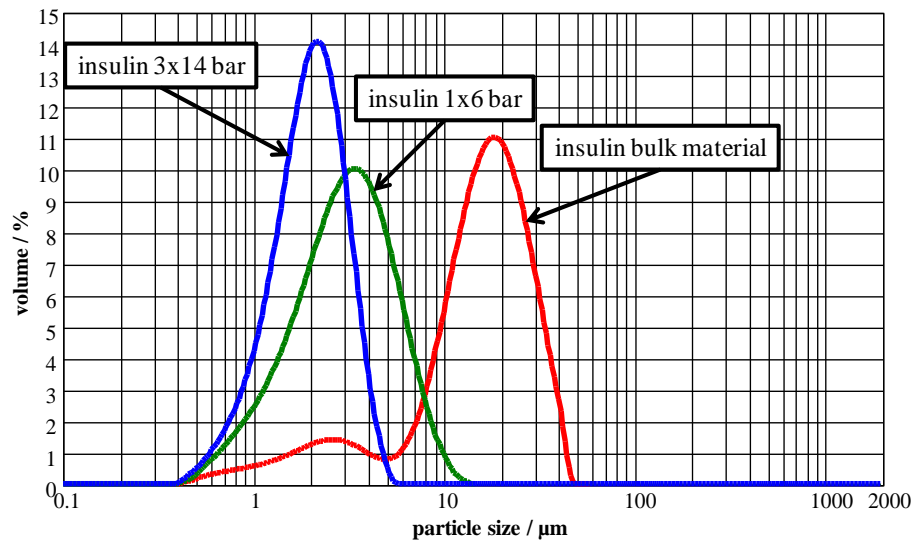
Fig. 4.1 size distributions of insulin micronized without cooling
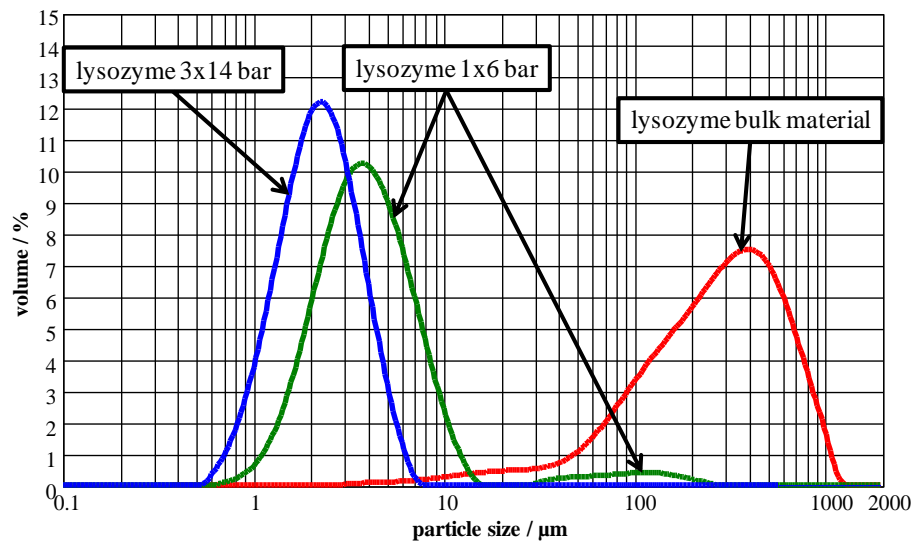
Fig. 4.2 size distributions of lysozyme micronized without cooling
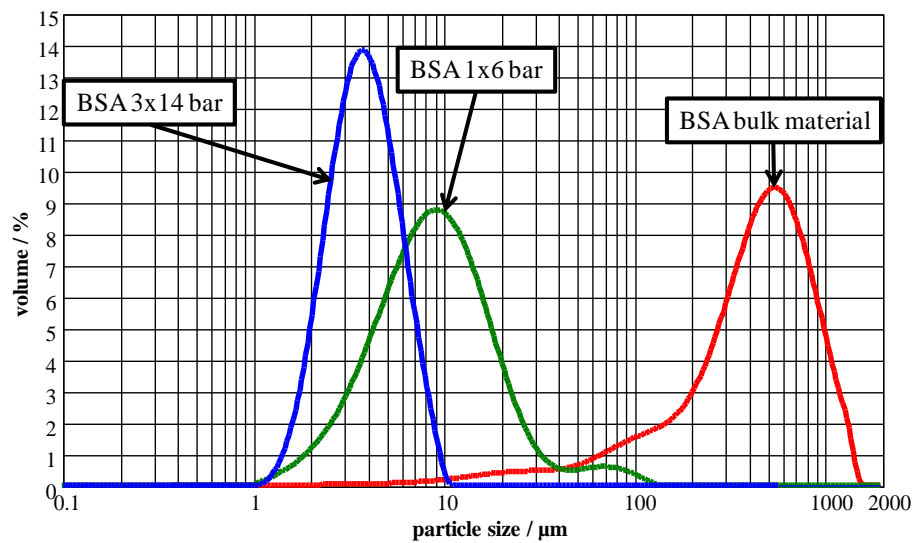
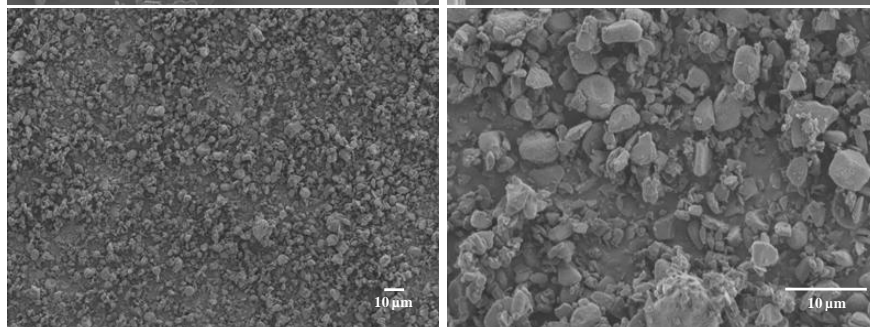*Fig. 4.3 size distribution of BSA after micronization without cooling*

Particle morphology

To verify the results measured by laser light diffraction SEM micrographs were taken from the micronized protein powders. SEM pictures (fig. 4.4, 4.5 and 4.6) show the protein particles before milling and after one micronization cycle at 6 and after three cycles at 14 bar without and with cooling. It is clearly visible that in spite of the very different morphology of the bulk material, after micronization the resulting particles look very similar. For insulin it was obvious that the nearly cubic crystals of the raw material were no more detectable after micronization. The micronization process resulted in very small and sometimes rounded fragments. The rounded shape of the jet milled particles is the typical particle morphology after jet milling and is assigned to attrition of the particles on each other or the walls of the mill [83,150]. This also explains the increasing incidence of these rounded particles with higher number of milling cycles. There is no difference in morphology between the samples ground without and with cooling. Obviously, the pictures confirm the particle size measurements by laser light diffraction.

insulin bulk material		
insulin 1x6 bar		
insulin 3x14 bar		
insulin 1x6 bar milled at cryogenic conditions		
insulin 3x14 bar milled at cryogenic conditions		
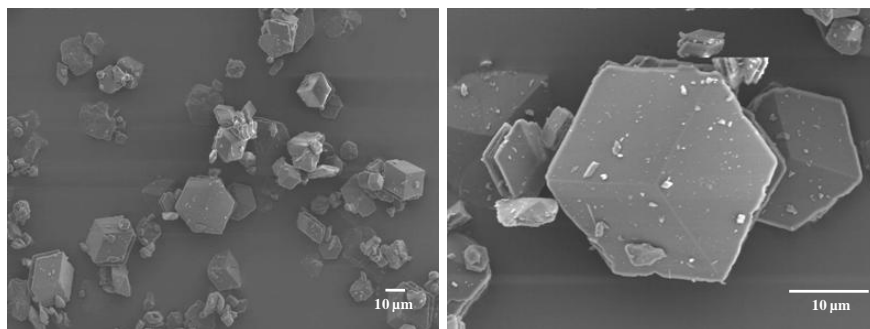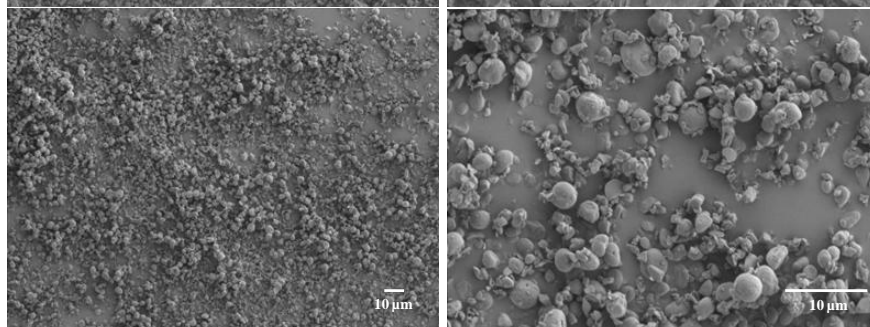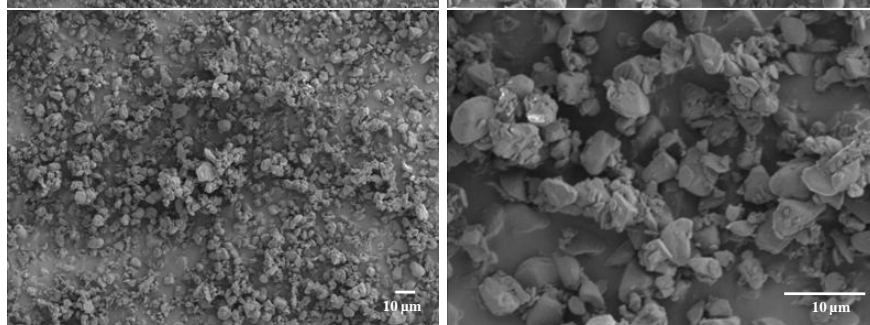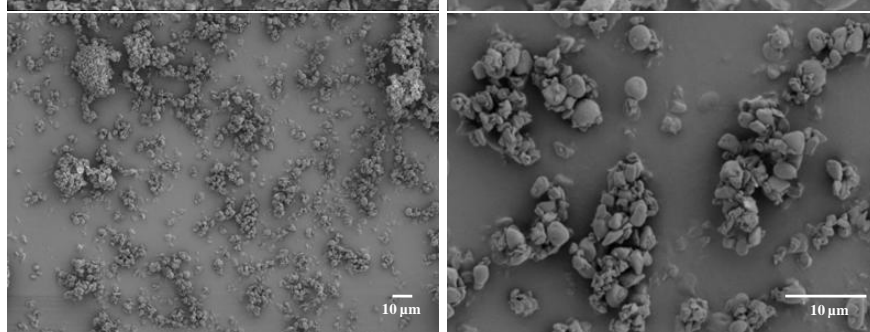
Fig. 4.4 SEM pictures of insulin micronized under different conditions compared to the bulk material

lysozyme bulk material
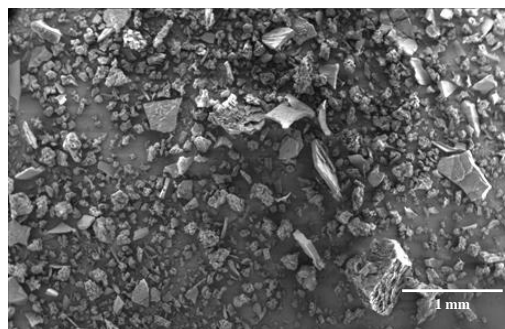
lysozyme 1x6 bar
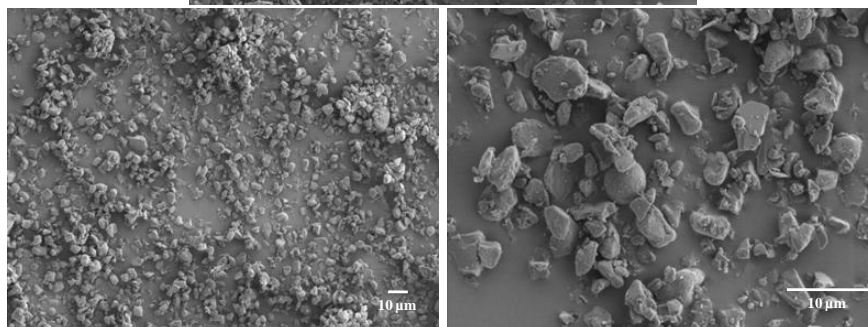
lysozyme 3x14 bar
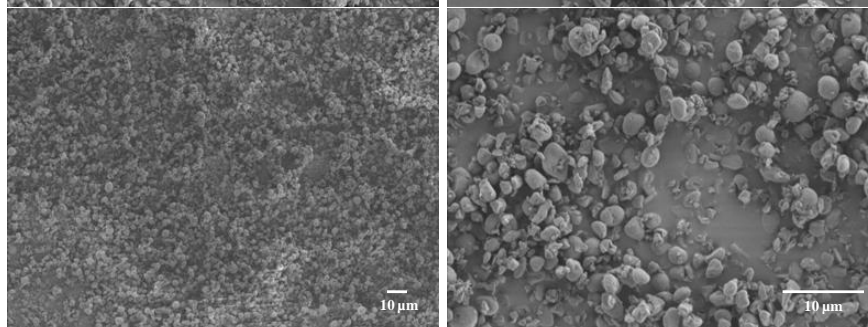
lysozyme 1x6 bar milled at cryogenic conditions
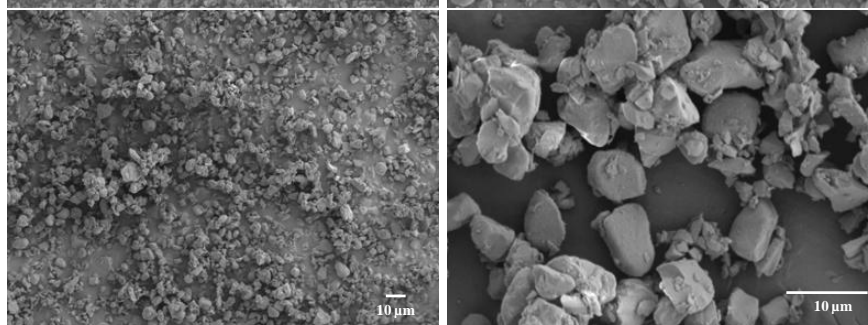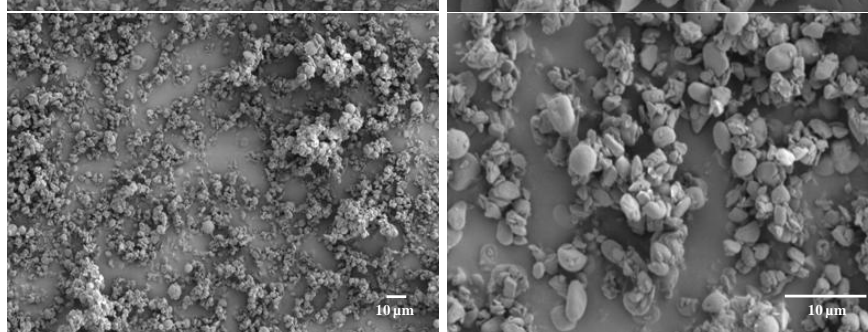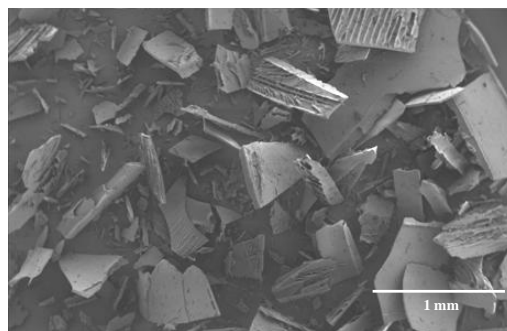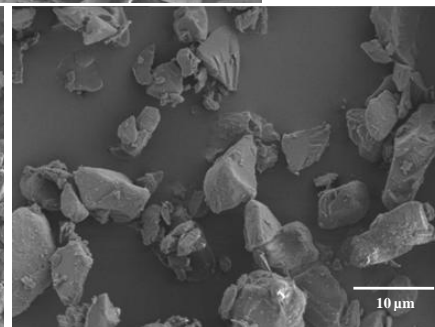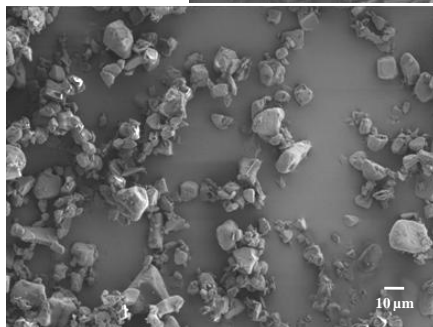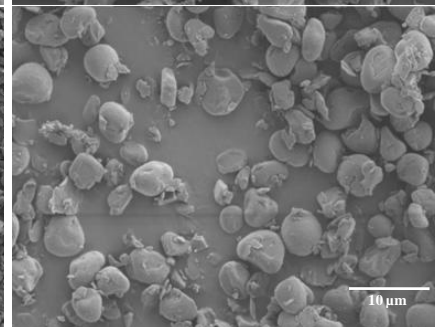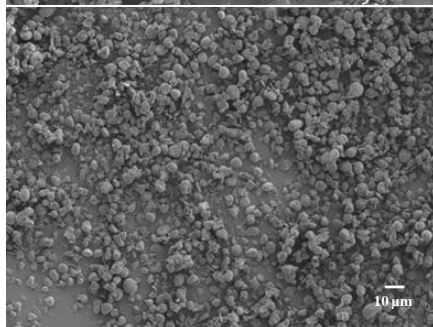
lysozyme 3x14 bar milled at cryogenic conditions

Fig. 4.5 SEM pictures of lysozyme micronized under different conditions compared to the bulk material

Fig. 4.6 SEM pictures of BSA micronized under different conditions compared to the bulk material
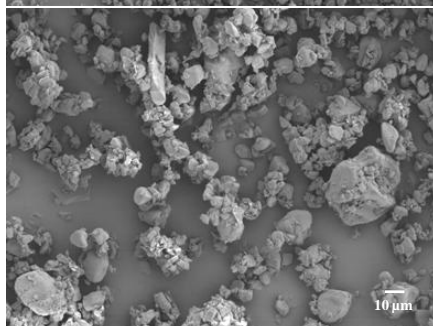
BSA bulk material

BSA 1x6 bar

BSA 3x14 bar

BSA 1x6 bar milled at cryogenic conditions
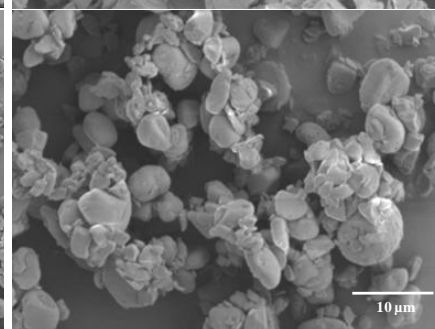
BSA 3x14 bar milled at cryogenic conditions

Analysis of the results by DoE
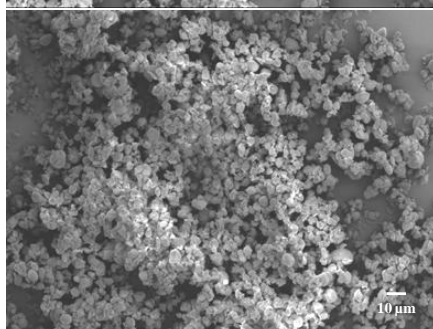
By using statistical analyses it was possible to fit a mathematical model based on equation 2.1 to the data obtained from the particle size (d90 value) measurements after micronization. The factors milling pressure (x_1), number of milling cycles (x_2) and temperature of the milling gas (x_3) were taken into account. It was obvious that higher milling pressure and higher number of milling cycles were decreasing the resulting d90 value for all three proteins, indicated by the negative coefficients. Differences were calculated for the significance of the other coefficients. Especially the impact of the milling gas temperature differed as mentioned before, which is reflected in the resulting equations, too. For insulin the temperature effect was not significantly different from zero and was therefore excluded from the model, but for lysozyme a small loss in milling efficiency was measured for the samples milled at temperatures about -60°C. The negative coefficient (x_3) indicates that by raising the temperature from low to high level smaller particle sizes are obtained. In contrast to these results lower temperatures improved the milling efficiency for the jet milling of BSA. It is noticeable that for insulin a quite simple model was obtained with only two significant factors, one quadratic coefficient and no interactions between the three factors could be detected and therefore were excluded from the model. While for lysozyme all three factors had a significant impact and for BSA additionally all quadratic coefficients and even two interactions showed an effect on the d90 value.

insulin:

$$y=0.5879-0.0791x_1-0.0643x_2+0.0892x_1^2 \tag{4.1}$$

lysozyme:

$$y=0.7681-0.0649x_1-0.0793x_2-0.0537x_3+0.0228x_2^2 \tag{4.2}$$

BSA:

$$y=1.1160-0.1038x_1-0.1119x_2+0.0217x_3+0.0504x_1^2+0.0399x_2^2-0.2698x_3^2+0.0417x_1x_2-0.0941x_1x_3 \tag{4.3}$$

The 3D surface response diagrams, visualizing these results and the impact of the different parameters on the d90 value, are shown in figures $4.7 - 4.11$. The different impact of the milling gas temperature on the resulting particle size of lysozyme and BSA is clearly visible. For insulin temperature was excluded as an insignificant factor. Therefore, it was possible to display the calculated results according to equation 4.1 in only one diagram. The mentioned

grinding limit is visible by the decreasing slope of the diagrams with higher pressure and higher number of milling cycles.

The quality of the fit of the models is described by R^2, the fraction of the variation of the response explained by the model, and Q^2, the fraction of the variation of the response that can be predicted by the model. Therefore, R^2 is an overestimated measure, and Q^2 is an underestimated measure of the goodness of fit of the model. Large Q^2, 0.7 or larger, indicates that the model has good predictive ability and will have small prediction errors [141]. The model fitted for insulin resulted in $R^2 = 0.893$ and $Q^2 = 0.821$, for lysozyme in $R^2 = 0.945$ and $Q^2 = 0.903$ and for BSA $R^2 = 0.959$ and $Q^2 = 0.909$ were calculated. These are very good parameters for the calculated models, which allows the prediction of particle sizes with new parameter combinations within the investigated range. These results also confirm that the selection of the investigated milling parameters included in the experimental setup was reasonable. As most material properties like hardness, brittleness and number and size of initial flaws, which are mentioned in chapter 1, are not known and hard to determine, it was not possible to correlate the differences of the equations of the calculated models to any material properties. Therefore, further experiments with new proteins are necessary.
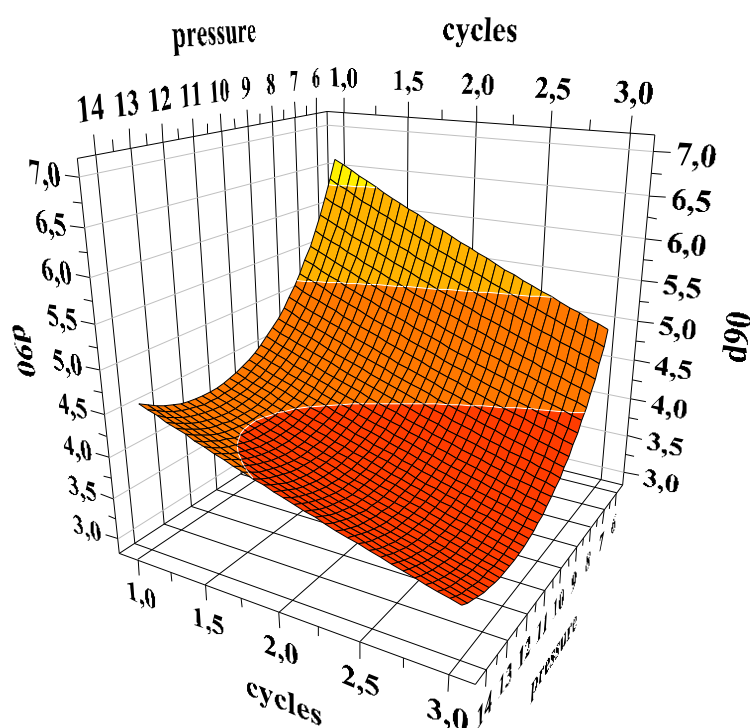

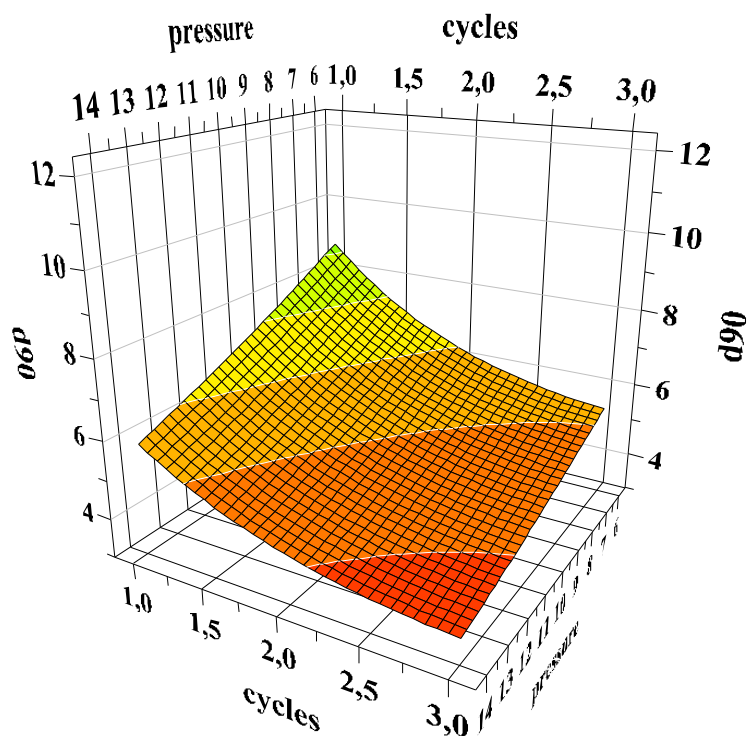*Fig. 4.7 Surface response diagram of insulin (d90 value)*

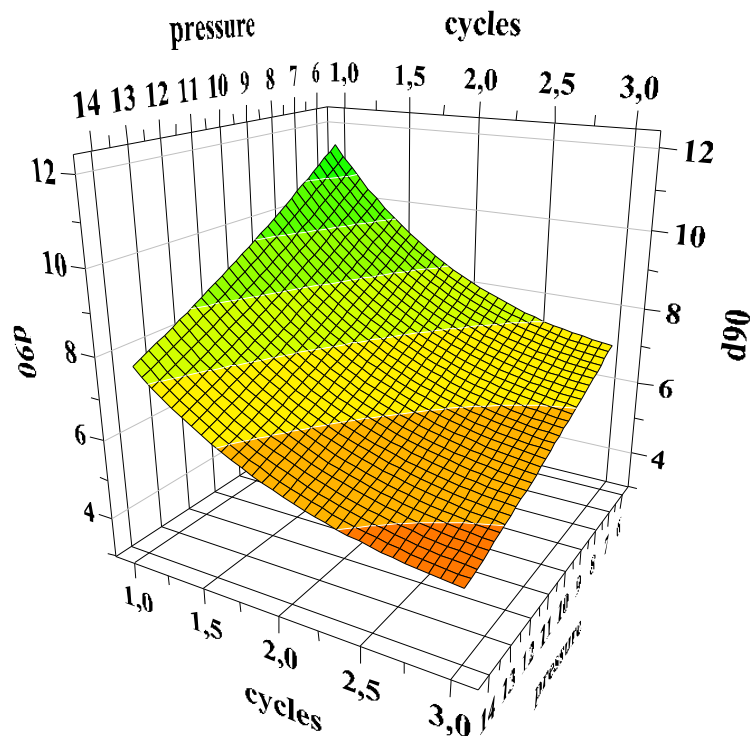*Fig. 4.8 Surface response diagram of lysozyme (d90 value) at room temperature*

Fig. 4.9 Surface response diagram of lysozyme (d90 value) at cryogenic conditions
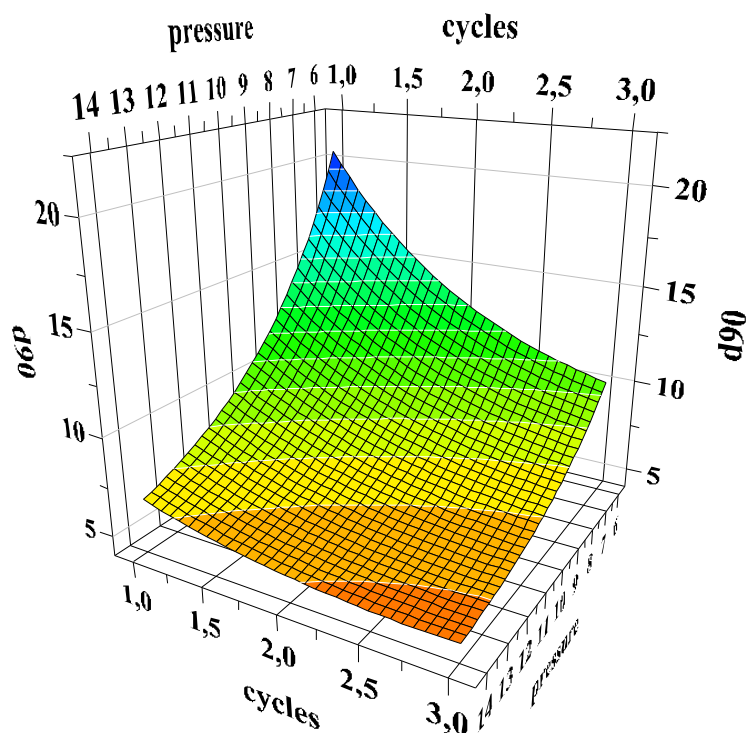
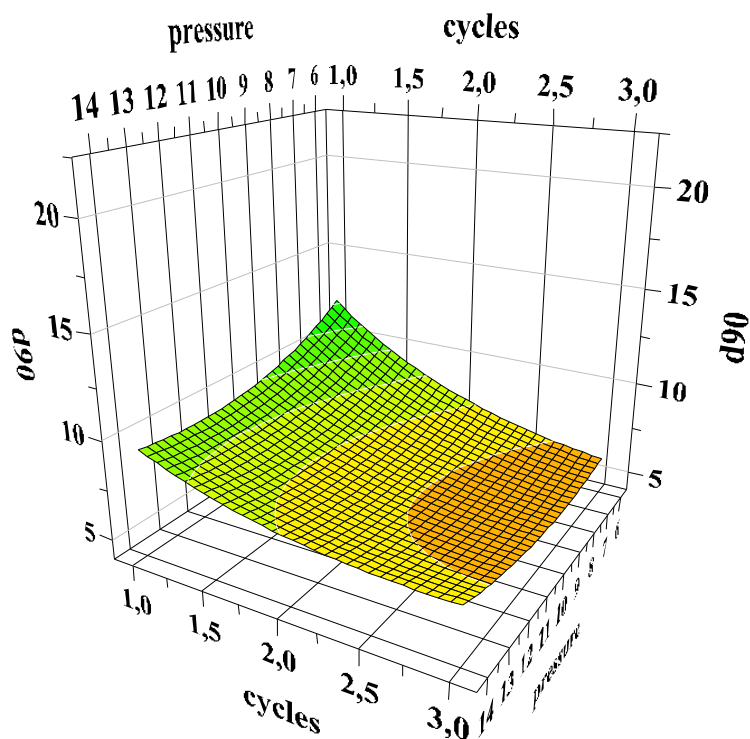*Fig. 4.10 Surface response diagram of BSA (d90 value) at room temperature*

Fig. 4.11 Surface response diagram of BSA (d90 value) at cryogenic conditions

Changes in particle size during storage

A problem of some milled products is that during storage particle growth due to the activated surfaces of the particles appears [151]. The comparison of the particle sizes of the freshly milled samples with the results of the same sample after 4 weeks of storage at -20°C verified that the particles are stable during storage. Figure 4.12. shows the results for the micronized BSA powder samples. No particle growth or aggregation could be detected after measuring the particles by laser light diffraction.
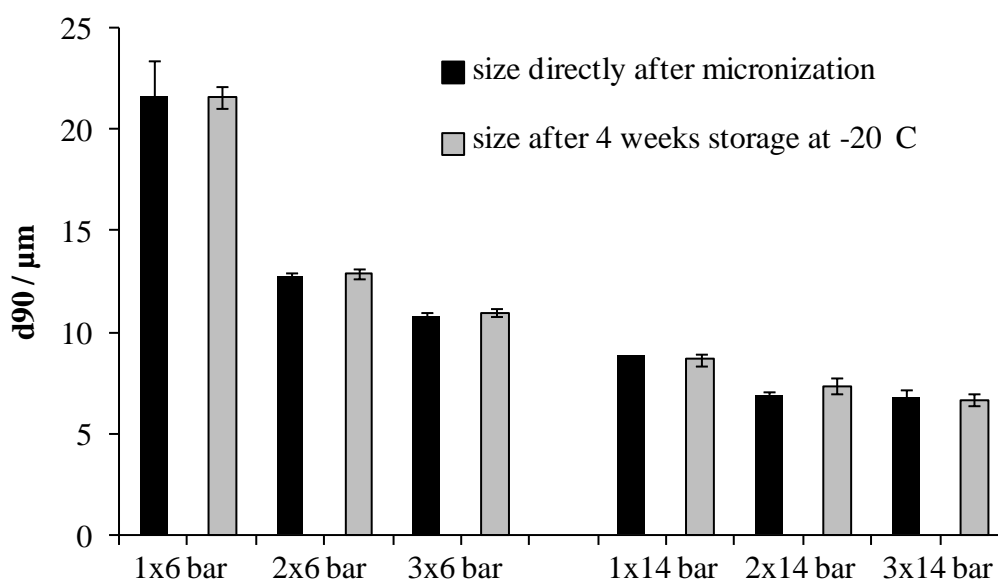

Fig.4.12 d90 value of micronized BSA directly after jet milling and after 4 weeks of storage

Summary

For all three proteins jet milling proved to be a powerful tool for size reduction. The yield of about 80% per milling cycle is very good taking the very small amount of milled substance into account. In most cases particle size distributions with a d90 value below 10 μm were achieved. Based on the resulting size distribution curves the particle size of the bulk material was identified as one factor having a significant effect on the resulting distribution. By applying statistical experimental design it was possible to describe the impact of the different factors qualitatively and quantitatively. The occurring differences between the tested proteins could not completely be explained, but were a good indicator for the complexity of the process. Nevertheless, the chosen factors milling pressure, number of milling cycles and milling gas temperature proved to be the most important factors of the process, because being indicated by the R^2 and Q^2 values, which are close to 1, nearly all effects could be described by these parameters. Finally, the storage stability of the micronized protein powders was demonstrated, which is an important factor for using these powders as drugs.

Chapter 5

Impact

of

Jet Milling

on

Bovine Insulin

Introduction

Insulin is one of the most important and best investigated proteins and can be called in many ways the prototypic biopharmaceutical [152]. Its success is based on different factors, it was quite easily available in good purity even before recombinant protein production had been developed and on the other side the epidemiology of diabetes mellitus itself. The WHO estimates that in 2030 more than 350 million people will be suffering from diabetes, which makes insulin research an urgent and financially promising topic. Therefore many research groups are working on the processing and delivery of insulin [92,153,154]. Insulin is so far the only protein administered in crystalline form and was the first biopharmaceutical approved for delivery by the pulmonary route [13]. Therefore, insulin is the optimal therapeutic protein for testing the suitability of jet milling for the micronization of proteins.

Insulin is an anabolic hormone with an important role in glucose and fat metabolism. The bovine insulin used for our experiments consists of 51 amino acids organized in two peptide chains A and B. Interchain disulfide bonds are located between the cysteines at positions A7 and B7 and between positions A20 and B19. An intrachain disulfide bond occurs between the cysteines at A6 and A11. Bovine insulin differs from human insulin at the following positions: alanine for threonine at A8, valine for isoleucine at A10, and alanine for threonine at the carboxyl terminal of the B-chain [155]. For bioactivity testings a chondrocyte cell assay is available [123].

Results and discussion

Chemical stability of insulin

First the impact of the jet milling process on the chemical stability of bovine insulin was investigated. HPLC experiments were performed to detect occurring degradation products. Figure 5.1 shows the results of these experiments.
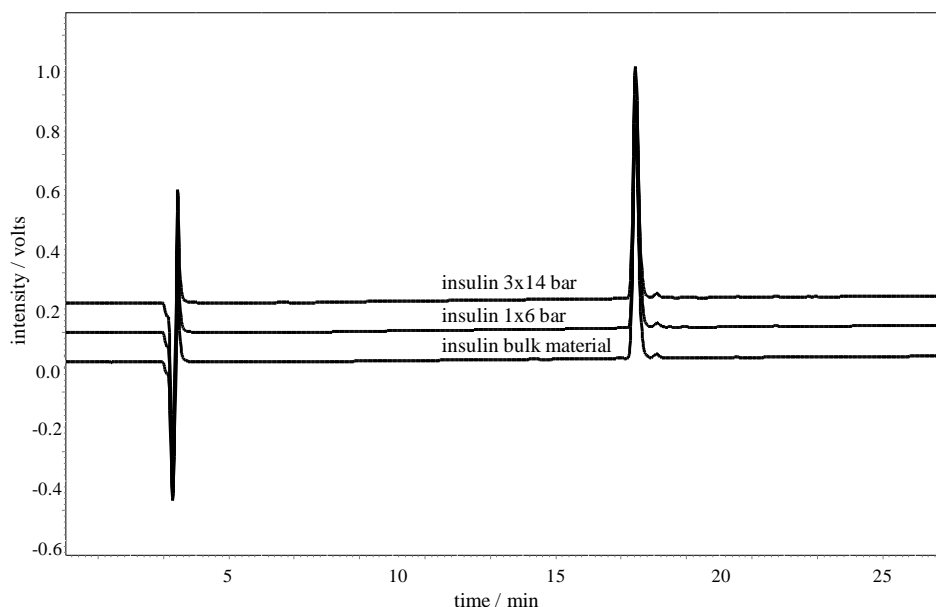

Fig. 5.1 RP-HPLC chromatogram of insulin at a detector wavelength of 210 nm

No differences between the unprocessed control and the samples micronized sample could be detected. For all samples a main peak at 17.4 min and a small side peak appeared (retention time 18.1 min). The main peak was assigned to insulin and the small peak was identified as desamidoinsulin in an earlier study by Maschke et al. [92]. The ratio between these two peaks did not change comparing the unprocessed bulk material with the samples jet milled once at 6 bar or three times at 14 bar. Similar results were found for the analysis of the samples by MALDI-ToF (fig. 5.2). The spectra of the bulk material and powder three times micronized at 14 bar showed no significant differences. The main peak was at a molecular mass of 5736.0 Da for the unprocessed material and at 4735.8 Da for the micronized sample.

Overall the chemical stability of bovine insulin did not seem to be influenced by the micronization process in a jet mill.
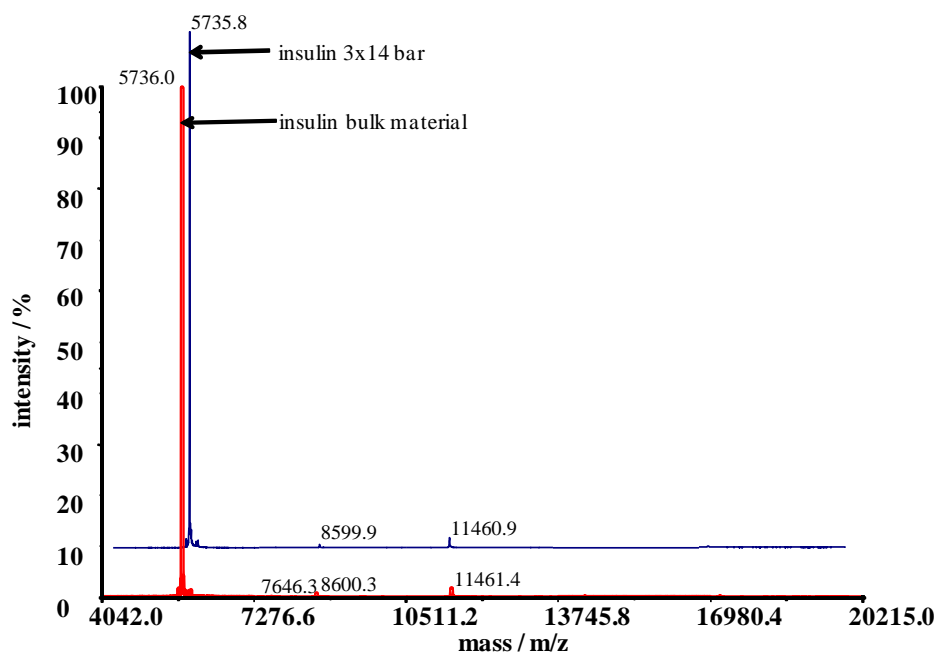
Fig. 5.2 MALDI-ToF spectra of insulin

Impact on secondary and tertiary structure

The influence of the milling process on the structure of insulin in solution was analyzed by fluorescence methods and CD spectroscopy.

Analysis of insulin solutions by CD spectroscopy revealed that only insignificant differences between the tested micronized and unprocessed samples were detectable (fig. 5.3).

Fig. 5.3 CD spectra of insulin before and after micronization

Intrinsic fluorescence measurements at an excitation wavelength of 280 nm resulted for all samples in emission maximum at 308 nm. As shown in fig. 5.4 small differences in the

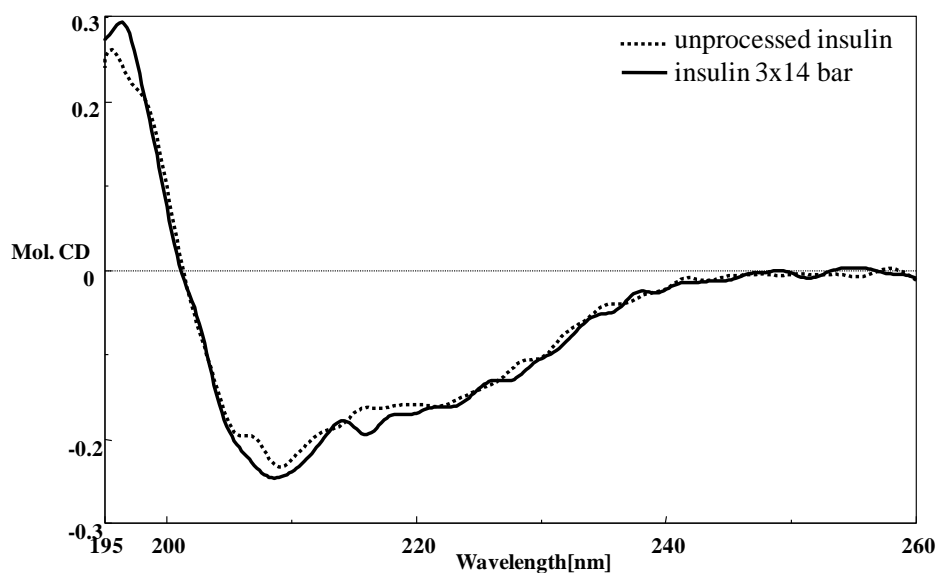maximum intensity were detected. Tyrosin fluorescence intensity dropped from 522 for the control to 487 for the samples micronized three times at 14 bar. Normally the two tyrosins in position A14 and A19 produce no fluorescence, because they are buried in the hydrophobic core and H-bonded to carbonyls [156]. Therefore, changes in the environment of the tyrosin residues in positions B16 and B26 have to be responsible for the reduced intensity after micronization. This effect can be caused by carbonyls or disulfide bonds which changed their relative position to these residues.

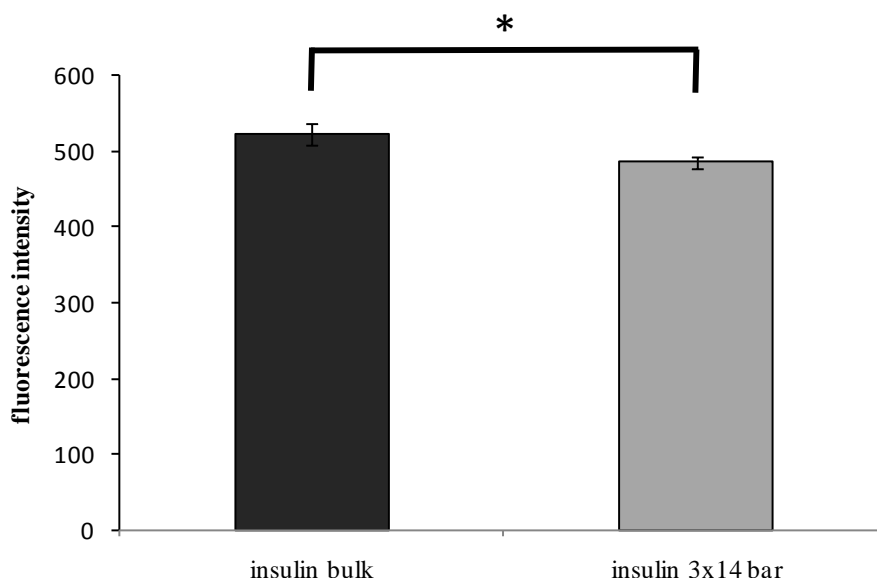*Fig. 5.4 intrinsic fluorescence of insulin at 308 nm upon excitation at 280 nm (p<0.05)*

For further investigations the relative surface hydrophobicity of the protein in solution was analyzed by addition of a fluorescent probe (ANS). Again small differences were detected. The surface hydrophobicity of the sample micronized three times at 14 bar increased by 12 % compared to the unprocessed bulk material (fig 5.5).
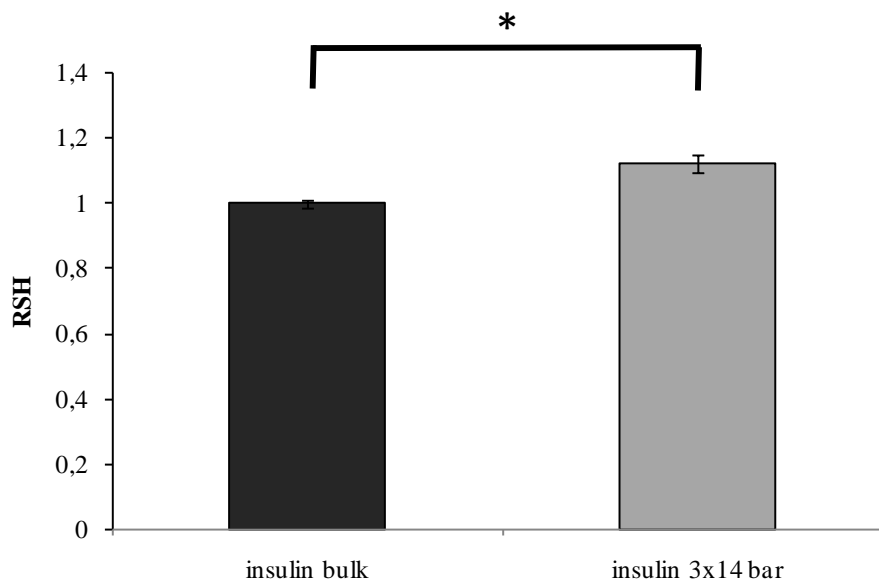
Fig. 5.5 relative surface hydrophobicity (RSH) of insulin measured after addition of fluorescent probe ANS.

All three methods revealed small differences in the secondary and tertiary structure of insulin. An important question is now, if these small differences have an effect on the bioactivity of the bovine insulin.

Bioactivity assay for insulin

Maintaining the bioactivity is the most important parameter while processing proteins. The bioactivity of insulin was tested by using a bovine chondrocyte cell assay utilizing the effect on cell proliferation and production of extracellular matrix. As illustrated in fig. 5.6 after 5 weeks of cultivation no differences in cell number of the groups supplied with the micronized insulin compared to the groups with unprocessed insulin were visible. Pressure, milling cycles and temperature of the milling gas had no effect on the bioactivity of the bovine insulin.
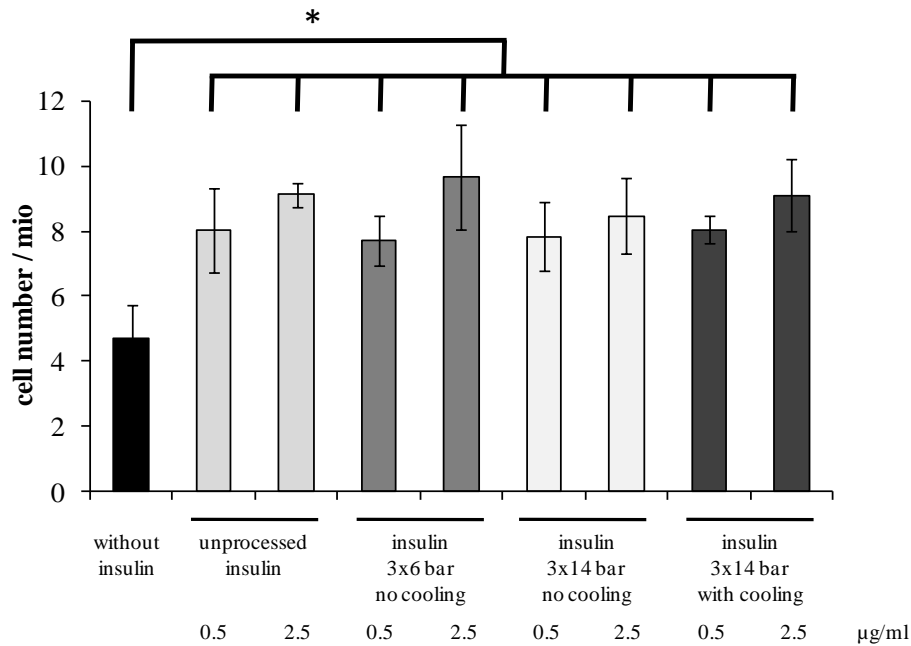
Fig. 5.6 cell number of chondrocytes after 5 weeks of cultivation after having added different samples of insulin at two concentrations

Additionally, histological cross sections of the chondrocyte containing fibrin gels were stained with safranin-O in order to visualize the glycosaminoglycans (GAG), an important compound of the extracellular matrix. As shown in fig. 5.7 the intensity of the red staining is much higher in the insulin containing groups. But no difference between unprocessed and micronized insulin supplied groups was visible, which supports the results of the cell number analysis.

Fig. 5.7 Histological cross-sections after 5 weeks of cultivation, stained red for glycosaminoglycans (GAG) with safranin-O. a) Without insulin (control), b) with unprocessed insulin 2.5 µg/ml and c) with insulin micronized 3 times at 14 bar 2.5 µg/ml.

Summary and conclusion

The micronization process seems to have only a small impact on the crystalline insulin. Analysis by HPLC and MALDI-ToF revealed no changes in the chemical structure and stability of the insulin molecules. Small changes were detected by fluorescence analysis. The intrinsic fluorescence was reduced and the relative surface hydrophobicity (RSH) increased, indicating small alterations in the tertiary structure of insulin. Nevertheless, these changes had no influence on the bioactivity of insulin tested in a chondrocyte cell assay. Nevertheless, regarding the sensitivity of the cell culture assay, which is lower than e.g. for an enzymatic assay, an impact of jet milling on insulin bioactivity cannot totally be excluded.

Overall, the jet milling process seems to be a suitable method for the micronization of insulin and is a promising approach for the preparation of micron sized protein particles.

Chapter 6

Impact

of

Jet Milling

on

Hen egg-white Lysozyme

Introduction

Lysozyme is an often used model in protein research [5,157,158]. Its properties and structure are very well investigated, because since the 1960s it has been in the focus of protein research [159–161]. Additionally its bioactivity is easly accessible by measuring the lysis of micrococcus luteus cells turbidimetrically [125]. Therefore, lysozyme was chosen as a model substance for our jet milling experiments.

Lysozymes are a group of enzymes defined as 1,4-β-N-acetylmuramidases cleaving the glycosidic bond between the C-1 of N-acetylmuramic acid and the C-4 of N-acetyl-glucosamine in the bacterial peptidoglycan [161]. They are found in many tissues and secretions of vertebrates, invertebrates as well as bacteria, phages and plants. In the human body the highest concentration can be found within the tear fluid. As the main function a basic defense against infections is assumed.

Chicken egg white lysozyme is a single chain polypeptide of 129 amino acids cross-linked with four disulfide bridges, containing 3 tyrosine, 6 tryptophan and 2 methionine [162] resulting in a molecular weight of 14307 Da.

Results and discussion

Chemical stability of lysozyme

The impact of the micronization process on lysozyme in solid state on the formation of degradation products was investigated by HPLC and MALDI-ToF analysis.

The analysis of lysozyme by HPLC revealed no differences of the micronized samples to the unprocessed substance (fig. 6.1). No other peaks beside the main peak at 20.9 min were detectable for each sample.
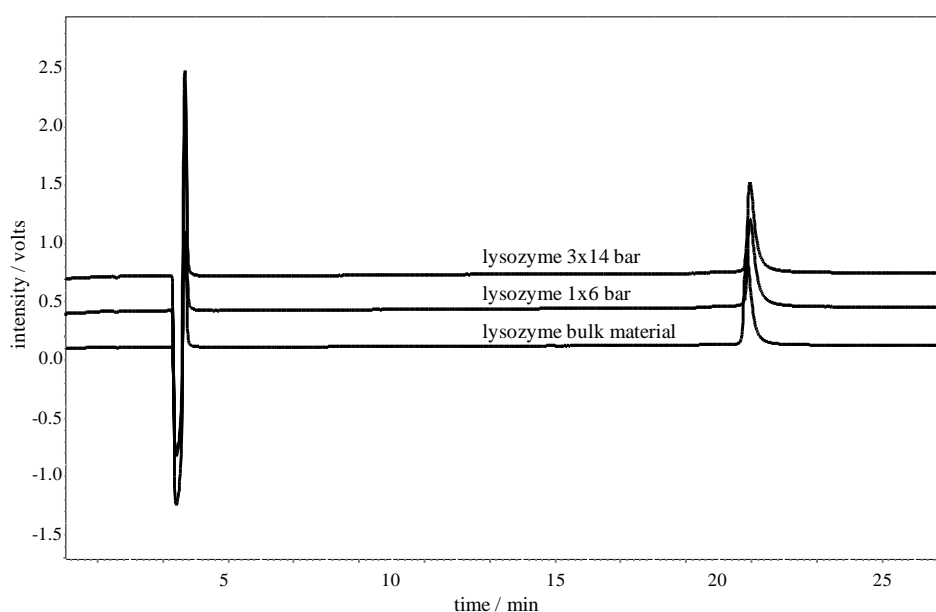
Fig. 6.1 HPLC chromatogram of lysozyme at a detector wavelength of 210 nm

Also the mass analysis by MALDI-ToF showed no significant differences between the samples (fig. 6.2). The main peak at 7145.5 Da and 7156.0 Da respectively are due to double charged molecules and the peaks at 14304.0 Da and 14304.0 Da are due to the single charged molecules. For the sample micronized three times at 14 bar no additional peaks compared to the reference were detectable.
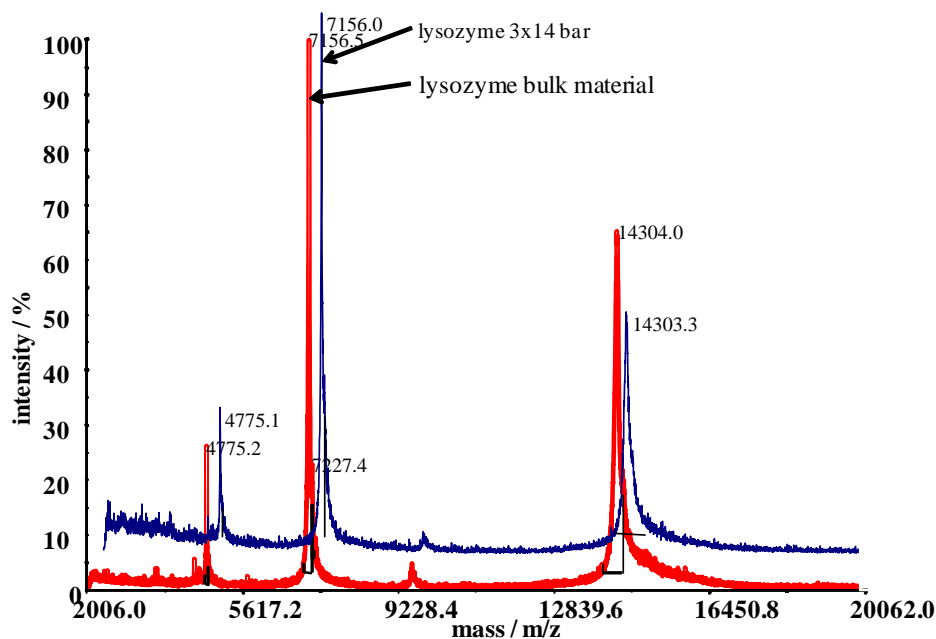
Fig. 6.2 MALDI-ToF spectra of lysozyme; lower spectrum in red shows results for the unprocessed bulk material, upper spectrum in blue the results after jet milling three times at 14 bar

Impact on secondary and tertiary structure

The effect of the jet milling process on the secondary structure of lysozyme in solution was investigated by CD measurements and subsequent analysis of the structure composition by applying the CDNN algorithm.

The results for lysozyme shown in fig. 6.3 demonstrate that no significant changes in the secondary structure in solution could be detected. Consequently no differences in the analysis of the structure composition by using CDNN algorithm were determined (fig 6.4).
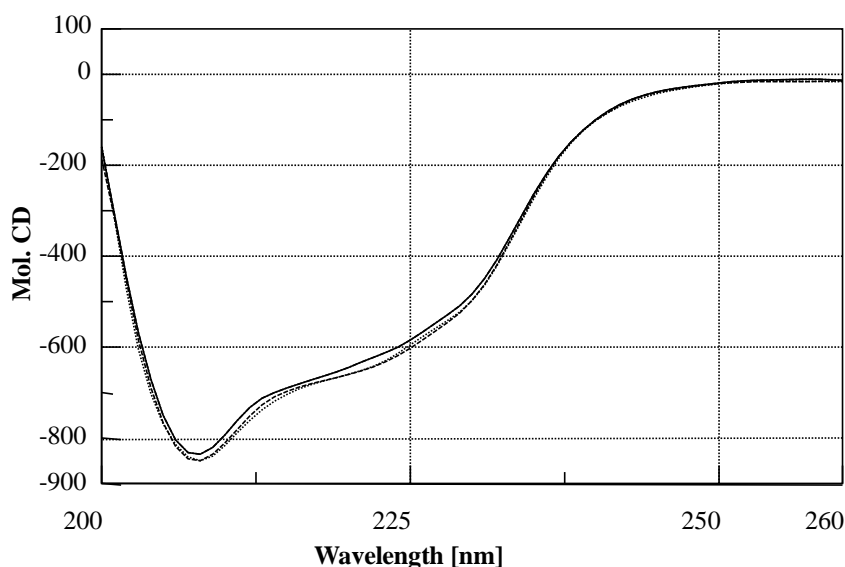
Fig. 6.3 CD spectra of lysozyme (control, 1x14bar, 2x14bar, 3x14bar)

	control	1x14 bar	2x14 bar	3x14 bar
Helix	21.0%±1.68	21.4%±2.38	21.1%±2.44	20.9%±2.25
Antiparallel	19.7%±1.52	18.6%±1.73	19.1%±2.06	19.5%±1.98
Parallel	5.5%±0.10	5.5%±0.05	5.4%±0.06	5.5%±0.05
Beta-Turn	18.4%±0.29	18.1%±0.33	18.3%±0.37	18.3±0.33
Random Coil	33.1%±1.11	33.1%±2.01	30.4%±6.29	33.0%±1.65

Fig. 6.4 Results of secondary structure composition analysis by CDNN algorithm

Similar to insulin lysozyme was analyzed by two different fluorescence methods for changes in tertiary structure. The intrinsic fluorescence measurements were performed at a wavelength of 295 nm for the excitation of the 6 tryptophan residues. The maximum of the tryptophan fluorescence was at about 394.5 nm for all samples and depending on the number of milling cycles the intensity was reduced from 200 for the control to 175 measured for the sample milled three times at 14 bar (fig. 6.5). Possible reasons for a reduction of tryptophan fluorescence are that the residues are now in a more hydrophobic environment, quenched by disulfide bonds or a greater distance to tyrosin residues, which can intensify tryptophane fluorescence via nonradiative energy transfer, if the distance between them is smaller than 10-18Å [163].
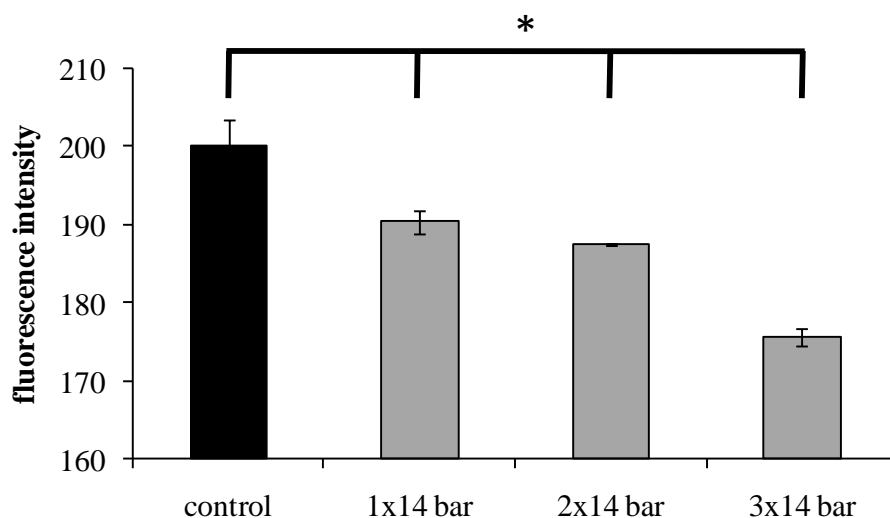
Fig. 6.5 Intrinsic fluorescence of lysozyme at an excitation wavelength of 295 nm (p<0.05)

After having added ANS as a hydrophobic probe the relative surface hydrophobicity of the protein in solution was determined. A 12-fold increase of relative surface hydrophobicity indicates dramatic changes in the tertiary structure of lysozyme (fig. 6.6). Nevertheless, by comparing the secondary structure of the reconstituted micronized proteins with that of the native proteins in solution measured by circular dichroism spectroscopy no significant changes were visible. This observation of an increasing surface hydrophobicity without changes in secondary structure of lysozyme was already described by Lechevalier et al. [129].
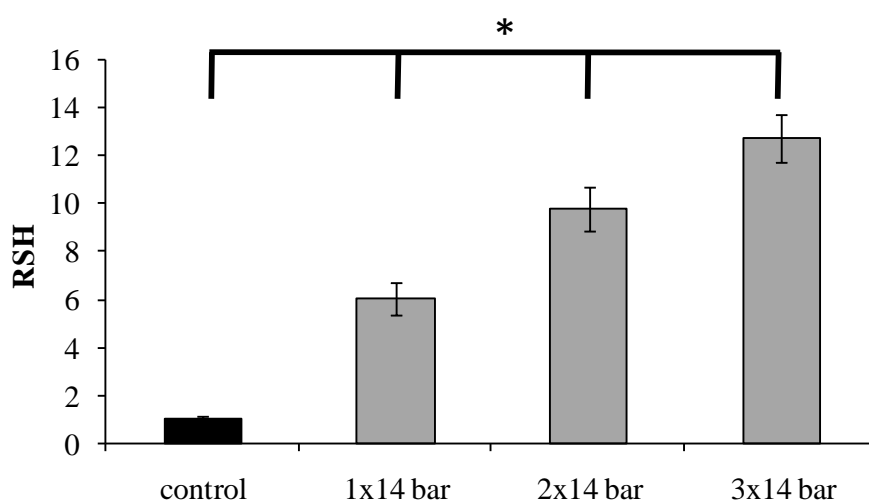
Fig. 6.6 Relative surface hydrophobicity (RSH) of lysozyme in solution with ANS as hydrophobic probe (p<0.05)

Bioactivity assay for lysozyme

For the analysis of the bioactivity of lysozyme all samples were tested using the micrococcus assay. Examination of the results showed that at the harshest conditions lysozyme activity decreased to 88 % compared to the unprocessed sample. Analyzing the results for the influence of the milling parameters it became clear that temperature of the milling gas had no significant effect on the resulting bioactivity. The decrease depended significantly on the chosen milling pressure and number of milling cycles. It was possible to fit a model describing the obtained data ($R^2 = 0.776$, $Q^2 = 0.706$). Figure 6.7 illustrates the impact of milling cycles (x_2) and of the used pressure (x_1). Performing the experiments in presence of 1mM Detapac for complexation of iron ions had no effect on measured bioactivity.
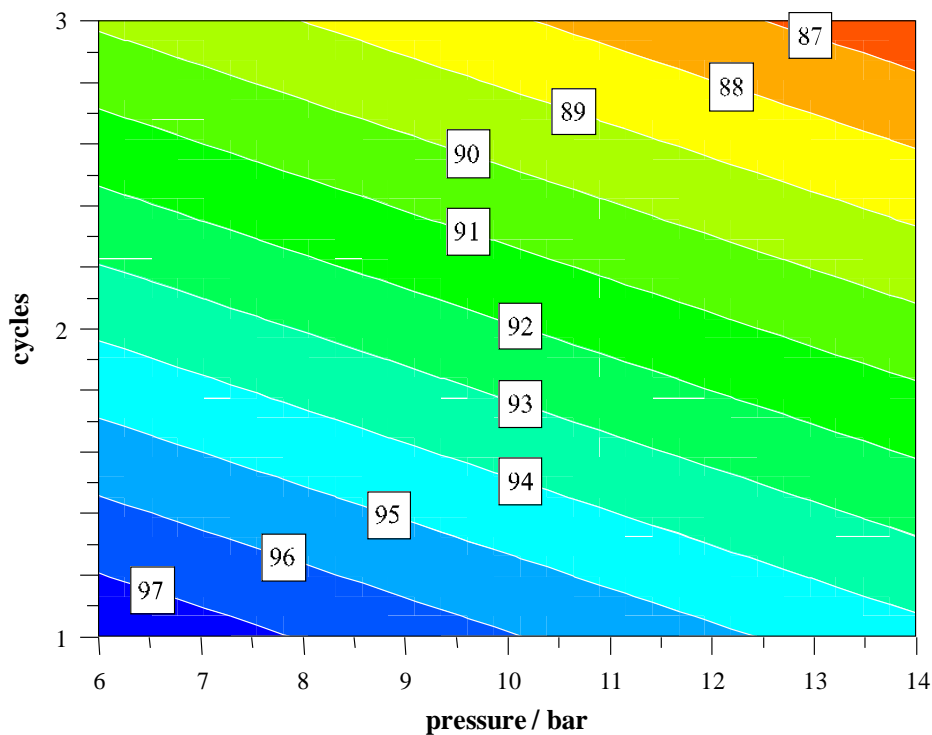
Fig. 6.7 Activity of lysozyme in percent depending on number of milling cycles and milling pressure. Both factors decrease activity of lysozyme, but the number of milling cycles has a bigger effect ($y = 92.0864 - 1.3292x_1 - 3.0048x_2$)

Based on the equation in fig. 6.7 you can state that the number of milling cycles had a bigger impact on the activity of lysozyme than the applied pressure. In literature the negative effect of acceleration in a jet stream and following impaction on bioactivity of catalase particles is described [17]. When comparing the bioactivity results of insulin and lysozyme it is important

to keep in mind that the sensitivity of the enzymatic assay of lysozyme is much higher than for the chondrocyte cell assay of insulin. Nevertheless, for insulin the mechanical stress in the jet mill seemed not to influence its bioactivity. One reason for these different results could be the much larger lysozyme particles in the beginning. Due to this fact particles had to undergo many more breakage events to reach the same sizes as determined for insulin. During breakage events temperatures of several hundred Kelvin may occur at the newly created surfaces [107], which may lead to persisting changes in the molecules at the particle surface.

Determination of the iron content

Another factor which may decrease the bioactivity of lysozyme and cause a drop in fluorescence intensity is metal wear of the mill components. The iron content was measured for selected lysozyme samples by ICP-OES. A slight increase depending on the number of milling cycles was detected (fig. 6.8). The content of the unprocessed control sample was 6.32 ppm, which increased to 8.9 ppm after three cycles at 14bar.
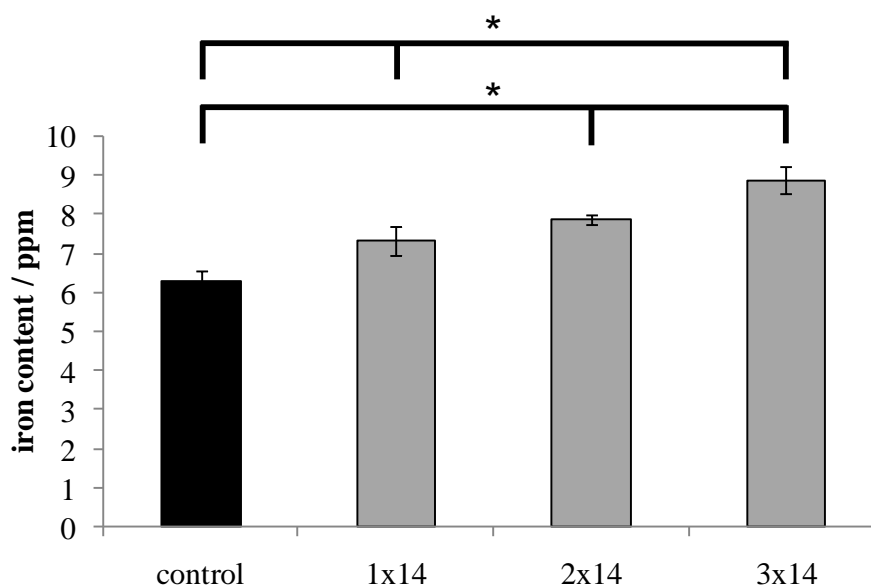

Fig. 6.8 Iron content of lysozyme powder determined by ICP-OES measurements (p<0.05)

Platz et al. described that after micronization of human growth hormone 40 % of the powder was insoluble in water [81]. It was possible to reduce this fraction to 2.5 to 7.5 % by

exchanging some silver soldered joints and copper gas lines with more inert materials like stainless steel. However, with the used setup for these experiments only stainless steel and PTFE came in contact with the proteins. An effect of iron, which is the essential element in stainless steel, on lysozyme was described by Sellak et al. [164]. It was published that lysozyme is able to bind iron and is then much more sensitive to damages by radicals which results in a loss of bioactivity. Additionally, a decrease in tryptophan fluorescence was described. However, these results were described for concentrations higher than 1800 ppm and our results showed only a small increase from 6 to 9 ppm of iron content within the milled powder, which is probably due to attrition in the milling chamber. As mentioned before the addition of an iron complexing agent (Detapac) to the tested protein solutions did not show any improvement in lysozyme bioactivity. Therefore, a reduction of the bioactivity of lysozyme by metal contamination due to attrition can be neglected.

Impact of jet milling on lysozyme crystals

Another interesting question was, if the solid state itself has an effect on the protein stability. As described before, no loss in activity was determined for the crystalline insulin but for the freeze dried lysozyme. Therefore, the impact of the jet milling process on lysozyme crystals was tested, too.

The crystals, obtained by a method described in chapter 2, showed a broad size distribution between 1 and 1000 μm with a d90 value of 85.6 μm (fig. 6.9). After one cycle at 14 bar the d90 was reduced to 6.9 μm with some coarser particles still present. Three cycles at 14 bar resulted in narrow distribution with a d90-value of 4.3 μm, which is slightly smaller than for the freeze dried powder.
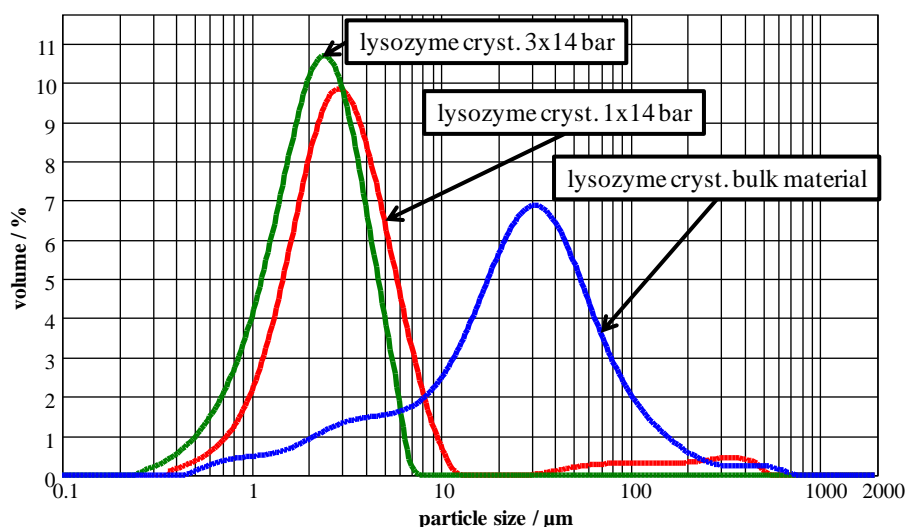
Fig. 6.9 Size distribution of lysozyme crystals before and after micronization

The bioactivity experiments revealed that even for the lysozyme crystals a drop in activity was present. Similar to the previous results the activity was reduced to 89 % after three milling cycles at 14 bar (fig. 6.10). For lysozyme the crystalline form seemed not to increase the stability against changes due to the mechanical stressing by the milling process.
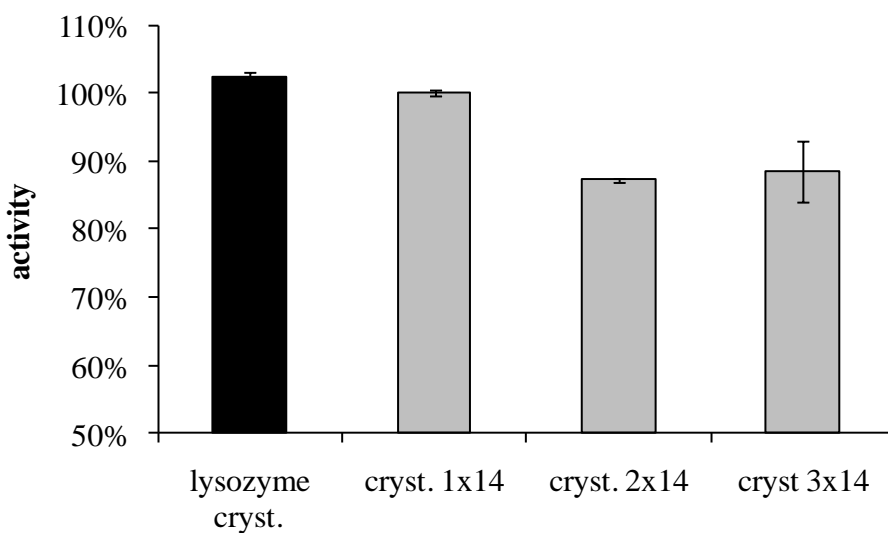
Fig. 6.10 Bioactivity of crystalline lysozyme before and after micronization

Summary and conclusion

The experiments with lysozyme revealed that the chemical stability was not influenced by the micronization process. By HPLC and MALDI-ToF no changes due to the milling process were determined. Also no significant differences in the secondary structure analyzed by CD spectroscopy were visible. However, by fluorescence measurements significant differences between bulk material and the micronized powder were detected indicating changes in the tertiary structure of the protein. The intrinsic fluorescence due to tryptophane decreased by about 12% and the surface hydrophobicity (RSH) in solution increased 12-fold compared to the reference. These changes seemed to be the reason for the drop in activity determined after micronization. Higher iron content due to attrition in the milling chamber was excluded as a reason for this decrease. This effect was not influenced by the solid state of lysozyme. The investigated crystals showed similar results as the freeze dried form.

As a conclusion it can be stated that there are structural changes within the protein molecules induced by the jet milling process resulting in a decrease in bioactivity. As the most critical parameter seems to be the number of milling cycles, repeated milling should be avoided.

Chapter 7

Impact

of

Jet Milling

on

BSA

Introduction

As third model protein for the micronization experiments BSA was chosen. It is a well-studied protein often used as a model substance for example in controlled release experiments [165] or as reference and calibration substance in several methods for protein analytics, like in the bicinchonic acid assay for protein quantitation [126] or utilized to prevent protein adsorption to surfaces. As the most abundant plasma protein it is easily available in larger amounts by isolation from bovine plasma. BSA has a single polypeptide chain consisting of about 583 amino acid residues (66 430 Da [166]) building up three domains each stabilized by a network of in all 17 disulfide bonds and one free thiol group [167]. In-vivo it plays an important role in colloidal osmotic blood pressure and is responsible for the transport, distribution and metabolism of a variety of substances to which it binds (metals, fatty acids, hormones and therapeutic drugs) [168].

Results and discussion

Impact of jet milling on the solubility of BSA

While preparing the micronized BSA samples for analysis it occurred that it was not possible to completely dissolve the micronized sample in water. In order to investigate if this phenomenon is linked to some milling parameters, the amount of the insoluble fraction was determined. Fig. 7.1 shows the results for the different samples.
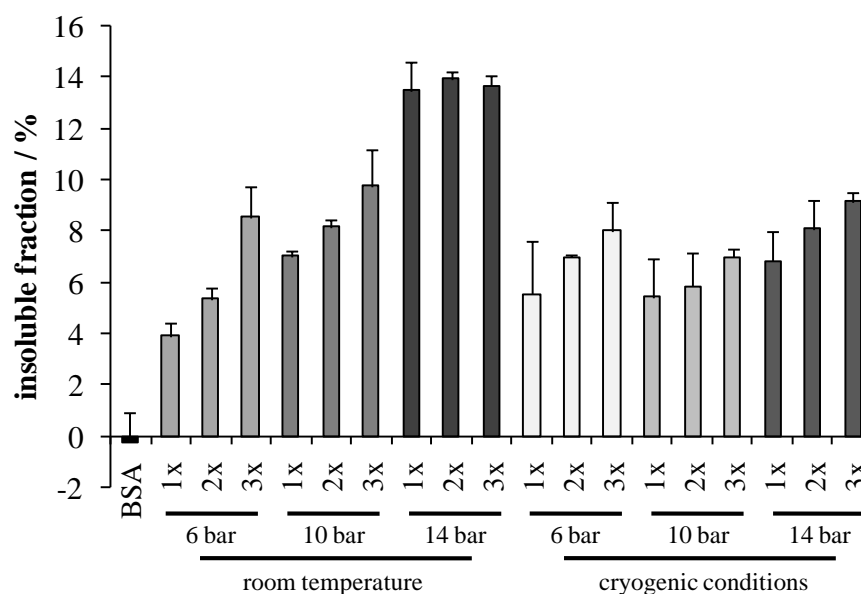
Fig. 7.1 influence of milling pressure (6 to 14 bar), number of milling cycles (1 to 3) and milling gas temperature on the amount of insoluble BSA fractions

A correlation between the milling parameters pressure, number of milling cycles and milling gas temperature is with the incidence and amount of insoluble fractions is clearly visible. For the samples ground at room temperature with increasing pressure and increasing number of milling cycles the amount of insoluble BSA increased significantly. Starting from 3.9 % for one cycle at 6 bar leading to a maximum of 13.9 % at 2 cycles at 14 bar. At 14 bar no further increase due to the milling cycles was detectable, since the values reached a plateau. For the samples processed at cryogenic conditions the results were different. Nearly no impact of the milling gas pressure was visible and only a small effect of the milling cycles. The amount of the insoluble fraction stayed constant in a range of 6-9 %. For quantifying these effects the results were analyzed by statistical experimental design methods using the same setup as for the particle size analysis, but using the amount of the insoluble fraction in percent as the response parameter.

A model with a Q^2 value (the fraction of the variation of the response that can be predicted by the model) of 0.923 and a R^2 value (the fraction of the variation of the response explained by the model) of 0.972, which are both indicating an excellent fitted model. The calculations resulted in the following equation:

$$y=7.1230+2.1300x_1+1.2549x_2+1.3323x_3+1.7027x_1^2-0.4677x_1x_2+1.5983x_1x_3$$

The highest factor for x_1 indicates that the applied milling pressure had the biggest impact on the creation of insoluble BSA fractions. Also the effect of the temperature is confirmed. This is a hint that the process leading to the insoluble fractions is partly temperature dependent and may be due to the created heat at the breakage surfaces of the protein particles [107].

Based on these results two questions occurred. First: what changes in the solid BSA powder are induced by the milling process and second: is it possible to prevent the creation of insoluble fractions?

SEM pictures of the remainder
The SEM pictures of the insoluble fraction gave no hint about the underlying mechanism. As shown in fig.7.2 only an unstructured mass was visible, due to agglomeration and the centrifugation steps.
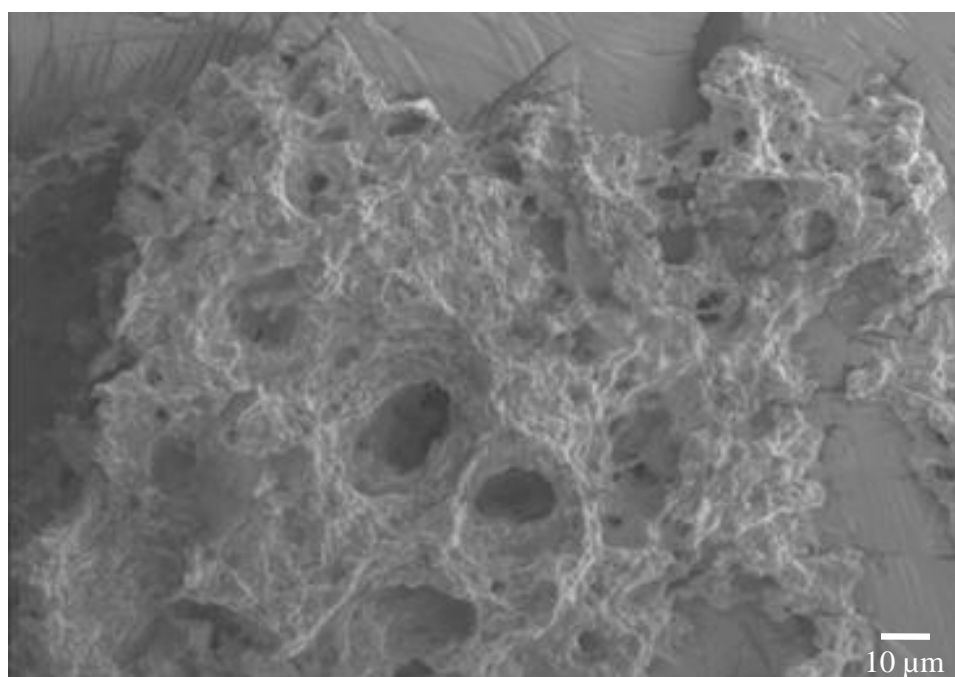

Fig. 7.2 SEM picture of the remainder after dissolving micronized BSA in water

Dissolution tests with the water insoluble BSA fractions

To identify the changes within the BSA several solvents were tested in order to get the remainder into solution. The results showed that the water-insoluble BSA fraction was dissolved only by a combination of denaturizing and reducing agents. 6M urea or 6M guanidine HCl both in combination with 10mM dithioerythritol and 1mM EDTA were the only suitable solvents. For all other setups only the appearance of the sediment differed. In hydrophilic environment like water big flakes formed and in more lipophilic media the powder particles stayed separated. This indicates that the insoluble particles had a more lipophilic surface and wettability may be part of the problem. Nevertheless, only the combination with a reducing agent like dithioerythritol resulted in a clear solution. The fact that dithioerythritol alone was not able to dissolve the protein aggregates implied that the wettability of the particles by this solution was too low or that not all the disulfide bonds were accessible and only the combination with the denaturizing agents loosened the aggregates. Therefore, chemical reactions like a disulfide interchange were possible explanations for the creation of insoluble fractions. Similar results are known for the moisture-induced aggregation of BSA Liu et al. [169].

Nevertheless, the found solvents were not suitable for performing further analysis, because the molecule structure had been totally destroyed und all disulfide bonds had been broken up so that no differences between the samples were detectable. Therefore, further experiments were needed to investigate if sulfhydryl groups are responsible for the creation of the insoluble fraction.

Determination and blocking of free SH-groups

BSA contains 17 disulfide bonds and one free thiol group of a cysteine residue. This facilitates the possibility of a thiol-disulfide interchange by a nucleophilic attack of an ionized thiol on a disulfide linkage resulting in covalent protein aggregates. Therefore, the idea was to block the free thiol groups and investigate the effect on the solubility properties after micronization.

As described in chapter 2 the determination of free thiol groups was performed by using Ellman´s reagent. Fig. 7.3 shows the free thiol groups per molecule BSA before and after S-alkylation by iodoacetamide determined by this method. BSA provides 0.4 free SH-groups per molecule, which matches the values described in literature [165]. The fraction without a free sulfhydryl group is due to interaction with plasma cysteine and a less content with

glutathion [170,171]. By S-alkylation the content was reduced to 0.05 free SH-groups per molecule.
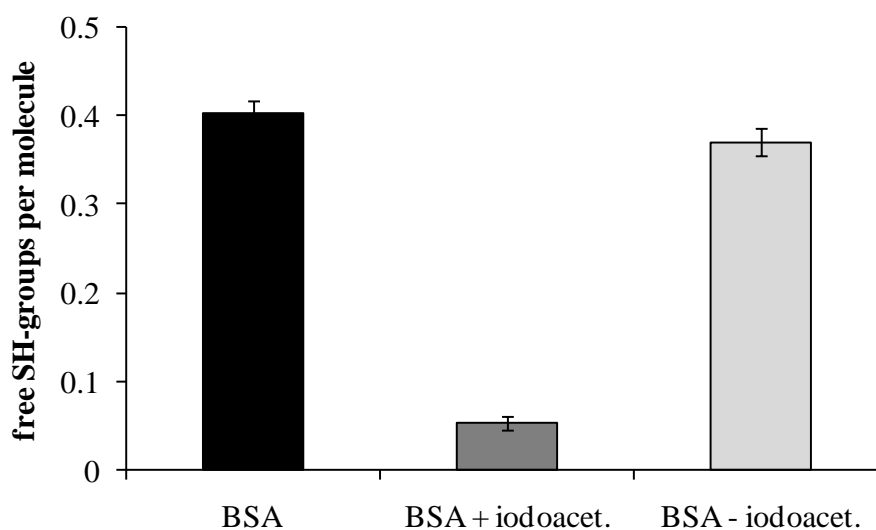
Fig. 7.3 SH-groups per molecule BSA. Left bar shows results for unprocessed BSA, middle bar shows effect of S-alkylation by iodoacetamide, right bar shows impact of the preparation process for S-alkylation without addition of iodoacetamide.

This modified BSA was now micronized at 14 bar one to three times. The unmodified BSA was micronized, too, because a new batch of BSA was used for these experiments. The following analysis of solubility in water showed that no significant difference between the samples was obtained (fig. 7.4). The slightly lower values compared to Fig. 7.1 are due to the used new batch of BSA despite the fact that for the old batch only 0.15 free thiols per molecule BSA were measured.

Therefore, the impact of the free SH-group on the creation of insoluble fractions by thiol disulfide interchange can be neglected.
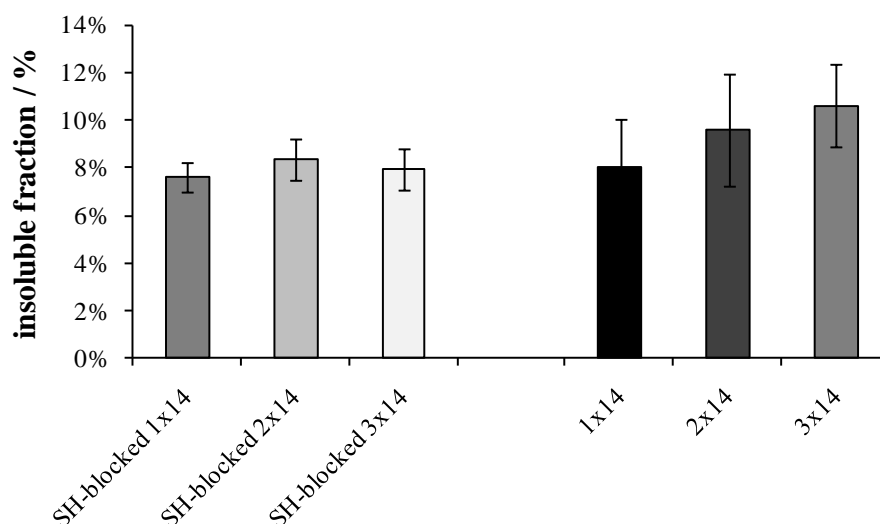
Fig. 7.4 comparison of the amount of insoluble BSA before and after S-alkylation micronized at 14 bar one to three times; left three bars show the results of SH-blocked BSA, as a comparison right three bars show results for unmodified BSA

HPLC analysis of soluble BSA fraction

The solution was also analyzed by HPLC. The comparison of the different samples revealed no changes for the SH-blocked samples. Nevertheless, a small difference was detected for unmodified BSA. A small peak visible in the unprocessed sample (retention time 15.3 min), not completely separated from the main peak (retention time 13.9 min), disappeared in the micronized sample (Fig. 7.5). Unfortunately it was not possible to increase the resolution or relate the peak to a specific substance.
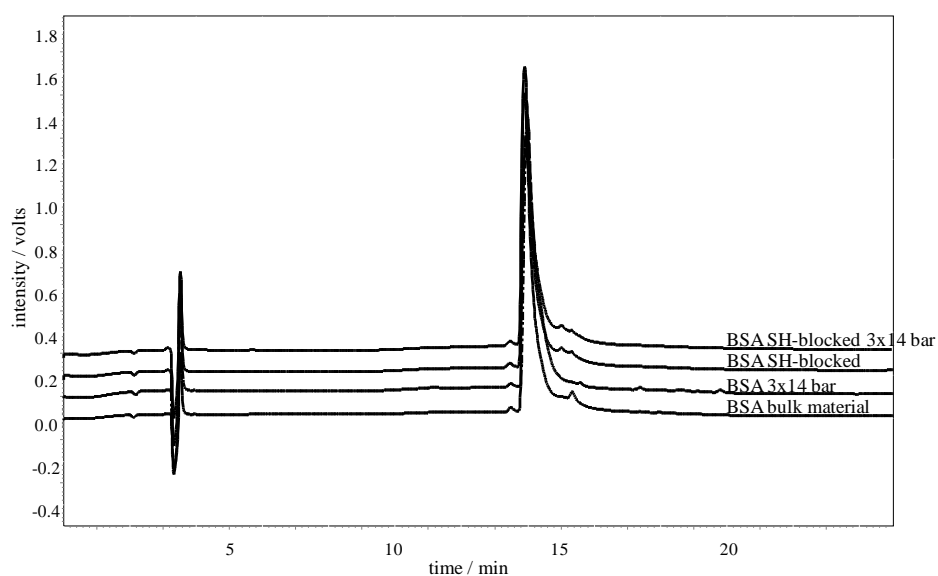
Fig. 7.5 HPLC analysis of different BSA samples at 210 nm

Micronization of l-glutathione (GSH)

In order to investigate if oxidative processes involving the free SH-group are responsible for the formation of intermolecular disulfide bonds, micronization experiments were performed with l-glutathione, a small and easy to analyze peptide with a free SH-group. For such a small peptide the probability of reactions should be increased and the formed aggregates should be soluble in water and therefore accessible to analytical methods.

The reduced form of GSH containing the free SH-group was micronized 3 times at 14 bar and afterwards was analyzed for changes by using the thiol assay and HPLC. Fig. 7.5 shows the free SH-groups per molecule of the unprocessed bulk material (GSH red) compared to the reference of the oxidized form (GSH ox) and to the three times micronized sample of the reduced form.
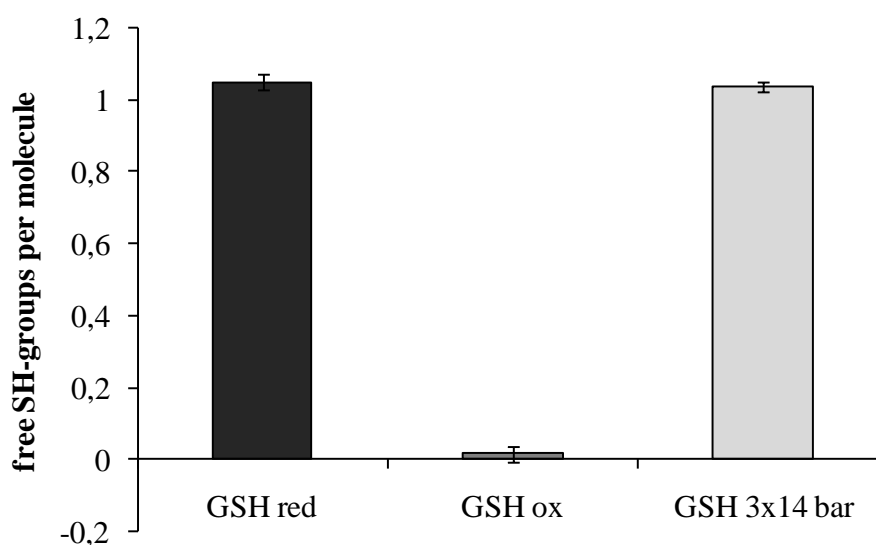
Fig. 7.5 Free thiol content per molecule GSH of the reduced (GSH red) and oxidized form (GSH ox) compared to the jet milled reduced form

No changes after the jet milling process compared to the unprocessed reference were visible. These results were confirmed by the results of the HPLC analysis of these samples (fig. 7.6). For the reduced form, one main peak related to the monomer with the free thiol groups and a small peak identical to the oxidized form was detected. After micronization the same chromatogram was obtained with no additional peaks and no changes in the peak to peak ratio.
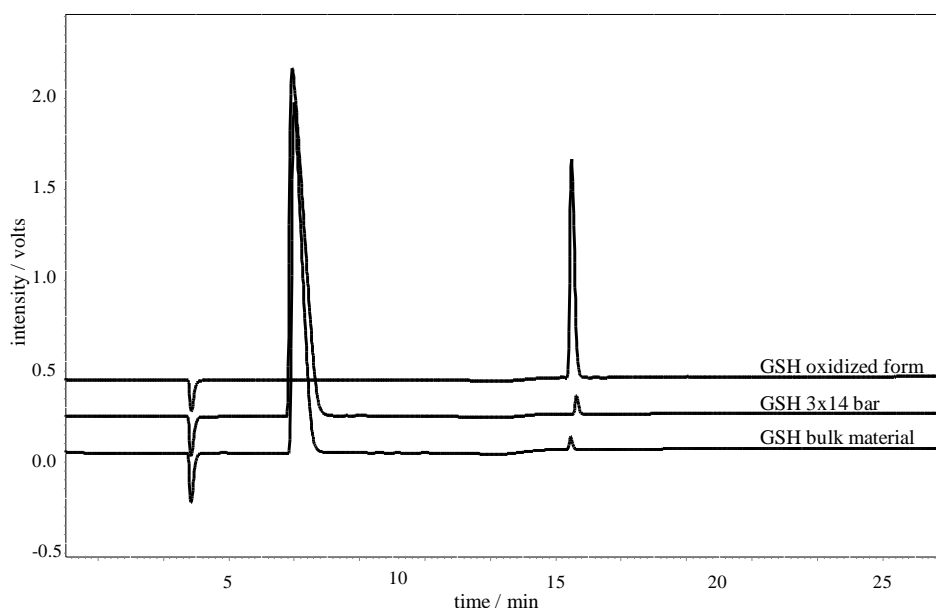
Fig. 7.6 HPLC chromatogram obtained at a detector wavelength of 210 nm of GSH in reduced and oxidized form and after jet milling three times at 14 bar

These results support the results from the BSA experiments, indicating that the free thiol groups are not reactive under the conditions during the jet milling process and are not responsible for the creation of insoluble fractions of BSA and therefore an alkylation of the free SH-group did not improve the results of the BSA micronization.

Micronization of fatty acid free BSA (BSA FAF)

Based on the results of the solvent experiments, another reason for the formation of insoluble particles may be an increased hydrophobicity on the surface of the micronized protein particles. Normally up to 3 mol/mol fatty acids are bound to BSA [172]. These consist mainly of mono unsaturated or saturated C_{16} and C_{18} fatty acids. In solution bound fatty acids result in compact conformation of the BSA molecule [173] and diminish the accessibility of albumins disulfide bonds in aqueous solutions [174]. Costantino et al. stated that the removal of the fatty acids increased the solid state aggregation of BSA [165]. Therefore, experiments were performed with fatty acid free BSA (fatty acid content <0.01 %).

Our experiments showed no significant difference (comparison of samples with the same number of milling cycles) of the fatty acid free samples to the fatty acid containing ones (fig. 7.7). Only a small trend to less insoluble fractions was visible, which is a contrast to the before mentioned literature results.
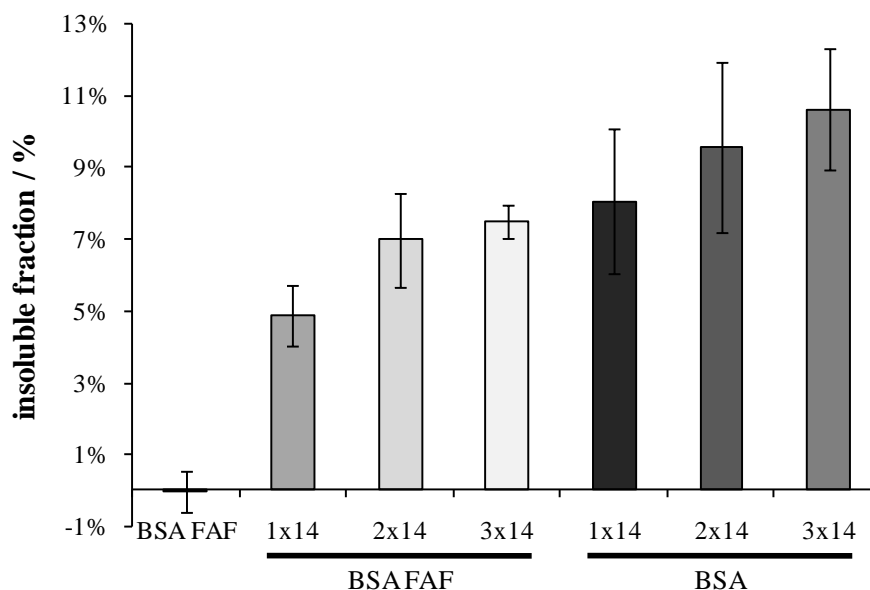
Fig. 7.7 Resulting insoluble fraction after micronization of fatty acid free BSA (BSA FAF) (bars 2, 3 and 4) compared to the fatty acid containing standard BSA (bars 5, 6 and 7); first bar shows results of the control group with unprocessed fatty acid free BSA

One possible reason may be a rearrangement of the fatty acids on the surface of the protein particles due to the micronization process increasing the surface hydrophobicity.

Fluorescence measurements of BSA in solution

Besides the insoluble fractions the characterization of the soluble fraction was important. The samples were analyzed for changes in the tertiary structure of BSA molecules by fluorescence methods. Intrinsic fluorescence measurements are a useful tool to identify structural changes within the tertiary structure of proteins, while the utilization of a hydrophobic probe like 8-anilino-1-naphtalenesulfonic acid ammonium salt (ANS) reveals changes at the surface of the protein molecule.

The intrinsic fluorescence measurements showed an emission maximum at 351 nm for all samples and the fluorescence intensity was equal for all samples (fig. 7.8). This indicates that no changes in the environment around the excited tryptophan residues were induced by the micronization process.
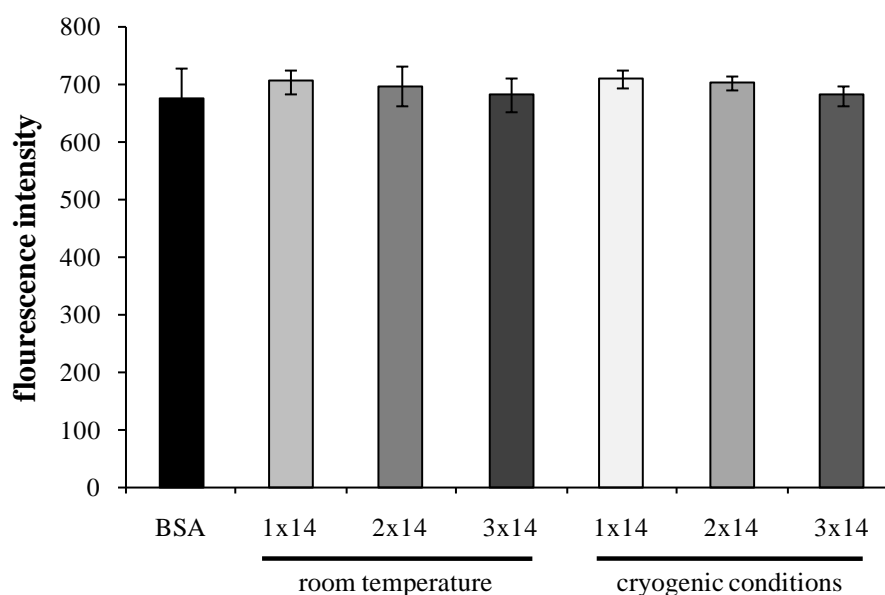
Fig. 7.8 intrinsic fluorescence intensity measured at a wavelength of 351 nm of BSA before and after micronization; first bar shows results of the unprocessed BSA in comparison to samples micronized at a pressure of 14 bar one to three times at room temperature (bars 2, 3 and 4) and at cryogenic conditions (bars 5, 6 and 7)

The surface hydrophobicity of the BSA molecules in solution was investigated by addition of ANS as a hydrophobic probe. In a hydrophobic environment, e.g. by hydrophobic amino acids on the surface of the protein, the fluorescence intensity of ANS is increased. The calculated relative surface hydrophobicity (RSH) revealed a significant decrease of hydrophobicity for the micronized samples compared to the unprocessed bulk material (fig. 7.9).
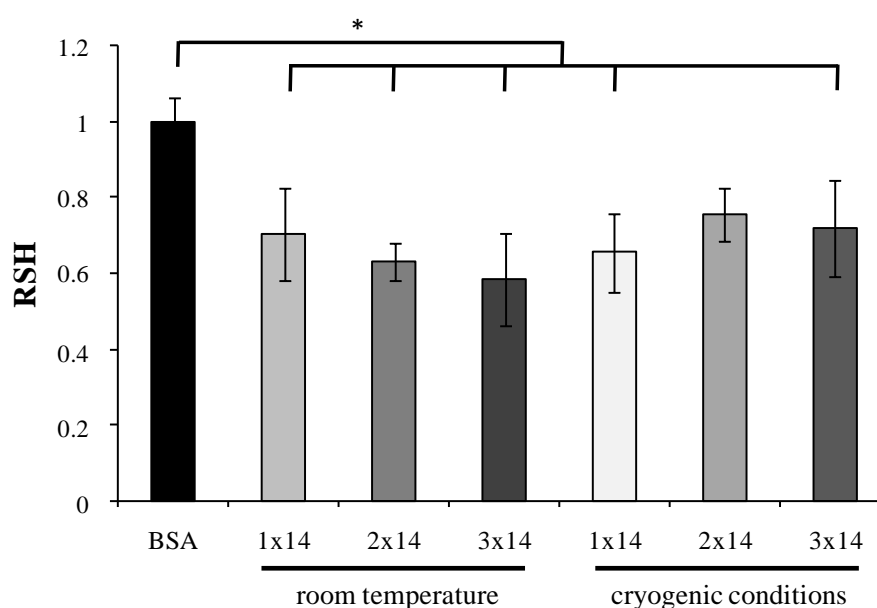
Fig. 7.9 Relative surface hydrophobicity (RSH) of BSA in solution; samples were jet milled at 14 bar one to three times at room temperature (bars 2, 3 and 4) and cryogenic conditions (bars 5, 6 and 7) compared to unprocessed BSA (left bar)

Between the samples jet milled at room temperature and these milled at cryogenic conditions no differences were visible. The observed decrease in surface hydrophobicity of the protein molecules in solution indicates a rearrangement of the surface structure presented to the water interface. Hydrophobic groups seem to be transferred to the interior of the molecules. Remarkably these changes had no effect on the intrinisic fluorescence measurements.

FT-IR analysis of the BSA powder

In order to get an idea of the structural changes within the protein powder due to the micronization process FT-IR experiments were performed with the samples in solid state. By FT-IR measurements it is possible to investigate the secondary structure of proteins in solid state. Because it was not possible to dissolve the insoluble fraction without destroying the whole molecule structure, FT-IR analysis seemed to be a good option to get a closer look on the obvious changes induced by the jet milling process to part of the BSA proteins. Tests were performed with samples micronized at 14 bar, which were compared with the unprocessed BSA powder. Additionally a sample of the separated insoluble fraction was analyzed.

The evaluation of the second derivative analysis of the amide I region showed differences of the micronized samples to the reference (fig. 7.10).

wave number	1700-1687	1687-1681	1681-1674	1674-1668	1668-1659	1659-1644	1644-1633	1633-1618	1618-1610
Control	10.01%	7.74%	7.48%	6.57%	9.39%	24.95%	17.47%	16.31%	5.10%
1x14	5.35%	4.52%	4.47%	2.81%	6.70%	33.51%	24.90%	18.46%	1.60%
2x14	6.42%	5.18%	6.31%	3.05%	7.45%	34.99%	23.40%	15.37%	1.53%
3x14	7.85%	5.28%	6.61%	3.98%	8.45%	32.67%	23.08%	14.98%	1.40%
insoluble 3x14	11.63%	7.08%	8.18%	5.67%	9.81%	24.62%	17.08%	17.14%	3.64%

Fig. 7.10 Comparison between the areas under the different peaks visible in the second derivative of the measured absorption at different wavenumbers by FT-IR

Unexpectedly the isolated insoluble fraction showed no difference to the unprocessed BSA powder. The most probable reason is that the particle size of the samples had a significant effect on the measured result [193], because the sample of the insoluble fraction had been

obtained after centrifugation in water in order to separate it from the soluble fraction. The result was a flake-like structure. Although the samples were ground in an agate mortar before measurement no sizes below 10 μm were achieved like for the micronized samples.

Co-lyophilization of BSA with poly(ethylene glycol) (PEG)

So far three possible reasons for the formation of insoluble BSA fractions were discussed. First, the heat created during the milling process, indicated by the reduced amount of insoluble particles after jet milling under cryogenic conditions. Second, the formation of BSA aggregates and third, an increase of surface hydrophobicity of the particles. To inhibit these phenomenons the idea was to embed BSA into poly(ethylene glycol) (PEG) as a so-called bulking agent [175]. On the one side it would minimize the intermolecular contact between single BSA molecules and on the other side it could result in a hydrophilization of the resulting particles. To investigate the effect, BSA was mixed at different ratios with PEG 10 000, dissolved in water and freeze-dried afterwards. The freeze-dried powder was micronized in the jet mill under the same conditions as the pure BSA samples.

	after freeze-drying	**micronized 3x at 14 bar**
BSA		
BSA : PEG 9 : 1		
BSA : PEG 1 : 1		
BSA : PEG 1 : 9		
PEG		
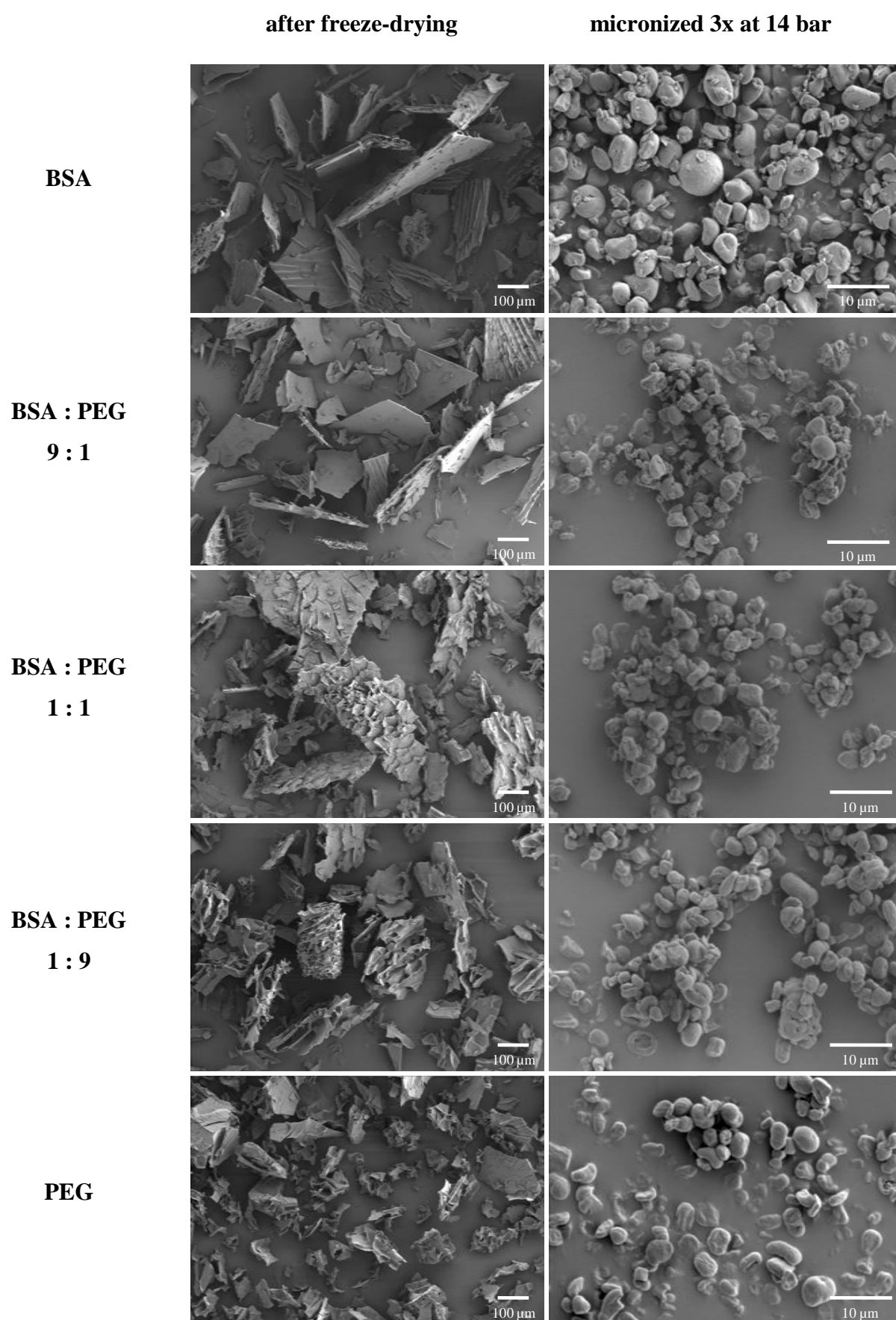
Fig. 7.11 SEM micrographs of BSA PEG mixtures after freeze-drying and after micronization

Particle size analysis revealed that depending on the ratio of BSA and PEG the d90-value changed. The higher the PEG content was the larger were the resulting particle sizes (fig. 7.12). Fluctuations after one milling cycle are mostly due to differences in the particle size distribution of the starting material after freeze-drying.
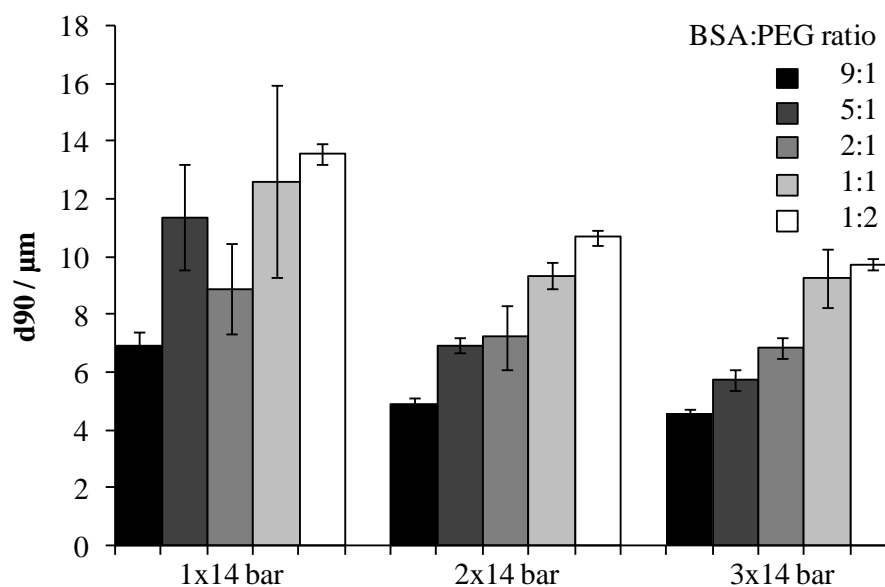
Fig. 7.12 Particle size (d90-value) after micronization at 14 bar for the different BSA PEG mixtures

Afterwards the amount of the insoluble fraction for the different samples was analyzed. It appeared that with increasing PEG ratio this fraction was decreased and at a ratio BSA to PEG of 2:1 no insoluble particles were detectable anymore (fig. 7.13).
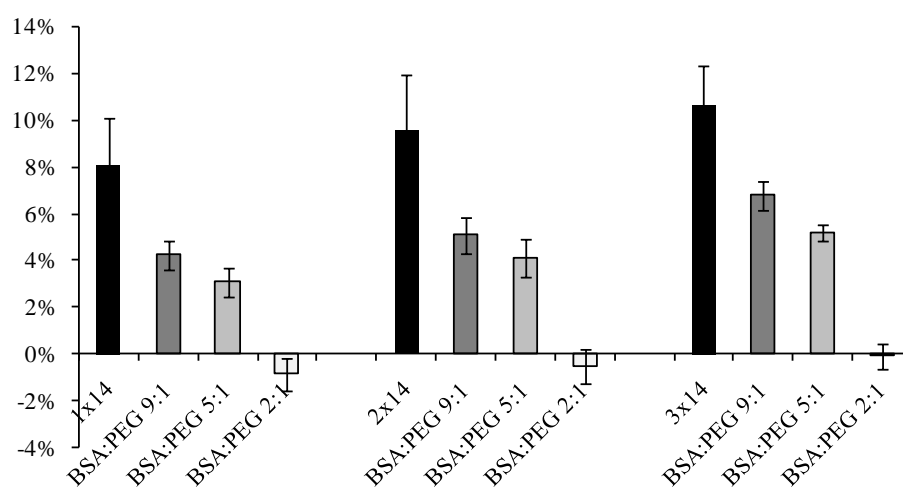
Fig. 7.13 Determination of the insoluble fraction of the different BSA PEG mixtures after micronization

This effect of PEG is probably due to the combination of the aforementioned effects of separating the BSA molecules and keeping the particles hydrophilic. Additionally the fact that with a higher amount of PEG more heat of the grinding process is transferred to PEG molecules than to BSA. That increased the protection of the BSA molecules furthermore.

Summary and conclusion

Due to the micronization of BSA by jet milling insoluble fractions of protein powder were created. Depending on the milling parameters the amount of this fraction reached up to 14 %. Three possible reasons for this phenomenon were discussed and investigated. First, the influence of possible heat creation on the particle surface during the particle breakage was confirmed by the positive effect of cryogenic milling gas temperatures on the reduction of the insoluble fraction. Second, thiol group reactions were investigated. Based on the fact that the remainder was only soluble by the combination of denaturizing and reducing agents, a thiol disulfide interchange as described by literature [169] was probable. Nevertheless, blocking the crucial free thiol group did not improve the milling results. Experiments with l-glutathion revealed that no oxidation of SH-groups took place caused by the applied milling conditions. Third, an increased surface hydrophobicity was suggested, but fluorescence measurements in solution were contradictory to this assumption. Nevertheless, micronization of fatty acid free BSA improved the results slightly.

No analytical method was found to characterize the insoluble fraction in detail. By dissolving the remainder with denaturizing and reducing agents the structure of the protein was totally destroyed and no hints for former changes were detectable. Unfortunately FT-IR measurements seemed to be influenced more by the particle size of the samples than by structural changes.

Nevertheless, besides the lowering of the milling gas temperature the mixture of BSA with PEG as a bulking agent was successful in lowering the amount of the insoluble fraction. Additionally it facilitated another parameter for controlling the final particle size.

Chapter 8

Lipid Microparticles

by

Jet Milling

Introduction

As mentioned in chapter 1, release systems which deliver proteins for several days or even months are investigated. They are one option of enhancing the compliance with protein drugs of the patients. Optimally, these devices are easily administrable and consist of a material that has an adjustable release profile, is biocompatible, biodegradable and does not harm but rather stabilizes the sensitive protein drugs. Several materials were tested during the last three decades, e.g. containing: (1) natural materials, like albumin, cellulose, chitosan, hyaluronic acid, dextran and starch; (2) synthetic polymers, like polyanhydrides, polyamides, polyesters and polyorthoesters; (3) hydrogels, consisting of alginates, collagen, fibrin or gelatine [176]; and (4) lipid materials, like cholesterol, fatty acids, lecithin, waxes, dipalmitoyl-phospatidylcholin, mono- and triglycerides [177]. They were applied as nano- or microparticles, cylindrical implants or scaffolds for tissue engineering, which are just some of the tested formulations.

Synthetic polymers like poly(lactid-co-glycolic acid) (PLGA) are most often used at the moment. They can be easily customized and have a defined structure and therefore well-defined degradation pathways [178]. Their acceptable biocompatibility is well investigated [179,180] and many are approved by the FDA. Nevertheless, some drawbacks in combination with protein drugs occurred. During the preparation steps high shear forces, temperature increase and the use of organic solvents are often necessary [181] and proteins may be harmed by the occurring interfaces [182]. Additionally, during the erosion of the polymers the microenvironment within the devices often changes. A drop of the pH, an increase of the osmotic pressure and acylating degradation products [183] are fatal factors for protein stability and bioactivity.

Lipid materials, like triglycerides, are one alternative group of materials for the development of controlled release drug delivery devices. They are generally recognized as biocompatible and biodegradable [184] due to the fact that they are substances physiologically found in the body. Several proteins, e.g. insulin [185], somatostatin [186], thymocartin [187], Interleukin-18 [79] and BSA [188] have been incorporated in different lipid formulation, like compressed cylinders or microparticles resulting in protein release over days or even months. Triglycerides proved to be promising material for protein release without the induction of protein degradation.

Nevertheless, the production of protein containing microparticle formulations tends to be a critical and difficult process. Especially formed interfaces and high shear forces during the

preparation step are very critical for protein stability. Solvent evaporation, melt dispersion techniques [189] or spray drying of O/W emulsions or of organic lipid solutions [190] are prone to harm proteins. So several excipients have to be added to maintain protein stability or increase encapsulation efficiency. Therefore, there are approaches to incorporate proteins into microparticles as solids. Maschke et al. encapsulated insulin into lipid microparticles with an average diameter of 230 μm by spray congealing of a protein suspension in molten lipid without any loss in protein integrity [185]. Nevertheless, structure modifications of the lipid were detected after this process due to the rapid freezing of the molten mass, which leads to recrystallization and structural change during storage and protein release.

Due to these observations the idea of jet milling of lipids to obtain microparticles was born. Jet milling is a well known method for powder micronization and is often indicated for the processing of heat sensitive substances. However, high temperatures occurring on the breakage surface are possible [107]. When micronizing lipids some questions should be investigated:

1. Is it possible to micronize lipids, as very soft substances, by jet milling and establishing it as an alternative method for lipid microparticle preparation?

2. How are the particle properties influenced by the milling process? Are there changes in structure or modification of the investigated lipid?

3. Is it possible to correlate these changes to process parameters of the milling process, like milling gas temperature, and may lipids be utilized as model substances to analyze energetic effects of jet mill grinding on products?

Some experiments were performed to get a basic understanding of the underlying processes.

Results and Discussion

Particle size and size distribution

The sieved glycerol tripalmitate was micronized at 4 bar at room temperature and under cryogenic conditions with a milling gas temperature of -65°C. Measurements by laser light diffraction revealed that after one milling cycle particles with a d50 value of 34.5 µm at room temperature and 24.5 µm after cryogenic grinding were obtained (fig. 8.1 and 8.2 upper graphics). However, the size distribution was very broad with particles up to 1000 µm indicating a large fraction of non-milled particles. The result was improved by repeated stressing of the lipid powder. After 3 milling cycles narrow size distributions with an average diameter of 9.7 µm at room temperature and 8.3 µm for the cryomilling experiments were determined. For both setups the d90 value was below 20 µm after the three milling cycles.

These results clearly show that for glycerol tripalmitate one milling cycle did not lead to a sufficient particle size reduction. Glycerol tripalmitate is quite a soft material which tends to deform plastically without initiating cracks due to mechanical stressing. Repeated stressing may induce an embrittlement of the substance and enhance the size reduction process [101]. Another factor influencing the resulting particle size was the milling gas temperature. Especially after the first milling cycle the difference was obvious, with d50 values discerning by 10 µm. The relatively low melting point of glycerol tripalmitate (onset 62.71°C, maximum 64.79°C) may be one reason why it tended to deform more plastically due to impact grinding at room temperature than at a milling gas temperature of -65°C. This effect is exploited for the cryogenic grinding of some rubber-like materials [136].

Particle size measurements were repeated after three weeks of storage at room temperature and compared to the aforementioned results, which were measured on the day of production. An increase of particle size was determined for all samples (fig. 8.1 and 8.2 lower graphs). The d50 values of the samples ground at room temperature increased from 34.5 µm up to 146.6 µm (1x4 bar) and from 9.6 µm to 13.6 µm (3x4 bar), respectively. Particle size of the cryomilled samples increased as well, from 24.5 µm to 30.7 µm and from 8.3 µm to 9.9 µm.

Jet milling seems to induce changes within the lipid particles which result in particle growth during storage of the samples. These changes may be caused by high temperatures occurring at the breakage surfaces as described by Weichert et al. [107]. Glycerol tripalmitate is a highly crystalline substance normally existing in the stable β-modification. The applied stress and increased temperatures could probably result in an amorphisation of the particle surfaces or

even in the formation of polymorphic structures. For glycerol tripalmitate an unstable α-modification and a metastable β´-modification are described [191,192].
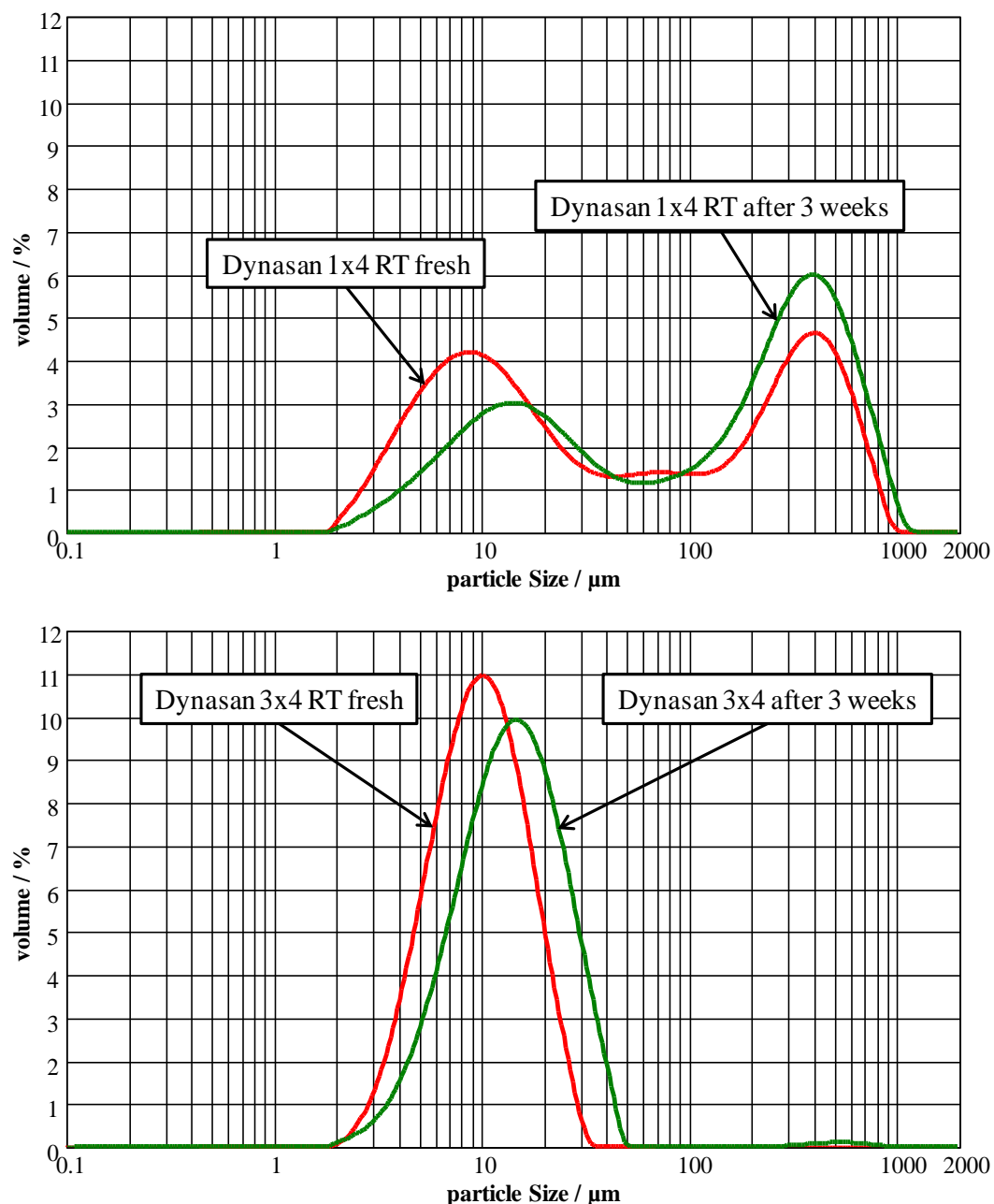
Fig. 8.1 Particle size distribution of lipid microparticles after jet milling at room temperature and 4 bar compared to the results after 3 weeks of storage
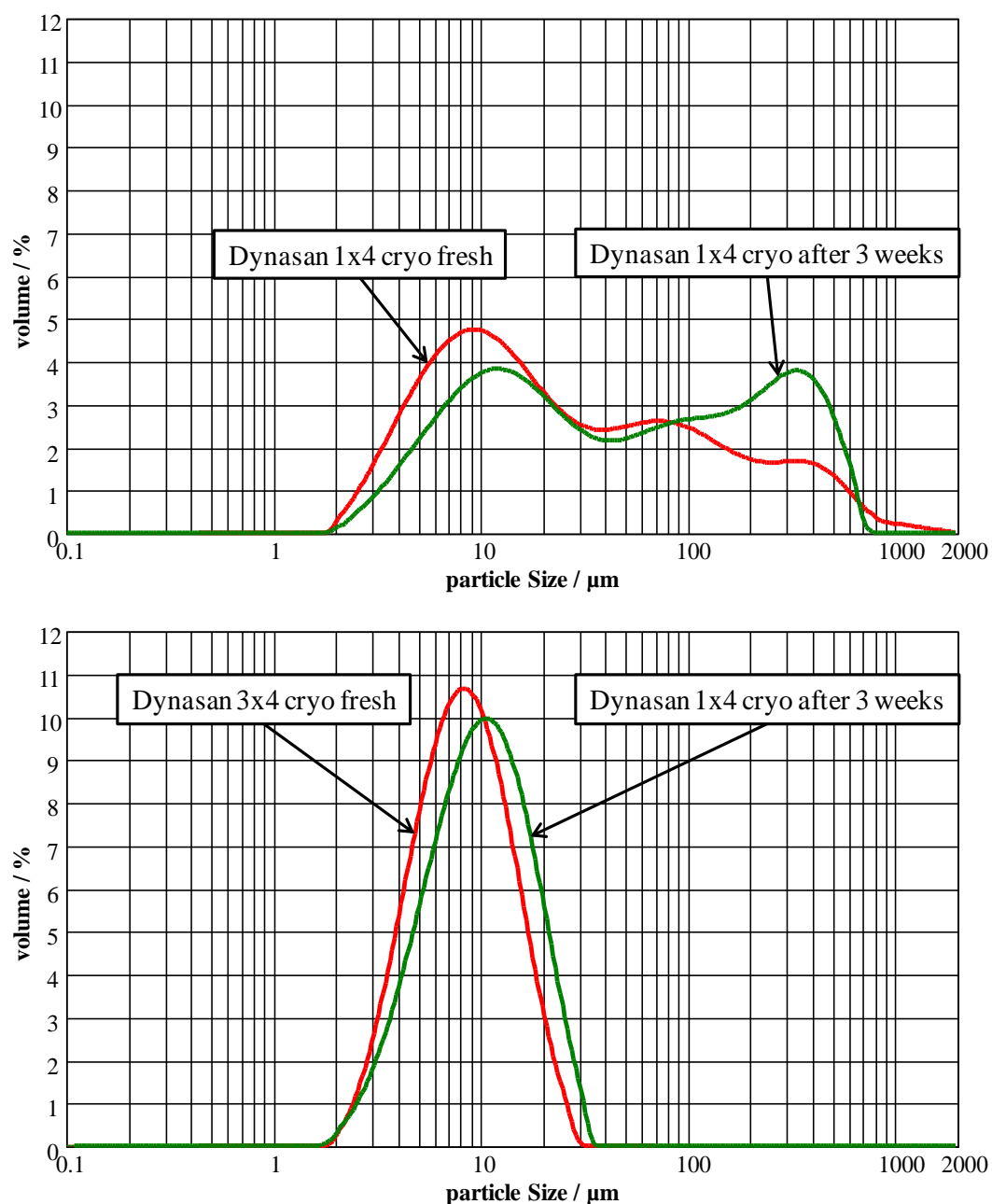
Fig. 8.2 Particle size distribution of lipid microparticles after jet milling under cryogenic conditions at 4 bar compared to the results after 3 weeks of storage

Particle morphology

First scanning electron microscopy was applied to see if the increase in particle size is visible by this method, too, and if it is possible to determine the reason for this particle growth. Figures 8.3 and 8.4 show glycerol tripalmitate particles directly after micronization and after three weeks of storage at room temperature, each in two different magnifications. For comparison reasons the starting material is visible in the first line.

The size reduction effect of jet milling on the lipid particles is clearly recognizable. The freshly ground material displays small particles without sharp edges and with a smooth surface. For the samples milled only once some larger particles were detectable. There were no obvious differences in morphology between the two different milling gas temperatures. After three weeks of storage a tremendous change in surface structure appeared. It changed to very rough and spiky structures, which indicates a crystallization process on the surface of the particles [185]. The SEM pictures of the three weeks old samples give an impressive insight into the events responsible for particle growth. Particles were highly agglomerated and interconnected due to the grown spikes on the surface. When having a closer look, the changes on the cryomilled particles seemed to be less prominent and the spikes were smaller.

bulk
Dynasan 116
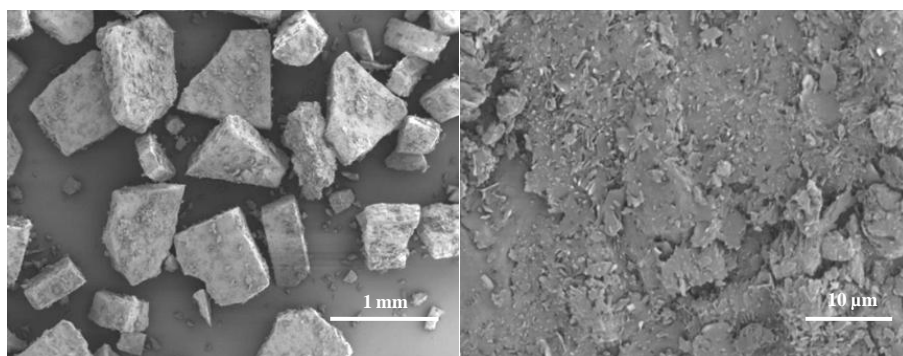
1x4 bar
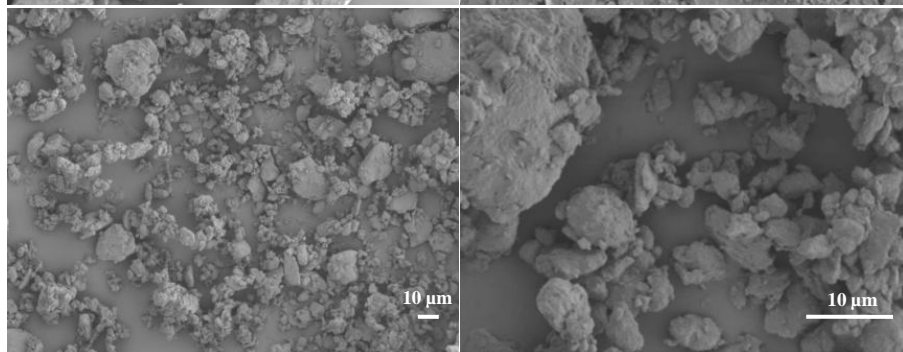
3x4 bar
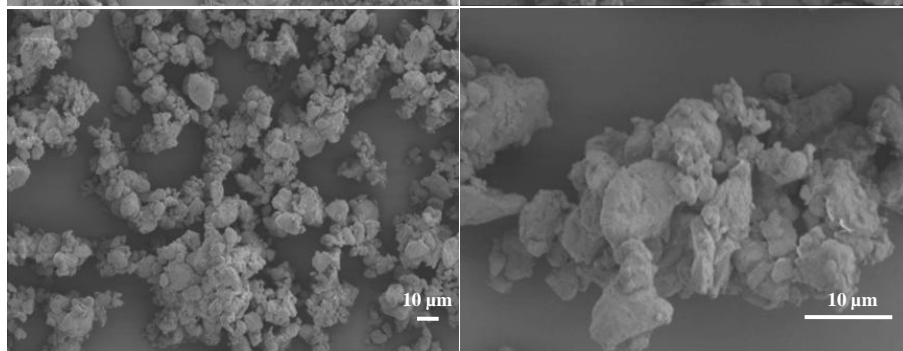
1x4 bar
3 weeks later

3x4 bar
3 weeks later

Fig. 8.3 SEM picture of glycerol tripalmitate milled at room temperature and 4 bar directly after micronization and after 3 weeks of storage at room temperature
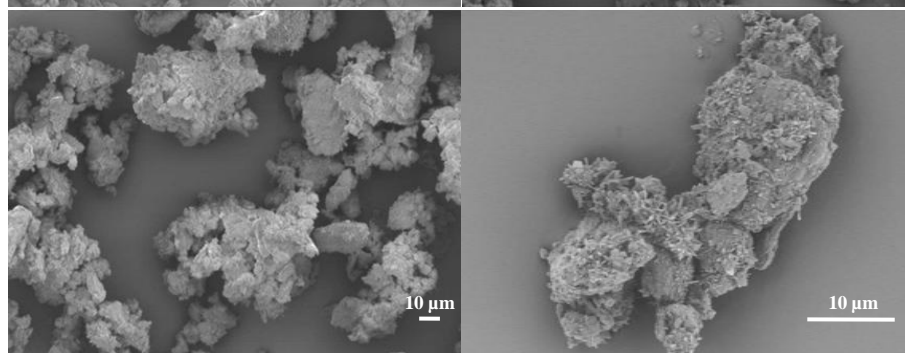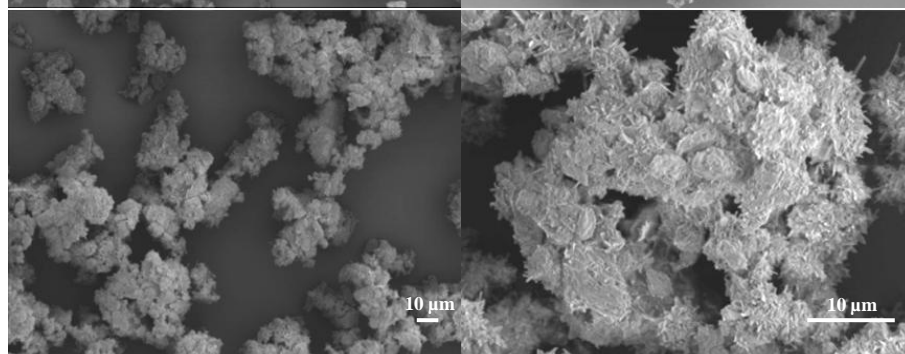
Fig. 8.4 SEM picture of glycerol tripalmitate milled at cryogenic conditions and 4 bar directly after micronization and after 3 weeks of storage at room temperature

Thermal behavior of micronized lipid particles

Thermal analysis is the standard method for investigating lipids. Therefore, DSC measurements were applied to verify the visible changes within the particle structure and to detect probable differences between the samples. Figure 8.5 shows the thermogram of the glycerol tripalmitate bulk material showing one endothermal event with an onset at 62.71°C and a maximum at 64.79°C, which are typical values for the melting point of this material. The micronized samples were analyzed by DSC at the same time points as investigated with the other methods before. For comparison figures 8.6 and 8.7 show thermograms zoomed in on the area of interest.

Each freshly micronized sample showed an exothermal event in the area between 35 and 50°C. A dependence of the number of milling cycles is clearly visible as with each additional milling cycle the exothermal event increased. This effect was reduced by applying the cooled milling gas for the milling process. The detected differences were less prominent, indicating that alteration of the surface is due to heat generated during the milling process. After three weeks still some differences were detectable for the room temperature milled samples, but the curves were much closer to the "baseline" of the bulk material. After three weeks the cryomilled samples were not any more distinguishable from the bulk material. The energy input by heat due to particle breakage induces the creation of unordered structures on the particle surfaces. During storage these activated structures return to the low energy and stable crystalline state by recrystallization, an exothermic process.
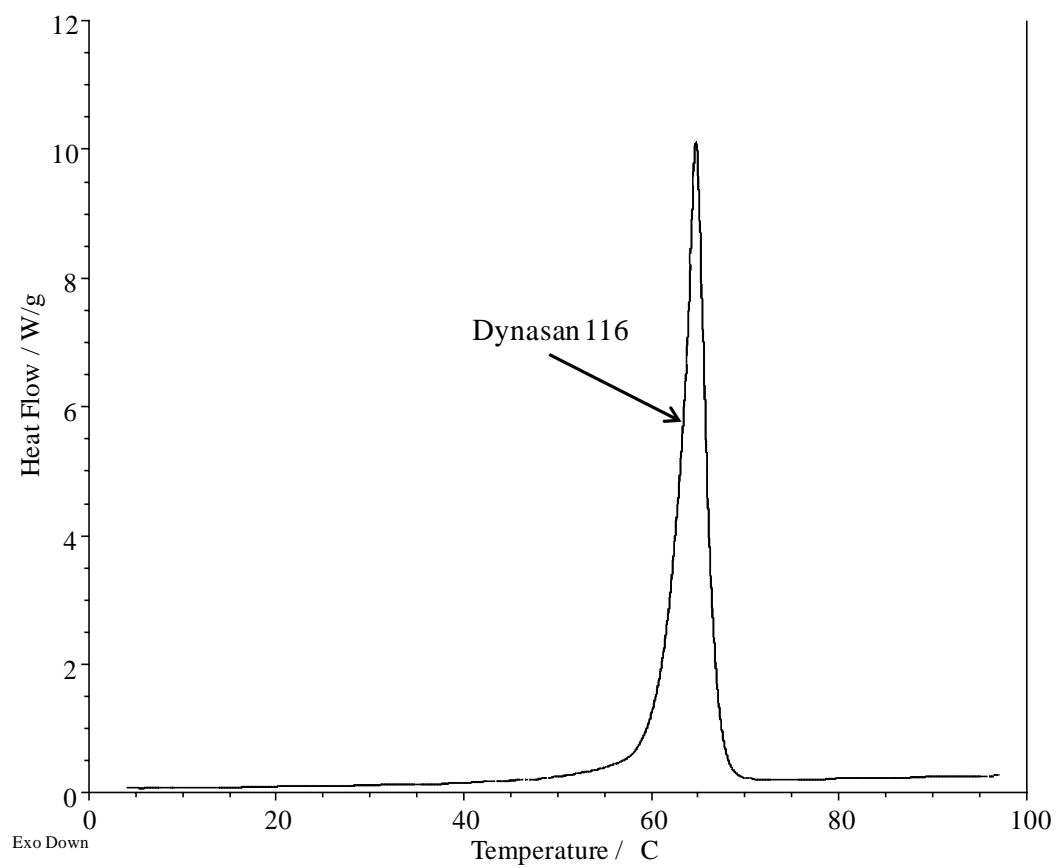
Fig. 8.5 DSC melting curve of glycerol tripalmitate bulk material
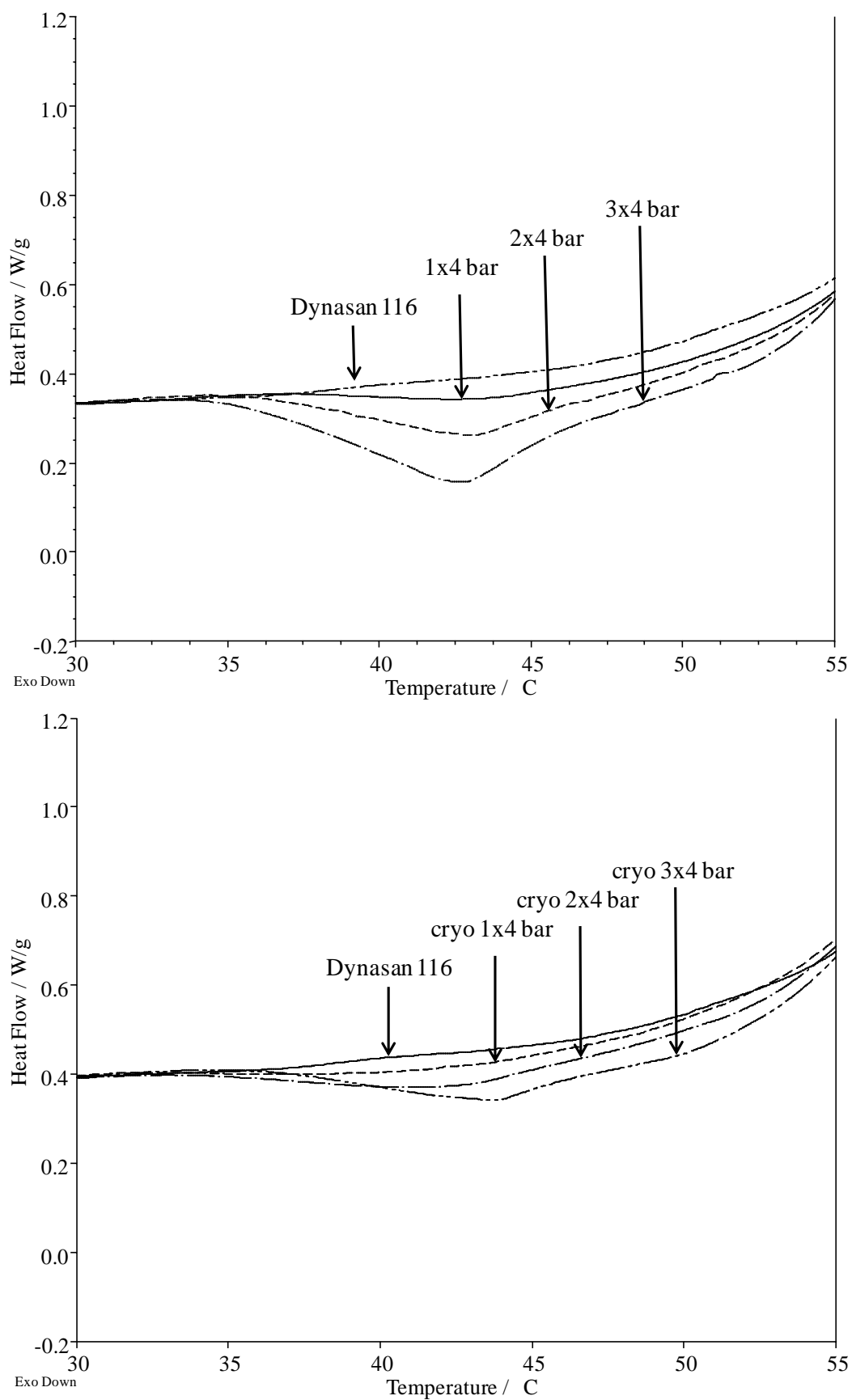
Fig. 8.6 Comparison of micronized lipid processed at different temperatures, analyzed by DSC directly after production
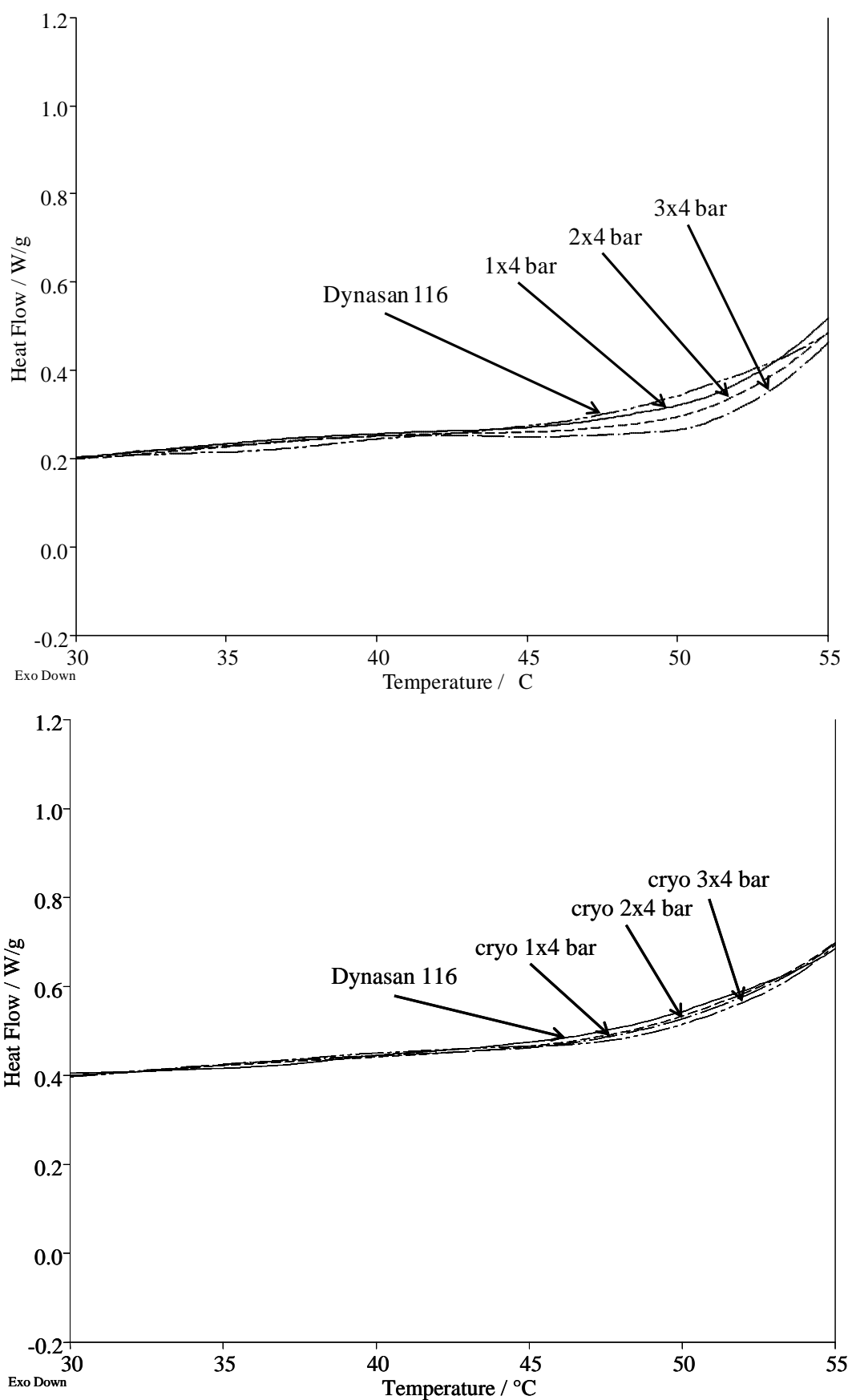
Fig. 8.7 Comparison of micronized dynasan 116 processed at different temperatures and stored for 3 weeks at room temperature, analyzed by DSC

Summary

The experiments demonstrated that it is possible to obtain microparticles of glycerol tripalmitate as an example for lipid materials by jet milling. However, only repetitive milling resulted in a narrow size distribution with most particles below 20 μm. Cryomilling improves the result significantly. By utilizing lipids as milling samples it was possible to prove surface activation effects due to the jet milling process. As demonstrated in chapter 3 this process is not initiated by a heating up of the milling gas, but the changes are caused by heat created by the impact itself and by the heat occurring during the crack propagation of particle breakage [107]. This effect can be influenced by reducing the temperature of the milling gas, but cannot be totally prevented. Unstructured areas with a higher energy level were created on the particle surface leading to recrystallization processes on the surface of the lipid particles, which resulted in particle growth during storage.

Jet milling is often indicated for the micronization of heat sensitive substances due to the cooling effect of the expanding gas stream. Nevertheless, the energy induced by the high velocity impacts and particle breakage may result in alterations of the substance. This effect may be also responsible for the observations made for protein grinding described in the previous chapters.

Lipids seem to be a useful and cheap tool for investigating energetic processes occurring during jet milling.

Chapter 9

Summary

and

Conclusions

Summary

The aim of this thesis was to provide more information about the jet milling of proteins, to identify important parameters and their effect on resulting particle size, chemical stability and bioactivity of the investigated proteins.

To perform the planned micronization experiments the MC One® of Jetpharma had to be modified. A cryogenic cooling system had been established facilitating milling gas temperatures of about -60°C in reproducible quality. To exclude possible effects of air humidity the whole setup was integrated into a glovebox filled with dry nitrogen. Therefore, it was possible to process amounts starting from 200 mg with yields of more than 80 % under constant environmental conditions. This way it was possible to attribute all the observed effects to controlled parameters (**chapter 3**).

The micronization of three different model proteins proved the size reduction potential of jet milling. It was possible to achieve narrow particle size distributions with d90 values below 10 μm for each of the three proteins. Chosen pressure and number of milling cycles had a significant impact on the milling results. For the first cycle the size distribution of the bulk material played an important role. Especially for the coarse BSA powder some larger particles were still present after the first milling cycle. A grinding limit existed for all model proteins at about 3-4 μm (d90), implicating that additional milling cycles would have no further effect on the particle size. The effect of the third investigated parameter, the milling gas temperature, was different for the proteins. No effect was detected for insulin; for lysozyme the particle size increased slightly under cryogenic conditions, while a clear decrease was detected for BSA. By applying statistical design it was possible to fit mathematical models to all the three micronization processes, describing the qualitative and quantitative impact of the parameters on the resulting particle size. So the prediction of milling results of not tested parameter combinations within the investigated range was enabled (**chapter 4**).

It was the second focus of the thesis was to investigate the effect of the jet milling process on the chemical stability and the bioactivity of proteins. For insulin no chemical changes were observed. The analysis of secondary and tertiary structures revealed slight changes. Nevertheless, they seemed to have no effect on the bioactivity investigated, using a chondrocyte proliferation assay (**chapter 5**).

After micronization chemically no changes were detected for lysozyme compared to the unprocessed bulk material. The analysis of the secondary protein structure by CD-spectroscopy showed no difference either. Regarding the tertiary structure fluorescence

analysis revealed significant changes. Especially the relative surface hydrophobicity was affected by a 12-fold increase after three milling cycles at 14 bar. Due to these changes the bioactivity decreased depending on applied pressure and milling cycles. For three cycles at 14 bar 87 % of the former activity were measured. In particular repeated milling seemed to have a negative effect. The milling gas temperature had no significant effect. An influence of increased iron content due to attrition during the milling process was excluded by ICP measurements. The attempt of reducing the decrease in bioactivity by using crystalline lysozyme brought no advantage for the process (**chapter 6**).

For BSA the most prominent effect of the micronization process was the formation of an insoluble fraction of the protein. Experiments revealed that all the three investigated milling parameters affected this result. With higher pressure and more milling cycles the insoluble fraction increased to 14 %. By applying cryogenic conditions the amount had been decreased to 6-9 %. This indicates that heat creation on the particle surface may play a role in this process, inducing changes within the particles. Different possible reasons for this phenomenon were investigated. Covalent protein aggregates due to thiol-disulfide interchange could be excluded as a reason as well as oxidation processes of this free thiol group. Increased surface hydrophobicity by rearrangement of fatty acids present at the molecule surface could be neglected by micronizing fatty acid free BSA. However, changes in relative surface hydrophobicity were detected by fluorescence analysis. The micronization process resulted in a significant decrease of this value while the intrinsic fluorescence was not affected. A correlation to the insoluble BSA fraction was not possible. Attempts to analyse the insoluble fraction itself brought no results. Nevertheless, beside the cryomilling approach of reducing this fraction, the co-lyophilization of BSA with PEG showed good results. With increasing amounts of PEG in the mixture the insoluble fraction decreased. At a BSA PEG ratio of 2:1 no insoluble BSA could be detected anymore. This effect was referred to the separation of the BSA molecules by PEG, preventing intermolecular reactions, and of the hydrophilic properties of PEG (**chapter 7**).

Processing of glycerol tripalmitate revealed that it is possible to micronize even such a soft material by jet milling. It resulted in d90 values below 20 µm. During storage an increase in particle size had been observed due to changes in surface structure of the micronized particles. DSC analysis revealed that the micronization process induces an activation at the surface. During storage these activated areas recrystallized. It was possible to correlate this effect to the number of milling cycles and the milling gas temperature. With more milling cycles the

effect was more prominent, which was significantly reduced by applying cryogenic conditions (**chapter 8**).

Conclusion

In conclusion the micronization process of proteins by jet milling was clarified in more detail. Particle size reduction was possible for all the tested substances, but different effects on chemical stability and bioactivity were revealed, strongly depending on the investigated substance. Especially repeated stressing of the materials seemed to have a negative effect and should be avoided for sensitive substances. Some effects like the formation of insoluble fractions for BSA or structural changes in glycerol tripalmitate were induced by heat formation at the breakage surface. In these cases cryomilling had a protective effect and it may be worth the additional costs. Therefore, for each new substance the milling conditions should be tested carefully. Application of design of experiments for these investigations proved to be a useful and cost saving tool.

References

References

[1]   M.P. Mullarney, N. Leyva, Modeling pharmaceutical powder-flow performance using particle-size distribution data, Pharm. Technol. 33 (2009) 126, 128-130, 132-134.

[2]   A. Miranda, M. Millan, I. Carballo, Investigation of the influence of particle size on the excipient percolation thresholds of HPMC hydrophilic matrix tablets, J. Pharm. Sci. 96 (2007) 2746–2756.

[3]   S. Koennings, A. Sapin, T. Blunk, P. Menei, A. Goepferich, Towards controlled release of BDNF - Manufacturing strategies for protein-loaded lipid implants and biocompatibility evaluation in the brain, Journal of Controlled Release 119 (2007) 163–172.

[4]   N. Rasenack, B.W. Mueller, Poorly water-soluble drugs for oral delivery - A challenge for pharmaceutical development. Part II: Micronization technologies and complex formaton, Pharmazeutische Industrie 67 (2005) 447–451.

[5]   S. Koennings, J. Tessmar, T. Blunk, A. Göpferich, Confocal Microscopy for the Elucidation of Mass Transport Mechanisms Involved in Protein Release from Lipid-based Matrices, Pharmaceutical Research 24 (2007) 1325–1335.

[6]   D.I. Daniher, J. Zhu, Dry powder platform for pulmonary drug delivery, Particuology 6 (2008) 225–238.

[7]   G. Walsh, Biopharmaceuticals: Approval trends in 2005, BioPharm International 19 (2006) 58-60, 62, 64, 66, 68.

[8]   J. Samuel, Protein drugs come of age, Trends in Biotechnology 20 (2002) 132-132.

[9]   P.M. Bummer, S. Koppenol, Chemical and physical considerations in protein and peptide stability, Drugs and the Pharmaceutical Sciences 99 (2000) 5–69.

[10]   W. Wang, Protein aggregation and its inhibition in biopharmaceutics, International Journal of Pharmaceutics 289 (2005) 1–30.

[11]   G. Mustata, S.M. Dinh, Approaches to oral drug delivery for challenging molecules, Critical Reviews in Therapeutic Drug Carrier Systems 23 (2006) 111–135.

[12]   M. Torres-Lugo, N.A. Peppas, Transmucosal delivery systems for calcitonin: a review, Biomaterials 21 (2000) 1191–1196.

[13]   S. White, D.B. Bennett, S. Cheu, P.W. Conley, D.B. Guzek, S. Gray, J. Howard, R. Malcolmson, J.M. Parker, P. Roberts, N. Sadrzadeh, J.D. Schumacher, S. Seshadri, G.W. Sluggett, C.L. Stevenson, N.J. Harper, EXUBERA: Pharmaceutical Development of a Novel Product for Pulmonary Delivery of Insulin, Diabetes Technology & Therapeutics 7 (2005) 896–906.

[14]   A.P. Sayani, Y.W. Chien, Systemic delivery of peptides and proteins across absorptive mucosae, Critical Reviews in Therapeutic Drug Carrier Systems 13 (1996) 85–184.

[15]   Y.-C. Lee, P. Simamora, S. Pinsuwan, S.H. Yalkowsky, Review on the systemic delivery of insulin via the ocular route, International Journal of Pharmaceutics 233 (2002) 1–18.

[16]   L. Jin; J. Pei; M. Duan; Y. Zheng, A rectum suppository of protein and its preparation method and the use, 2006, 2006 33p.

[17]   A.S. Ziegler, E. Schluecker, P. Reichel-Lesnianski, N. Alt, G. Lee, Inactivation effects on proteins in a needle-free vaccine injector, Engineering in Life Sciences 6 (2006) 384–393.

[18]   J.W. Lee, J.-H. Park, M.R. Prausnitz, Dissolving microneedles for transdermal drug delivery, Biomaterials 29 (2008) 2113–2124.

[19]   W. Wang, Lyophilization and development of solid protein pharmaceuticals, International Journal of Pharmaceutics 203 (2000) 1–60.

[20]   R. Vehring, Pharmaceutical Particle Engineering via Spray Drying, Pharmaceutical Research 25 (2008) 999–1022.

[21]   K. Masters, Spray Drying Handbook. 5th Ed, Longman, New York, 1991.

[22]   K.A. Johnson, Preparation of peptide and protein powders for inhalation, Advanced Drug Delivery Reviews 26 (1997) 3–15.

[23]   Y.-F. Maa, S.J. Prestrelski, Biopharmaceutical powders: particle formation and formulation considerations, Current Pharmaceutical Biotechnology 1 (2000) 283–302.

[24]   P. Labrude, M. Rasolomanana, C. Vigneron, C. Thirion, B. Chaillot, Protective effect of sucrose in spray drying of oxyhemoglobin, Journal of Pharmaceutical Sciences 78 (1989) 223–229.

[25]   J. Broadhead, S.K.E. Rouan, I. Hau, C.T. Rhodes, The effect of process and formulation variables on the properties of spray-dried b-galactosidase, Journal of Pharmacy and Pharmacology 46 (1994) 458–467.

[26]   M. Irngartinger, V. Camuglia, M. Damm, J. Goede, H.W. Frijlink, Pulmonary delivery of therapeutic peptides via dry powder inhalation: effects of micronization and manufacturing, European Journal of Pharmaceutics and Biopharmaceutics 58 (2004) 7–14.

[27]   H.-K. Chan, Dry Powder Aerosol Delivery Systems: Current and Future Research Directions, Journal of Aerosol Medicine 19 (2006) 21–27.

[28]   S.A. Shoyele, S. Cawthorne, Particle engineering techniques for inhaled biopharmaceuticals, Advanced Drug Delivery Reviews 58 (2006) 1009–1029.

[29]   M. Mumenthaler, C.C. Hsu, R. Pearlman, Feasibility study on spray-drying protein pharmaceuticals: recombinant human growth hormone and tissue-type plasminogen activator, Pharmaceutical Research 11 (1994) 12–20.

[30]   Y.-H. Liao, M.B. Brown, S.A. Jones, T. Nazir, G.P. Martin, The effects of polyvinyl alcohol on the in vitro stability and delivery of spray-dried protein particles from surfactant-free HFA 134a-based pressurised metered dose inhalers, International Journal of Pharmaceutics 304 (2005) 29–39.

[31]   J.D. Andya, Y.-F. Maa, H.R. Costantino, P.-A. Nguyen, N. Dasovich, T.D. Sweeney, C.C. Hsu, S.J. Shire, The effect of formulation excipients on protein stability and aerosol performance of spray-dried powders of a recombinant humanized anti-IgE monoclonal antibody, Pharmaceutical Research 16 (1999) 350–358.

[32]   C. Bosquillon, V. Preat, R. Vanbever, Pulmonary delivery of growth hormone using dry powders and visualization of its local fate in rats, Journal of Controlled Release 96 (2004) 233–244.

[33]   M. Adler, M. Unger, G. Lee, Surface composition of spray-dried particles of bovine serum albumin/trehalose/surfactant, Pharmaceutical Research 17 (2000) 863–870.

References

[34]   W.R. Gombotz; M.S. Healy; L.R. Brown; H.E. Auer, Process for producing small particles of biologically active pharmaceuticals, 1990, 1990 28 p.

[35]   Z.H. Chang, J.G. Baust, Ultra-rapid freezing by spraying/plunging: pre-cooling in the cold gaseous layer, Journal of microscopy 161 (1991) 435-444.

[36]   Y.-F. Maa, M. Ameri, C. Shu, L.G. Payne, D. Chen, Influenza vaccine powder formulation development: Spray-freeze-drying and stability evaluation, Journal of Pharmaceutical Sciences 93 (2004) 1912–1923.

[37]   Y.-F. Maa, P.-A. Nguyen, T. Sweeney, S.J. Shire, C.C. Hsu, Protein inhalation powders: spray drying vs spray freeze drying, Pharmaceutical Research 16 (1999) 249–254.

[38]   H.R. Costantino, L. Firouzabadian, K. Hogeland, C. Wu, C. Beganski, K.G. Carrasquillo, M. Cordova, K. Griebenow, S.E. Zale, M.A. Tracy, Protein spray-freeze drying. Effect of atomization conditions on particle size and stability, Pharmaceutical Research 17 (2000) 1374–1383.

[39]   S.D. Webb, S.L. Golledge, J.L. Cleland, J.F. Carpenter, T.W. Randolph, Surface adsorption of recombinant human interferon-g in lyophilized and spray-lyophilized formulations, Journal of Pharmaceutical Sciences 91 (2002) 1474–1487.

[40]   Z. Yu, K.P. Johnston, R.O. Williams, Spray freezing into liquid versus spray-freeze drying: Influence of atomization on protein aggregation and biological activity, European Journal of Pharmaceutical Sciences 27 (2006) 9–18.

[41]   M.C. Heller, J.F. Carpenter, T.W. Randolph, Protein formulation and lyophilization cycle design: Prevention of damage due to freeze-concentration induced phase separation, Biotechnology and Bioengineering 63 (1999) 166–174.

[42]   T.L. Rogers, A.C. Nelsen, J. Hu, J.N. Brown, M. Sarkari, T.J. Young, K.P. Johnston, R.O. Williams, A novel particle engineering technology to enhance dissolution of poorly water soluble drugs: spray-freezing into liquid, European Journal of Pharmaceutics and Biopharmaceutics 54 (2002) 271–280.

[43]   Z. Yu, T.L. Rogers, J. Hu, K.P. Johnston, R.O. Williams, Preparation and characterization of microparticles containing peptide produced by a novel process: spray freezing into liquid, European Journal of Pharmaceutics and Biopharmaceutics 54 (2002) 221–228.

[44]   Z. Yu, A.S. Garcia, K.P. Johnston, R.O. Williams, III., Spray freezing into liquid nitrogen for highly stable protein nanostructured microparticles, European Journal of Pharmaceutics and Biopharmaceutics 58 (2004) 529–537.

[45]   J.D. Engstrom, D.T. Simpson, C. Cloonan, E.S. Lai, R.O. Williams, III, G.B. Kitto, K.P. Johnston, Stable high surface area lactate dehydrogenase particles produced by spray freezing into liquid nitrogen, European Journal of Pharmaceutics and Biopharmaceutics 65 (2007) 163–174.

[46]   G.L. Gilliland, M. Tung, J.E. Ladner, The Biological Macromolecule Crystallization Database: crystallization procedures and strategies, Acta Cryst (2002) 916–920.

[47]   S.K. Basu, C.P. Govardhan, C.W. Jung, A.L. Margolin, Protein crystals for the delivery of biopharmaceuticals, Expert Opinion on Biological Therapy 4 (2004) 301–317.

[48]   B. Shenoy, Y. Wang, W. Shan, A.L. Margolin, Stability of crystalline proteins, Biotechnology and Bioengineering 73 (2001) 358–369.

[49] A.A. Elkordy, R.T. Forbes, B.W. Barry, Integrity of crystalline lysozyme exceeds that of a spray-dried form, International Journal of Pharmaceutics 247 (2002) 79–90.

[50] I. Pasquali, R. Bettini, F. Giordano, Solid-state chemistry and particle engineering with supercritical fluids in pharmaceutics, European Journal of Pharmaceutical Sciences 27 (2006) 299–310.

[51] A. Jen, H.P. Merkle, Diamonds in the rough: protein crystals from a formulation perspective, Pharmaceutical Research 18 (2001) 1483–1488.

[52] M.-J. Lee, J.-H. Kwon, J.-S. Shin, C.-W. Kim, Microcrystallization of a-lactalbumin, Journal of Crystal Growth 282 (2005) 434–437.

[53] M.X. Yang, B. Shenoy, M. Disttler, R. Patel, M. McGrath, S. Pechenov, A.L. Margolin, Crystalline monoclonal antibodies for subcutaneous delivery, Proceedings of the National Academy of Sciences of the United States of America 100 (2003) 6934–6939.

[54] P. Reichert; P.C. Weber; R.F. Choudrie; B.O. Stuart; T. Nagabhushan; A. Ganguly, Crystalline interferon alpha for pulmonary delivery, 1995 424085100, 1995 5 p.

[55] J.F. Brennecke, C.A. Eckert, Phase equilibria for supercritical fluid process design, AIChE Journal 35 (1989) 1409–1427.

[56] Y. Liu, W. Lin, S. Bai, Z. Wang, Supercritical fluid extraction technology and its application in tobacco industry, Huagong Shikan 22 (2008) 56–60.

[57] R.L. Mendes, Supercritical fluid extraction of active compounds from algae, Supercritical Fluid Extraction of Nutraceuticals and Bioactive Compounds (2008) 189–213.

[58] D.-R. Wu, L. Leith, The impact of chiral supercritical fluid chromatography in drug discovery, American Pharmaceutical Review 10 (2007) 84–87.

[59] P. Chattopadhyay, B.Y. Shekunov, D. Yim, D. Cipolla, B. Boyd, S. Farr, Production of solid lipid nanoparticle suspensions using supercritical fluid extraction of emulsions (SFEE) for pulmonary delivery using the AERx system, Advanced Drug Delivery Reviews 59 (2007) 444–453.

[60] M. Habulin, M. Primozic, Z. Knez, Supercritical fluids as solvents for enzymatic reactions, Acta Chimica Slovenica 54 (2007) 667–677.

[61] H. Okamoto, K. Danjo, Application of supercritical fluid to preparation of powders of high-molecular weight drugs for inhalation, Advanced Drug Delivery Reviews 60 (2008) 433–446.

[62] P. York, Strategies for particle design using supercritical fluid technologies, Pharmaceutical Science & Technology Today 2 (1999) 430–440.

[63] A. Tandya, F. Dehghani, N.R. Foster, Micronization of cyclosporine using dense gas techniques, Journal of Supercritical Fluids 37 (2006) 272–278.

[64] P.G. Debenedetti; G.B. Lim; R.K. Prud'homme, Formation of protein microparticles by antisolvent precipitation, 1992, 1992 11 p.

[65] G. Muhrer, M. Mazzotti, Precipitation of Lysozyme Nanoparticles from Dimethyl Sulfoxide Using Carbon Dioxide as Antisolvent, Biotechnology Progress 19 (2003) 549–556.

References

[66]   R. Thiering, F. Dehghani, A. Dillow, N.R. Foster, The influence of operating conditions on the dense gas precipitation of model proteins, Journal of Chemical Technology & Biotechnology 75 (2000) 29–41.

[67]   S.-D. Yeo, P.G. Debenedetti, S.Y. Patro, T.M. Przybycien, Secondary Structure Characterization of Microparticulate Insulin Powders, Journal of Pharmaceutical Sciences 83 (1994) 1651–1656.

[68]   S.D. Yeo, G.B. Lim, P.G. Debenedetti, H. Bernstein, Formation of microparticulate protein powders using a supercritical fluid antisolvent, Biotechnology and Bioengineering 41 (1993) 341–346.

[69]   R.T. Bustami, H.-K. Chan, F. Dehghani, N.R. Foster, Generation of microparticles of proteins for aerosol delivery using high pressure modified carbon dioxide, Pharmaceutical Research 17 (2000) 1360–1366.

[70]   J.Y.H. Blue, Successful lyophilization development of protein therapeutics, Am. Pharm. Rev. 12 (2009) 90–96.

[71]   J.F. Carpenter, B.S. Chang, T.W. Randolph, Physical damage to proteins during freezing, drying, and rehydration, Biotechnol.: Pharm. Aspects 2 (2004) 423–442.

[72]   P. Matejtschuk, Lyophilization of proteins, Methods Mol. Biol. (Totowa, NJ, U. S.) 368 (2007) 59–72.

[73]   J. Zhang, F. Huang, K. Wang, Lyophilization and development of protein pharmaceuticals, Zhongguo Yaoye 15 (2006) 25–27.

[74]   I.G.M.N. Roy, Freeze-drying of proteins: some emerging concerns, Biotechnol. Appl. Biochem. 39 (2004) 165–177.

[75]   S.L. Nail, S. Jiang, S. Chongprasert, S.A. Knopp, Fundamentals of freeze-drying, Pharm. Biotechnol. 14 (2002) 281–360.

[76]   L.A. Gatlin, T. Auffret, E.Y. Shalaev, S.M. Speaker, D.L. Teagarden, Freeze-drying concepts: the basics, Drugs and the Pharmaceutical Sciences 175 (2008) 177–195.

[77]   T. Morita, Y. Horikiri, H. Yamahara, T. Suzuki, H. Yoshino, Formation and isolation of spherical fine protein microparticles through lyophilization of protein-poly(ethylene glycol) aqueous mixture, Pharmaceutical Research 17 (2000) 1367–1373.

[78]   I.J. Castellanos, G. Cruz, R. Crespo, K. Griebenow, Encapsulation-induced aggregation and loss in activity of g-chymotrypsin and their prevention, Journal of Controlled Release 81 (2002) 307–319.

[79]   S. Koennings, E. Garcion, N. Faisant, P. Menei, J.P. Benoit, A. Goepferich, In vitro investigation of lipid implants as a controlled release system for interleukin-18, International Journal of Pharmaceutics 314 (2006) 145–152.

[80]   W. Yuan, F. Wu, Y. Geng, S. Xu, T. Jin, Preparation of dextran glassy particles through freezing-induced phase separation, International Journal of Pharmaceutics 339 (2007) 76–83.

[81]   R.M. Platz; A. Ip; C.L. Whitham, Process for preparing micronized polypeptide drugs, 1993 424489000, 1993 5 p Cont.-in-part of U.S. Ser. No. 823,218, abandoned.

[82]   E. Phillips, E. Allsopp, T. Christensen, M. Fitzgerald, L. Zhao, Size reduction of peptides and proteins by jet-milling, Respiratory Drug Delivery VI: Biological, Pharmaceutical, Clinical and Regulatory Issues Relating to Optimized Drug Delivery by

Aerosol, the International Symposium, 6th, Hilton Head, S. C., May 3-7, 1998 (1998) 161–168.

[83]   W. Schlocker, S. Gschliesser, A. Bernkop-Schnuerch, Evaluation of the potential of air jet milling of solid protein-poly(acrylate) complexes for microparticle preparation, European Journal of Pharmaceutics and Biopharmaceutics 62 (2006) 260–266.

[84]   K.G.E. Backstrom; C.M.O. Dahlback; P. Edman; A.C.B. Johansson, Therapeutic preparation for inhalation, 1996 514004000, 1996 16 p, Cont.-in-part of U.S. 5,518,998.

[85]   S. Kobayashi, S. Kondo, K. Juni, Pulmonary delivery of salmon calcitonin dry powders containing absorption enhancers in rats, Pharmaceutical Research 13 (1996) 80–83.

[86]   Z. Herceg, V. Lelas, G. Kresic, Influence of tribomechanical micronization on the physical and functional properties of whey proteins, International Journal of Dairy Technology 58 (2005) 225–232.

[87]   Z. Herceg, V. Lelas, M. Skreblin, Influence of tribomechanical micronisation on the rheological properties of whey proteins, Food Technology and Biotechnology 40 (2002) 145–155.

[88]   Lizio R, Damm M, Sarlikiotis A W, Bauer H H, Lehr C M, Low-temperature micronization of a peptide drug in fluid propellant: case study cetrorelix, AAPS PharmSciTech 2 (2001) E12.

[89]   S. Schultz, G. Wagner, K. Urban, J. Ulrich, High-pressure homogenization as a process for emulsion formation, Chemical Engineering & Technology 27 (2004) 361–368.

[90]   T. Shah, D. Patel, J. Hirani, A.F. Amin, Nanosuspensions as a drug delivery system: a comprehensive review, Drug Delivery Technology 7 (2007) 42, 44, 46, 48-50, 52-53.

[91]   J. Hou, S.-w. Zhou, New research on development of solid lipid nanoparticles, Journal of Medical Colleges of PLA 22 (2007) 385–390.

[92]   A. Maschke, N. Cali, B. Appel, J. Kiermaier, T. Blunk, A. Goepferich, Micronization of insulin by high pressure homogenization, Pharmaceutical Research 23 (2006) 2220–2229.

[93]   M.H. Prior, H. Prem, M.J. Rhodes, Principles of powder technology. Size Reduction, Wiley, Chichester, 1993.

[94]   T. Onishi; S. Mitsumura; Y. Tsuji, Jet mill and manufacture of electrophotographic toner using the same, 1997, 1997 31 p.

[95]   K. Brodka-Pfeiffer, H. Haeusler, P. Grass, P. Langguth, Air jet milling with homogeneous premixes of fenoterol hydrobromide and glucose for the application in dry powder inhalers, Pharmazeutische Industrie 67 (2005) 713–719.

[96]   K. Marquardt, Untersuchungen zum Zerkleinerungsverhalten kristalliner Stoffe in einer Spiralstrahlmühle. Dissertation, Würzburg, 2004.

[97]   R. Skelton, A.N. Khayyat, R.G. Temple, Fluid energy milling. An investigation of micronizer performance, Fine Particles Processing 1 (1980) 113–125.

[98]   H. Kuerten, H. Rumpf, Zerkleinerungsuntersuchungen mit tribolumineszierenden Stoffen, Chemie-Ing.-Techn. 38 (1966) 331–342.

[99]   H. Rumpf, Versuche zur Bestimmung der Teilchenbewegung in Gasstrahlen und des Beanspruchungsmechanismus in Strahlmühlen, Chemie-Ing.-Techn. 32 (1960) 335–342.

References

[100]   G. Abramovich, The Theory of turbulent Jets, M.I.T. Press, Cambridge, 1963.

[101]   H. Rumpf, Strain theory of impact comminution, Chemie Ingenieur Technik 31 (1959) 323–337.

[102]   H. Rumpf, Prinzipien der Prallzerkleinerung und ihre Anwendung bei der Strahlmahlung, Chemie-Ing.-Techn. 32 (1960) 129–135.

[103]   W. Bohl, Technische Strömungslehre, Vogel Verlag, Würzburg, 1994.

[104]   M. Benz, H. Herold, B. Ulfik, Performance of a fluidized bed jet mill as a function of operating parameters, International Journal of Mineral Processing 44-45 (1996) 507–519.

[105]   K. Nielsen, T. Malvik, Grindability enhancement by blast-induced microcracks, Powder Technology 105 (1999) 52–56.

[106]   K. Schoenert, K. Steier, Die Grenzen der Zerkleinerung bei kleinen Korngrößen, Chemie-Ing.-Techn. 43 (1971) 773–777.

[107]   R. Weichert, K. Schoenert, Temperature at the point of fracture, Chemie Ingenieur Technik 48 (1976) 543–544.

[108]   H. Rumpf, Physical Aspects of Comminution and New Formulation of a Law of Comminution, Powder Technology (1973) 145–159.

[109]   K. Schoenert, Advances in comminution fundamentals and impacts on technology, Aufbereitungs Technik (1960-1989) 32 (1991) 487-90, 492-4.

[110]   O. de Vegt, H. Vromans, F. Faassen, K. van der Voort Maarschalk, Milling of Organic Solids in a Jet Mill. Part 1: Determination of the Selection Function and Related Mechanical Material Properties, Particle & Particle Systems Characterization 22 (2005) 133–140.

[111]   H.A. Lieberman, L. Lachman, J.B. Schwartz, Pharmaceutical Dosage Forms: Tablets, Vol. 2, Marcel Dekker, New York/Basel, 1990.

[112]   M. Zogg, Einführung in die Mechanische Verfahrenstechnik, B.G. Teubner, Stuttgart, 1993.

[113]   M. Sokolowski, A new idea of a general law of comminution and establishing energy indices, Aufbereitungs-Technik 36 (1995) 107-10, 112-16.

[114]   H.T. Ozkahraman, A meaningful expression between bond work index, grindability index, and friability value, Minerals Engineering 18 (2005) 1057–1059.

[115]   L. Vogel, W. Peukert, Breakage behaviour of different materials-construction of a mastercurve for the breakage probability, Powder Technology 129 (2003) 101–110.

[116]   O. de Vegt, H. Vromans, F. Faassen, K. van der Voort Maarschalk, Milling of Organic Solids in a Jet Mill. Part 2: Checking the Validity of the Predicted Rate of Breakage Function, Particle & Particle Systems Characterization 22 (2005) 261–267.

[117]   P.B. Rajendran Nair, Breakage parameters and the operating variables of a circular fluid energy mill: Part I. Breakage distribution parameter, Powder Technology 106 (1999) 45–53.

[118]   P.B. Rajendran Nair, Breakage parameters and the operating variables of a circular fluid energy mill: Part II. Breakage rate parameter, Powder Technology 106 (1999) 54–61.

[119]   H. Berthiaux, J. Dodds, A new estimation technique for the determination of breakage and selection parameters in batch grinding, Powder Technology 94 (1997) 173–179.

[120] H.R. Costantino, R. Langer, A.M. Klibanov, Solid-Phase Aggregation of Proteins under Pharmaceutically Relevant Conditions, Journal of Pharmaceutical Sciences 83 (1994) 1662–1669.

[121] Y.F. Maa, P.A. Nguyen, J.D. Andya, N. Dasovich, T.D. Sweeney, S.J. Shire, C.C. Hsu, Effect of spray drying and subsequent processing conditions on residual moisture content and physical/biochemical stability of protein inhalation powders, Pharmaceutical Research 15 (1998) 768–775.

[122] B. Cervelle, F. Cesbron, J. Berthou, P. Jolles, Morphology and optical properties of tetragonal and orthorhombic hen lysozyme crystals, Acta Crystallographica, Section A: Crystal Physics, Diffraction, Theoretical and General Crystallography 30A (1974) 645–648.

[123] D. Eyrich, F. Brandl, B. Appel, H. Wiese, G. Maier, M. Wenzel, R. Staudenmaier, A. Goepferich, T. Blunk, Long-term stable fibrin gels for cartilage engineering, Biomaterials 28 (2006) 55–65.

[124] Y.J. Kim, R.L.Y. Sah, J.Y.H. Doong, A.J. Grodzinsky, Fluorometric assay of DNA in cartilage explants using Hoechst 33258, Analytical Biochemistry 174 (1988) 168–176.

[125] D. Shugar, The measurement of lysozyme activity and the ultra-violet inactivation of lysozyme, Biochim Biophys Acta 8 (1952) 302–309.

[126] J.M.(.). Walker, The Protein Protocols Handbook, 2nd Edition, Humana Press Inc., Totowa, NJ, 1996.

[127] J.K.F. Noel, M.J. Hunter, Bovine Mercaptalbumin and Non-mercaptalbumin Monomers. Interconversions and Structural Differences, J. Biol. Chem. 247 (1972) 7391–7406.

[128] G. Bohm, R. Muhr, R. Jaenicke, Quantitative analysis of protein far UV circular dichroism spectra by neural networks, Protein Eng 5 (1992) 191–195.

[129] V. Lechevalier, T. Croguennec, S. Pezennec, C. Guerin-Dubiard, M. Pasco, F. Nau, Ovalbumin, Ovotransferrin, Lysozyme: Three Model Proteins for Structural Modifications at the Air-Water Interface, Journal of Agricultural and Food Chemistry 51 (2003) 6354–6361.

[130] J.D. Meyer, M.C. Manning, J.F. Carpenter, Effects of potassium bromide disk formation on the infrared spectra of dried model proteins, Journal of Pharmaceutical Sciences 93 (2004) 496–506.

[131] S. Krimm, J. Bandekar, Vibrational spectroscopy and conformation of peptides, polypeptides, and proteins, Advances in Protein Chemistry 38 (1986) 181–364.

[132] T.P. Shakhtshneider, F. Danede, F. Capet, J.F. Willart, M. Descamps, S.A. Myz, E.V. Boldyreva, V.V. Boldyrev, Grinding of drugs with pharmaceutical excipients at cryogenic temperatures. Part I. Cryogenic grinding of piroxicam-polyvinylpyrrolidone mixtures, Journal of Thermal Analysis and Calorimetry 89 (2007) 699–707.

[133] C.T. Murthy, S. Bhattacharya, Cryogenic grinding of black pepper, Journal of Food Engineering 85 (2007) 18–28.

[134] S. Li, S. Ge, Z. Huang, Q. Wang, H. Zhao, H. Pan, Cryogenic grinding technology for traditional Chinese herbal medicine, Cryogenics 31 (1991) 136–137.

[135] S.B. Liang, D.P. Hu, C. Zhu, A.B. Yu, Production of fine polymer powder under cryogenic conditions, Chemical Engineering & Technology 25 (2002) 401–405.

References

[136] S.B. Liang, Y.C. Hao, A novel cryogenic grinding system for recycling scrap tire peels, Advanced Powder Technology 11 (2000) 187–197.

[137] T. Vu-Khanh, Z. Yu, Mechanisms of brittle-ductile transition in toughened thermoplastics, Theoretical and Applied Fracture Mechanics 26 (1997) 177–183.

[138] C. Butcher, Cryogenic grinding: An independent voice, Chemical Engineer 713 (2000) 19–21.

[139] S.P. Schwendeman, J.H. Lee, R.K. Gupta, H.R. Costantino, G.R. Siber, R. Langer, Inhibition of moisture-induced aggregation of tetanus toxoid by protecting thiol groups, Proceedings of the International Symposium on Controlled Release of Bioactive Materials 21ST (1994) 54–55.

[140] H.R. Costantino, R. Langer, A.M. Klibanov, Moisture-induced aggregation of lyophilized insulin, Pharmaceutical Research 11 (1994) 21–29.

[141] E. Johansson, N. Kettaneh-Wold, C. Wikstrom, S. Wold, L. Ericksson, Design of Experiments - Principles and Application, Umetrics Acedamy, Umea, 2000.

[142] J. Dong, C.-F. Mandenius, M. Luebberstedt, T. Urbaniak, A.K.N. Nuessler, D. Knobeloch, J.C. Gerlach, K. Zeilinger, Evaluation and optimization of hepatocyte culture media factors by design of experiments (DoE) methodology, Cytotechnology 57 (2008) 251–261.

[143] Joelsson Daniel, Moravec Phil, Troutman Matthew, Pigeon Joseph, DePhillips Pete, Optimizing ELISAs for precision and robustness using laboratory automation and statistical design of experiments, J Immunol Methods 337 (2008) 35-41.

[144] D. Horvath, R. Noorani, M. Mendelson, Improvement of surface roughness on ABS 400 polymer materials using design of experiments (DOE), Materials Science Forum 561-565 (2007) 2389–2392.

[145] M. Castagne, Y. Bentolila, F. Chaudoye, A. Halle, F. Nicolas, D. Sinoquet, Comparison of engine calibration methods based on design of experiments (DoE), Oil & Gas Science and Technology 63 (2008) 563–582.

[146] International Conference on Harmonisation, Q1D Bracketing and Matrixing Designs for Stability Testing of New Drug Substances and Products, 2002.

[147] O. Vegt, H. Vromans, W. Pries, K. van der Voort Maarschalk, The effect of crystal imperfections on particle fracture behavior, International Journal of Pharmaceutics 317 (2006) 47–53.

[148] W. Peukert, Material properties in fine grinding, International Journal of Mineral Processing 74 (2004) S3-S17.

[149] M. Wilczek, J. Bertling, D. Hnitemann, Optimised technologies for cryogenic grinding, International Journal of Mineral Processing 2004 (2004) 425–434.

[150] R. Thibert, M. Akbarieh, R. Tawashi, Morphic features variation of solid particles after size reduction: sonification compared to jet mill grinding, International Journal of Pharmaceutics 47 (1988) 171–177.

[151] K. Brodka-Pfeiffer, H. Haeusler, P. Grass, P. Langguth, Conditioning Following Powder Micronization: Influence on Particle Growth of Salbutamol Sulfate, Drug Dev. Ind. Pharm. 29 (2003) 1077–1084.

[152] G. Walsh, Biopharmaceutical benchmarks 2006, Nature Biotechnology 24 (2006) 769–776.

[153] J. Zheng, X. Yue, Z. Dai, Y. Wang, S. Liu, X. Yan, Novel iron–polysaccharide multilayered microcapsules for controlled insulin release, Acta Biomaterialia 5 (2009) 1499–1507.

[154] B. Singh, N. Chauhan, Modification of psyllium polysaccharides for use in oral insulin delivery, Food Hydrocolloids 23 (2009) 928–935.

[155] R. Diamond et al., Molecular Structures in Biology, Oxford University Press, Oxford, 1993.

[156] G.K. Iwamoto, R.A. van Wagenen, J.D. Andrade, Insulin adsorption: intrinsic tyrosine interfacial fluorescence, Journal of Colloid and Interface Science 86 (1982) 581–585.

[157] A. Malzert, F. Boury, D. Renard, P. Robert, L. Lavenant, J.P. Benoit, J.E. Proust, Spectroscopic studies on poly(ethylene glycol)–lysozyme interactions, International Journal of Pharmaceutics 260 (2003) 175–186.

[158] Q. Zhong, M. Jin, M. Davidson, S. Zivanovic, Sustained release of lysozyme from zein microcapsules produced by a supercritical anti-solvent process, Food Chemistry 115 (2009) 697–700.

[159] P. Jollès, Jollès J., What´s new in lysozyme research?, Molecular and Cellular Biochemistry 63 (1984) 165–189.

[160] C.C.F. Blake, D.F. Koenig, G.A. Mair, A.C.T. North, D.C. Phillips, V.R. Sarma, Structure of Hen Egg-White Lysozyme: A Three-dimensional Fourier Synthesis at 2 Å Resolution, Nature 206 (1965) 757–761.

[161] D.C. Phillips, The Three-dimensional Structure of an Enzyme Molecule, Scientific American 215 (1966) 79–90.

[162] W. Zhao, R. Yang, R. Lu, Y. Tang, W. Zhang, Investigation of the Mechanisms of Pulsed Electric Fields on Inactivation of Enzyme: Lysozyme, Journal of Agricultural and Food Chemistry 55 (2007) 9850–9858.

[163] J.R. Lakowicz, Principles of Fluorescence Spectroscopy, Plenum Press, New York, 1983.

[164] H. Sellak, E. Franzini, J. Hakim, C. Pasquier, Mechanism of lysozyme inactivation and degradation by iron, Archives of Biochemistry and Biophysics 299 (1992) 172–178.

[165] H.R. Costantino, L. Shieha, A.M. Klibanov, R. Langer, Heterogeneity of serum albumin samples with respect to solid-state aggregation via thiol-disulfide interchange — Implications for sustained release from polymers, Journal of Controlled Release 44 (1997) 255–261.

[166] K. Hirayama, S. Akashi, M. Furuya, K. Fukuhara, Rapid confirmation and revision of the primary structure of bovine serum albumin by ESIMS and Frit-FAB LC/MS, Biochem Biophys Res Commun. 173 (1990) 639–646.

[167] K. Murayama, M. Tomida, Heat-Induced Secondary Structure and Conformation Change of Bovine Serum Albumin Investigated by Fourier Transform Infrared Spectroscopy, Biochemistry 43 (2004) 11526–11532.

[168] T.J. Peters, Serum albumin, Advances in Protein Chemistry 37 (1985) 161–245.

[169] W.R. Liu, R. Langer, A.M. Klibanov, Moisture-induced aggregation of lyophilized proteins in the solid state, Biotechnology and Bioengineering 37 (1991) 177–184.

[170] T.P. King, On the Sulfhydryl Group of Human Plasma Albumin, J. Biol. Chem. 236 (1961) PC5.

References

[171] L.O. Andersson, The heterogeneity of bovine serum albumin, Biochim Biophys Acta 117 (1966) 115–133.

[172] R.F. Chen, Removal of Fatty Acids from Serum Albumin by Charcoal Treatment, J. Biol. Chem. 242 (1967) 173–181.

[173] F. Soetewey, M. Rosseneu-Motreff, R. Lamote, H. Peeters, Size and Shape Determination of Native and Defatted Bovine Serum Albumin Monomers: II. Influence of the Fatty Acid Content on the Conformation of Bovine Serum Albumin Monomers, J Biochem 71 (1972) 705–710.

[174] A.F. Habeeb, Immunochemistry of bovine serum albumin, Advances in experimental medcine and biology 98 (1978) 101–117.

[175] H.R. Costantino, K.G. Carrasquillo, R.A. Cordero, M. Mumenthaler, C.C. Hsu, K. Griebenow, Effect of excipients on the stability and structure of lyophilized recombinant human growth hormone, Journal of Pharmaceutical Sciences 87 (1998) 1412–1420.

[176] V.R. Sinha, A. Trehan, Biodegradable microspheres for protein delivery, Journal of Controlled Release 90 (2003) 261–280.

[177] S. Koennings, A. Goepferich, Lipospheres as delivery systems for peptides and proteins, Lipospheres in Drug Targets and Delivery (2005) 67–86.

[178] A. Goepferich, R. Langer, Modeling of polymer erosion in three dimensions: rotationally symmetric devices, AIChE Journal 41 (1995) 2292–2299.

[179] J.M. Anderson, M.S. Shive, Biodegradation and biocompatibility of PLA and PLGA microspheres, Advanced Drug Delivery Reviews 28 (1997) 5–24.

[180] B. Ronneberger, T. Kissel, J.M. Anderson, Biocompatibility of ABA triblock copolymer microparticles consisting of poly(L-lactic-co-glycolic-acid) A-blocks attached to central poly(oxyethylene) B-blocks in rats after intramuscular injection, European Journal of Pharmaceutics and Biopharmaceutics 43 (1997) 19–28.

[181] A. Brunner, K. Mader, A. Goepferich, The chemical microenvironment inside biodegradable microspheres during erosion, Proceedings of the International Symposium on Controlled Release of Bioactive Materials 25th (1998) 154–155.

[182] M. Morlock, H. Koll, G. Winter, T. Kissel, Microencapsulation of rh-erythropoietin, using biodegradable poly(D, L-lactide-co-glycolide). Protein stability and the effects of stabilizing excipients, European Journal of Pharmaceutics and Biopharmaceutics 43 (1997) 29–36.

[183] A. Lucke, J. Kiermaier, A. Gopferich, Peptide acylation by poly(a-hydroxy esters), Pharmaceutical Research 19 (2002) 175–181.

[184] C. Guse, S. Koennings, A. Maschke, M. Hacker, C. Becker, S. Schreiner, T. Blunk, T. Spruss, A. Goepferich, Biocompatibility and erosion behavior of implants made of triglycerides and blends with cholesterol and phospholipids, International Journal of Pharmaceutics 314 (2006) 153–160.

[185] A. Maschke, C. Becker, D. Eyrich, J. Kiermaier, T. Blunk, A. Goepferich, Development of a spray congealing process for the preparation of insulin-loaded lipid microparticles and characterization thereof, European Journal of Pharmaceutics and Biopharmaceutics 65 (2007) 175–187.

[186] H. Reithmeier, J. Herrmann, A. Goepferich, Development and characterization of lipid microparticles as a drug carrier for somatostatin, International Journal of Pharmaceutics 218 (2001) 133–143.

[187] H. Reithmeier, A. Goepferich, J. Herrmann, Preparation and characterization of lipid microparticles containing thymocartin, an immunomodulating peptide, Proceedings of the International Symposium on Controlled Release of Bioactive Materials 26th (1999) 681–682.

[188] W. Vogelhuber, E. Magni, M. Mouro, T. Spruss, C. Guse, A. Gazzaniga, A. Goepferich, Monolithic triglyceride matrixes: A controlled-release system for proteins, Pharmaceutical Development and Technology 8 (2003) 71–79.

[189] R. Cortesi, E. Esposito, G. Luca, C. Nastruzzi, Production of lipospheres as carriers for bioactive compounds, Biomaterials 23 (2002) 2283–2294.

[190] T. Eldem, P. Speiser, A. Hincal, Optimization of Spray-Dried and -Congealed Lipid Micropellets and Characterization of Their Surface Morphology by Scanning Electron Microscopy, Pharmaceutical Research 8 (1991) 47–54.

[191] B. Heurtault, P. Saulnier, B. Pech, J.-E. Proust, J.-P. Benoit, Physico-chemical stability of colloidal lipid particles, Biomaterials 24 (2003) 4283–4300.

[192] H. Bunjes, K. Westesen, M.H.J. Koch, Crystallization tendency and polymorphic transitions in triglyceride nanoparticles, International Journal of Pharmaceutics 129 (1996) 159–173.

[193] J.T. Luxon, D.J. Donald, R. Summitt, Effect of particle size and shape on the infrared absorption spectra of barium titanate and strontium titanate powders, Journal of Applied Physics 41 (1970) 2303-2307.

Appendices

Abbreviations

ANOVA	analysis of variances
ANS	8-anilino-1-naphtalenesolfonic acid
BSA	bovine serum albumin
CD	circular dichroism
CCF	face centered central composite design
Detapac	dieethylenetriamine-pentacetic acid
DMEM	Dulbecco's Modified Eagle's Medium
DMSO	dimethylsulfoxide
DoE	Design of Experiments
DSC	differential scanning calorimetry
DTNB	5,5´-dithiobis(2-nitrobenzoic acid), Ellman´s reagent
FBS	fetal bovine serum
FDA	Food and Drug Administration
GSH	l-glutathione
hGH	human growth hormone
ICH	International Conference on Harmonisation of Technical Requirements for Registration of Pharmaceuticals for Human Use
ICP-OES	inductively coupled plasma – optical emission spectroscopy
IGF	insulin-like growth factor
MALDI-ToF	matrix-assisted laser desorption/ionization time of flight mass spectrometer
PEG	polyethylene glycol
PLGA	poly(lactic-*co*-glycolic acid)
PSH	protein surface hydrophobicity

PTFE   polytetrafluoroethylene

RH   relative humidity

RSH   relative surface hydrophobicity

SCF   super critical fluid

SDS   sodium dodecyl sulfate

SEM   scanning electron microscope

SFD   spray freeze drying

SFL   spray freezing into liquid

SH   sulfhydryl

TFA   trifluoroacetic acid

Additional data for the experimental design

In this section the statistical data for all responses of the experimental design are given. The summary list for the statistical evaluation of the models, the ANOVA lists for the evaluation of the responses as well as the coefficient lists for the determination of the significance of the investigated factors and interactions thereof. All statistical data was evaluated at a confidence level of 0.95.

Particle size (d90-value) for insulin (chapter 4)

d90	Coeff. SC	Std. Err.	P	Conf. int(±)
Constant	0.70807	0.08918	4.06164e-006	0.1943
Pre	-0.08506	0.01011	2.23664e-006	0.02203
Cyc	-0.05011	0.01412	0.004	0.03076
Temp	0.00853	0.0138	0.54814	0.03006
Pre*Pre	0.0765	0.01687	0.00068	0.03675
Cyc*Cyc	0.00652	0.01491	0.66972	0.03248
Temp*Temp	-0.15922	0.11353	0.18613	0.24736
Pre*Cyc	-0.01062	0.01239	0.40824	0.027
Pre*Temp	-0.00054	0.01756	0.97596	0.03826
Cyc*Temp	-0.02281	0.01677	0.1986	0.03653

Table 1 coefficient list (significant factors printed in bold)

d90	Coeff. SC	Std. Err.	P	Conf. int(±)
Constant	0.58792	0.01058	1.36293e-021	0.02222
Pre	-0.07906	0.00965	1.75528e-007	0.02028
Cyc	-0.06434	0.00965	2.9787e-006	0.02028
Pre*Pre	0.08917	0.01432	7.10362e-006	0.03009

Table 2 coefficient list after exclusion of insignificant factors

d90	DF	SS	MS (variance)	F	p	SD
Total	22	9.10276	0.41376			
Constant	1	8.91457	8.91457			
Total Corrected	21	0.18819	0.00896			0.09467
Regression	3	0.16806	0.05602	50.0803	**0.000**	0.23668
Residual	18	0.02013	0.00112			0.03345
Lack of Fit (Model Error)	14	0.01422	0.00102	0.68664	**0.732**	0.03187
Pure Error (Replicate Error)	4	0.00592	0.00148			0.03846

Table 3 Anova list

	R2	R2 Adj.	Q2	SD	RSD	N	Model Validity	Reproducibility
d90	0.89301	0.87518	0.83723	0.09467	0.03345	22	0.92201	0.83495
		N = 22		DF = 18		Cond. no. =2.7386		Y-miss =0

Table 4 Summary list for statistical evaluation of experimental design for d90-value of insulin

Particle size (d90-value) for lysozyme (chapter 4)

d90	Coeff. SC	Std. Err.	P	Conf. int(±)
Constant	0.79691	0.07037	9.20315e-008	0.15333
Pre	-0.06524	0.00669	4.68248e-007	0.014573
Cyc	-0.07671	0.00673	8.55599e-008	0.014663
Temp	-0.05635	0.00668	2.18011e-006	0.01456
Pre*Pre	0.00941	0.00811	0.2683	0.01766
Cyc*Cyc	0.02083	0.00778	0.02016	0.01695
Temp*Temp	-0.03785	0.07522	0.62398	0.16389
Pre*Cyc	0.01175	0.00622	0.08329	0.01355
Pre*Temp	-0.00308	0.01341	0.82204	0.02921
Cyc*Temp	0.00854	0.00697	0.24409	0.01519

Table 5 coefficient list (significant factors printed in bold)

d90	Coeff. SC	Std. Err.	P	Conf. int(±)
Constant	0.76807	0.00975	3.09893e-023	0.02057
Pre	-0.06491	0.00675	2.7303e-008	0.01424
Cyc	-0.07925	0.00673	1.33813e-009	0.0142
Temp	-0.05372	0.00675	3.91394e-007	0.01424
Cyc*Cyc	0.02275	0.00754	0.00780	0.01592

Table 6 coefficient list after exclusion of insignificant factors

d90	DF	SS	MS (variance)	F	p	SD
Total	22	14.0147	0.63703			
Constant	1	13.7225	13.7225			
Total Corrected	21	0.2922	0.013914			0.11796
Regression	4	0.27604	0.06901	72.5879	**0.000**	0.2627
Residual	17	0.01616	0.00095			0.03083
Lack of Fit (Model Error)	13	0.01174	0.00090	0.818115	**0.651**	0.03006
Pure Error (Replicate Error)	4	0.00442	0.0011			0.03323

Table 7 Anova list

	R2	R2 Adj.	Q2	SD	RSD	N	Model Validity	Reproducibility
d90	0.944689	0.93167	0.90294	0.11796	0.03083	22	0.89271	0.92064
		N = 22		DF = 17		Cond. no. =2.6934		Y-miss =0

Table 8 Summary list for statistical evaluation of experimental design for d90-value of lysozyme

Particle size (d90-value) for BSA (chapter 4)

d90	Coeff. SC	Std. Err.	P	Conf. int($\pm$)
Constant	1.12121	0.08118	9.9557e-009	0.17688
pre	-0.10374	0.01024	3.11504e-007	0.02231
cyc	-0.11162	0.01035	1.57715e-007	0.02256
temp	0.02207	0.01028	0.05293	0.0224
pre*pre	0.05093	0.01658	0.00969	0.03613
cyc*cyc	0.0397	0.01577	0.02708	0.03437
temp*temp	-0.27678	0.10727	0.02409	0.23373
pre*cyc	0.04152	0.01263	0.0065	0.02752
pre*temp	-0.09533	0.02283	0.00129	0.04974
cyc*temp	-0.00388	0.01186	0.74906	0.02584

Table 9 coefficient list (significant factors printed in bold)

d90	Coeff. SC	Std. Err.	P	Conf. int($\pm$)
Constant	1.11603	0.07684	2.05311e-009	0.166
pre	-0.10375	0.00988	1.0209e-007	0.02135
cyc	-0.11185	0.00997	4.66039e-008	0.02154
temp	0.02166	0.00985	0.04652	0.02127
pre*pre	0.05044	0.01594	0.00745	0.03443
cyc*cyc	0.03988	0.01521	0.02114	0.03287
temp*temp	-0.26976	0.10144	0.01965	0.21914
pre*cyc	0.04175	0.01217	0.00448	0.0263
pre*temp	-0.09409	0.02173	0.00082	0.04693

Table 10 coefficient list after exclusion of insignificant factors

d90	DF	SS	MS (variance)	F	p	SD
Total	22	20.6863	0.94029			
Constant	1	20.3153	20.3153			
Total Corrected	21	0.37095	0.01766			0.13291
Regression	8	0.35581	0.04448	38.1953	**0.000**	0.2109
Residual	13	0.01514	0.001164			0.03412
Lack of Fit (Model Error)	9	0.00508	0.00056	0.22447	**0.971**	0.02376
Pure Error (Replicate Error)	4	0.01006	0.00251			0.05015

Table 11 Anova list

	R2	R2 Adj.	Q2	SD	RSD	N	Model Validity	Reproducibility
d90	0.95919	0.93408	0.90856	0.13291	0.03412	22	0.99255	0.85765
		N = 22		DF = 13		Cond. no. =26.8749	Y-miss =0	

Table 12 Summary list for statistical evaluation of experimental design for d90-value of BSA

Bioactivity of lysozyme (chapter 6)

Activity	Coeff. SC	Std. Err.	P	Conf. int(±)
Constant	89.1616	3.12135	2.10399e-012	6.8008
Pre	-1.29778	0.29666	0.0009	0.64637
Cyc	-3.00796	0.29849	3.29486e-007	0.65034
Temp	0.74775	0.29633	0.02674	0.64565
Pre*Pre	0.20269	0.35951	0.58328	0.78331
Cyc*Cyc	0.28067	0.34513	0.43193	0.75197
Temp*Temp	2.53408	3.33625	0.46218	7.26903
Pre*Cyc	-0.11668	0.27579	0.67973	0.6009
Pre*Temp	-0.68397	0.59462	0.27245	1.29557
Cyc*Temp	0.53595	0.30919	0.10862	0.67366

Table 13 coefficient list (significant factors printed in bold)

Activity	Coeff. SC	Std. Err.	P	Conf. int(±)
Constant	92,0864	0,37561	3,58467e-033	0,78914
Pre	-1,27052	0,38561	0,00403	0,81013
Cyc	-2,99871	0,38448	3,51184e-007	0,80776
Temp	0,68222	0,38563	0,09382	0,81019

Table 14 coefficient list after exclusion of insignificant factors (significant factors printed in bold)

Activity	Coeff. SC	Std. Err.	P	Conf. int(±)
Constant	92.0864	0.39584	2.73454e-034	0.82852
Pre	-1.32917	0.40516	0.00393	0.84802
Cyc	-3.00482	0.40516	5.06633e-007	0.84802

Table 15 coefficient list after exclusion of insignificant factors

Activity	DF	SS	MS (variance)	F	p	SD
Total	22	186850	8493.18			
Constant	1	186558	186558			
Total Corrected	21	292.203	13.9144			3.73021
Regression	2	226.706	113.353	32.8821	**0.000**	10.6467
Residual	19	65.4976	3.44724			1.85668
Lack of Fit (Model Error)	15	60.1043	4.00695	2.97178	**0.151**	2.00174
Pure Error (Replicate Error)	4	5.39334	1.34833			1.16118

Table 16 Anova list

	R2	R2 Adj.	Q2	SDY	RSD	N	Model Validity	Reproducibility
Activity	0.775851	0.752254	0.706127	3.73022	1.85668	22	0.526519	0.903098
	N = 22		DF = 19		Cond. no. =1.0235		Y-miss =0	

Table 17 Summary list for statistical evaluation of experimental design for bioactivity of lysozyme

Insoluble BSA fraction (chapter 7)

insoluble fraction	Coeff. SC	Std. Err.	P	Conf. int(±)
Constant	8.6635	1.12161	5.37506e-006	2.44377
pre	2.12488	0.14149	3.83282e-009	0.30827
cyc	1.27967	0.14302	1.17447e-006	0.31162
temp	1.43366	0.14203	3.23714e-007	0.30946
pre*pre	1.84723	0.22908	3.46603e-006	0.49912
cyc*cyc	-0.23992	0.21793	0.29253	0.47482
temp*temp	-1.94042	1.48207	0.21496	3.22914
pre*cyc	-0.42425	0.17452	0.03168	0.38025
pre*temp	1.23938	0.31541	0.002	0.68721
cyc*temp	0.14553	0.16383	0.39183	0.35694

Table 18 coefficient list (significant factors printed in bold)

insoluble fraction	Coeff. SC	Std. Err.	P	Conf. int(±)
Constant	7.12295	0.16027	2.43886e-017	0.34161
pre	2.12998	0.14661	3.04458e-010	0.31248
cyc	1.25493	0.14618	3.57311e-007	0.31157
temp	1.33229	0.12294	1.71859e-008	0.26204
pre*pre	1.70266	0.21743	1.1192e-006	0.46344
pre*cyc	-0.46773	0.17903	0.0196	0.38158
pre*temp	1.59827	0.16392	6.96364e-008	0.34939

Table 19 coefficient list after exclusion of insignificant factors

insoluble fraction	DF	SS	MS (variance)	F	p	SD
Total	22	1550	70.4545			
Constant	1	1411.2	1411.2			
Total Corrected	21	138.798	6.60942			2.57088
Regression	6	134.952	22.492	87.7324	**0.000**	4.74258
Residual	15	3.84557	0.256371			0.50633
Lack of Fit (Model Error)	11	3.01519	0.27411	1.3204	**0.426**	0.52355
Pure Error (Replicate Error)	4	0.83038	0.2076			0.45563

Table 20 Anova list

	R2	R2 Adj.	Q2	SDY	RSD	N	Model Validity	Reproducibility
insoluble fraction	0.97229	0.96121	0.92265	2.57088	0.50633	22	0.78636	0.96859
	N = 22		DF = 15		Cond. no. =2.7534		Y-miss =0	

Table 21 Summary list for statistical evaluation of experimental design for insoluble fraction of BSA

Curriculum vitae

Name: Axel Ehmer

Date of birth: August 22nd, 1978

Place of birth: Fulda

Education:

1984 – 1988   Elementary school Paul Gerhard, Hünfeld

1988 – 1997   Grammar school Wigbert Gymnasium, Hünfeld

Professional training and experiences:

10/1998 – 04/2003   Study of Pharmacy: Johannes Gutenberg-Universität, Mainz

11/2002 – 03/2003   Student assistant: Department of Pharmaceutical Biology, Johannes Gutenberg-Universität, Mainz

05/2003 – 10/2003   Pharmaceutical Traineeship: "Kantonsspital Baden", Baden, Switzerland

11/2003 – 04/2004   Pharmaceutical Traineeship: "Adler-Apotheke", Mainz

05/2004   Acquisition of the license to practice as pharmacist

08/2004 – 10/2008   PhD program at the Department of Pharmaceutical Technology, University of Regensburg, Prof. A. Göpferich

11/2008 – present   Bulk Manufacturing Manager, Spirig Pharma AG, Egerkingen, Switzerland

List of Publications

Publications:

A. Ehmer, C. Becker, D. Eyrich, A. Zaky, J. Teßmar, T. Blunk, A. Göpferich: Protein jet milling. *to be submitted*

Conference Abstracts:

2003

A. Ehmer, M. Lutters, P. Vonbach, A. Dubied: Optimierung der pharmazeutischen Betreuung durch verbesserte Arzneimittelinformation für den Pflegedienst. GSASA, St. Gallen

(*poster presenation*)

2006

A. Ehmer, S. Kolb, J. Teßmar, T. Blunk, A. Göpferich: Micronization of Proteins by Jet Milling. CRS German Chapter, Jena

(*poster presentation*)

A. Ehmer, A. Zaky, D. Eyrich, J. Teßmar, T. Blunk, A. Göpferich: Micronization of Insulin by Jet Milling. DPhG Jahrestagung - Joint Meeting, Marburg

(*poster presentation*)

C. Becker, A. Ehmer, A. Maschke, A. Meindorfer, D. Ausbacher, J. Teßmar, T. Blunk, A. Göpferich: Influence of Micronisation of Proteins on the Properties of Lipid Microparticles for Controlled Release. DPhG Joint Meeting, Marburg

(*poster presentation*)

2007

A. Ehmer, S. Kolb, C. Becker, J. Teßmar, A. Göpferich: Cryogenic Grinding by Jet Milling: A Promising Option for the Micronization of Proteins?. 2nd European Congress on Life Science Process Technology, Nuremberg

(*poster presentation*)

A. Ehmer, C. Becker, C. Popp, A. Zaky, J. Teßmar, T. Blunk, A. Göpferich: Impact of Jet Milling on Stability and Bioactivity of Proteins in Solid State. AAPS Annual Meeting, San Diego, The AAPS Journal Vol. 9, No. S2, Abstract T2350

(*poster presentation*)

A. Ehmer, C. Becker, J. Teßmar, T. Blunk, A. Göpferich: Parameters Influencing the Micronization of Proteins Investigated by Using Statistical Experimental Design. DPhG-Jahrestagung, Erlangen

(*oral presentation*)

2008

A. Ehmer, T. Blunk, J. Teßmar, A. Göpferich: Jet Milling of BSA: Stabilization by Low Temperature or Addition of Polyethylene Glycol. 6th World Meeting on Pharmaceutics Biopharmaceutics and Pharmaceutical Technology, Barcelona

(*poster presentation*)

2009

A. Zaky, A. Elbakry, A. Ehmer, M. Breunig, A. Göpferich: Protein Release Mechanism from Triglyceride Microspheres. DPhG-Jahrestagung, Jena

(*poster presentation)*

Danksagung

Zum Schluss möchte ich mich bei allen bedanken, die zum Gelingen dieser Arbeit beigetragen haben

Herrn Prof. Göpferich danke ich sehr für die Überlassung des interessanten Themas und die Betreuung der Arbeit. Die konstruktiven Anregungen während zahlreicher Meetings waren sehr hilfreich und motivierend. Besonders danke ich für die zahlreichen Gelegenheiten meine Ergebnisse auf nationalen und internationalen Konferenzen präsentiert haben zu dürfen.

Der Forschungsvereinigung der Arzneimittel-Hersteller e.V. (FAH) für die Finanzierung der Arbeit während der ersten 2 Jahre im Rahmen des Projektes „Mikronisierung von Proteinen und Verarbeitung zu Arzneiformen".

Bei Dr. Jörg Teßmar für sein immer offenes Ohr, seine fachlichen Ratschläge, für die Einführung der Superbowl Herrenabende und sein Einsatz für den gesamten Lehrstuhl beruflich und privat.

Dr. Torsten Blunk für seinen fachlichen Rat und seine Fähigkeit immer etwas Positives in Forschungsergebnissen zu finden

Bei Dr. Eduard Hochmuth für die Durchführung der MALDI Messungen.

Allen Mitstreitern beim jährlichen Jedermannzehnkampf.

Dr. Barbara Weiser für fachkompetente Gespräche (vor allem in Statistikfragen) und die Aufnahme von Fritzi.

Dr. Daniela Tausendpfund, Dr. Stephanie Könnings, Dr. Sigrid Grundsteiner und Dr. Christian Guse für die freundschaftliche Aufnahme in den Lehrstuhl und gemeinsame Freizeitgestaltung.

Dr. Stefan Rothschenk für 10 freundschaftliche gemeinsame Jahre an der Uni.

"He, who breaks a thing to find out what it is, has left the path of wisdom."

Lord of the Rings by J.R.R. Tolkien